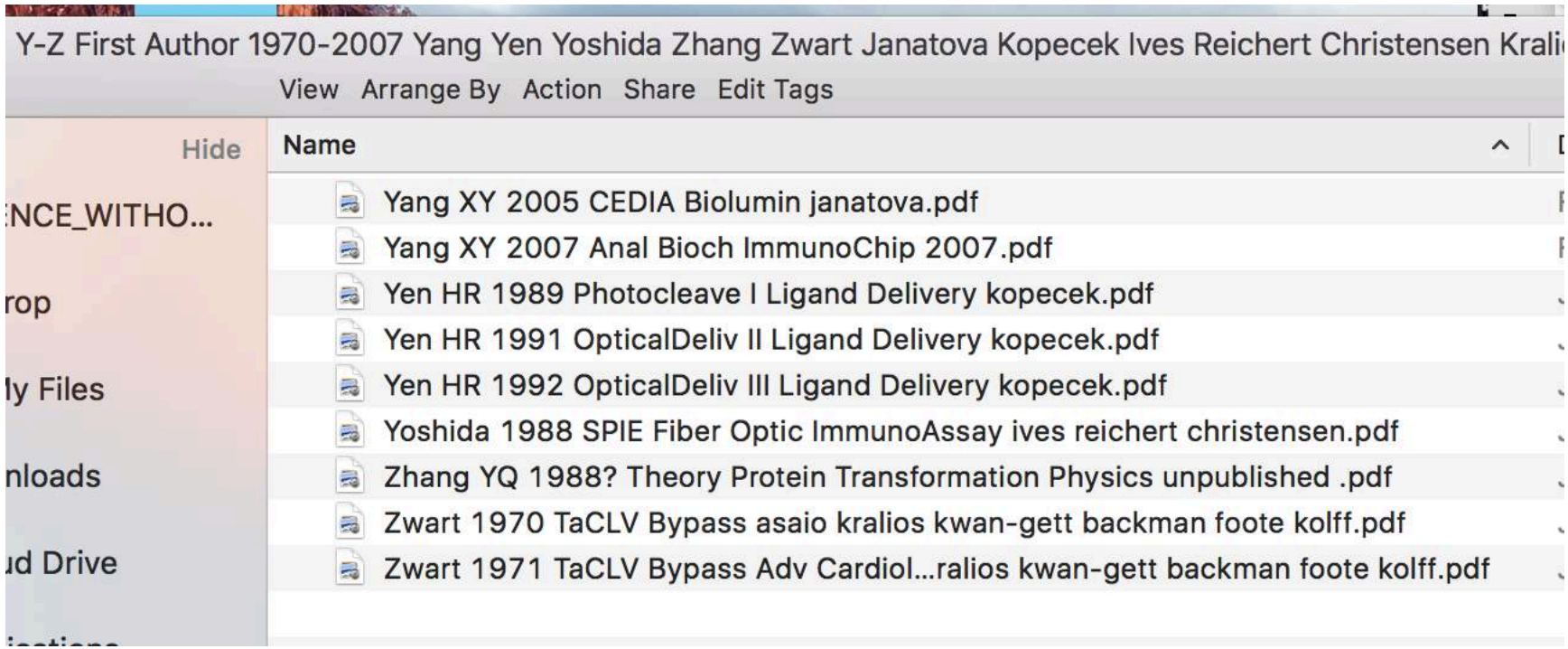
Y-Z First Author 1970-2007 Yang Yen Yoshida Zhang Zwart Janatova Kopecek Ives Reichert Christensen Krali
View Arrange By Action Share Edit Tags
Hide
Name
Yang XY 2005 CEDIA Biolumin janatova.pdf
Yang XY 2007 Anal Bioch ImmunoChip 2007.pdf
Yen HR 1989 Photocleave I Ligand Delivery kopecek.pdf
Yen HR 1991 OpticalDeliv II Ligand Delivery kopecek.pdf
Yen HR 1992 OpticalDeliv III Ligand Delivery kopecek.pdf
Yoshida 1988 SPIE Fiber Optic ImmunoAssay ives reichert christensen.pdf
Zhang YQ 1988? Theory Protein Transformation Physics unpublished .pdf
Zwart 1970 TaCLV Bypass asaio kralios kwan-gett backman foote kolff.pdf
Zwart 1971 TaCLV Bypass Adv Cardiol...ralios kwan-gett backman foote kolff.pdf

Available online at www.sciencedirect.com
SCIENCE DIRECT®
Analytical Biochemistry 336 (2005) 102–107
ANALYTICAL BIOCHEMISTRY
www.elsevier.com/locate/yabio

Homogeneous enzyme immunoassay modified for application to luminescence-based biosensors

Xiaoyun Yang, Jarmila Janatova, Joseph D. Andrade*

Department of Bioengineering, University of Utah, 50 South Central Campus Drive, Room 2480, Salt Lake City, UT 84112-9202, USA

Received 20 July 2004
Available online 10 November 2004

Abstract

Application of immunoassay to biosensors for use in the point-of-care setting ideally requires immunoassay without separation steps and with small volumes of both sample and reagents. The suitability of cloned enzyme donor immunoassay (CEDIA), one of a few homogeneous immunoassays available, was investigated for application to biosensors. This method is based on the bacterial enzyme β-galactosidase, which has been genetically engineered by others into two inactive fragments, enzyme donor (ED) and enzyme acceptor (EA). Association of the ED and EA fragments in the assay results in formation of active enzyme, which acts on substrate to generate a detectable signal. Sensitivity of commercially available CEDIA kits were compared, with respect to the sample and reagent volumes, using three different signal generation processes. The CEDIA kit for valproic acid and three substrates, a colorimetric (chlorophenol red-β-D-galactopyranoside), a chemiluminescent (Lumi-Gal 530), and a bioluminescent (Beta-Glo Assay System), were employed in the study. Our results indicate that the high sensitivity of the bioluminogenic substrate, D-luciferin-*O*-β-galactopyranoside, with short assay time and small volumes of sample and reagents required for the assay, simple handling, and relatively low expense, make this substrate, together with CEDIA, suitable for application to biosensors intended for drug and metabolite monitoring in the point-of-care setting.

Keywords: Homogeneous immunoassay; CEDIA; Spectrophotometry; Chemiluminescence; Bioluminescence; Substrates

There is a growing need for high-throughput analysis of small molecular substances [1]. For such analysis homogeneous rather than heterogeneous assays are preferred due to their simplicity, ease of automation, and higher throughput. A homogeneous immunoassay that employs complementation within the β-galactosidase system is known as CEDIA[1] [2,3]. CEDIA is based on the bacterial enzyme β-galactosidase, which has been genetically engineered into two inactive fragments, enzyme donor (ED) and enzyme acceptor (EA). When mixed together, the two fragments combine to form active enzyme; this process is termed "complementation." Covalent attachment of analyte to ED does not affect the ability of ED to associate with EA. Analyte present in a sample competes for binding to the limited number of antibody sites, making analyte–ED conjugate available for enzyme formation.

* Corresponding author. Fax: +1 801 585 5361.
E-mail addresses: joeandrade@uofu.net, joe.andrade@m.cc.utah.edu (J.D. Andrade).

[1] *Abbreviations used:* CEDIA, cloned enzyme donor immunoassay; CPRG, chlorophenol red-β-D-galactopyranoside; EA, enzyme acceptor; ED, enzyme donor; EDTA, ethylenediaminetetraacetic acid; GDP, 4-methoxy-4-(3-β-D-galactosidephenyl) spiro [1,2-dioxetane-3,2′-adamantane]; Hepes, *N*-2-hydroxyethylpiperazine-*N*′-2-ethane-sulfonic acid; R1, CEDIA reagent 1; R2, CEDIA reagent 2; TDM, therapeutic drug monitoring; VPA, valproic acid; RT, room temperature.

0003-2697/$ - see front matter © 2004 Elsevier Inc. All rights reserved.
doi:10.1016/j.ab.2004.09.026

The amount of active enzyme formed is directly proportional to the analyte concentration in the sample. During the assay, the level of enzyme with β-galactosidase activity can be determined either spectrophotometrically by the rate of chromogenic substrate hydrolysis or luminescently with chemi- or bioluminescent substrate. The CEDIA Kit for valproic acid (VPA), designed by Microgenics (Fremont, CA, USA) for use in automated analyzers, is a two-step procedure. For time saving, cost reduction, simplicity, and application to a ChemChip format [4], a one-step procedure introduced by Khanna et al. [5] was adapted and used in this study (Fig. 1). Based on simulation results, it is shown that one-step CEDIA has a wider analyte dynamic range than two-step CEDIA [6].

High-quality therapeutic drug monitoring (TDM) reagents, calibrators and controls for a number of drugs are available from Microgenics. This kit employs the standard two-step CEDIA procedure [3,6]. The commercial CEDIA kit for VPA contains the chromogenic substrate chlorophenol red-β-D-galactopyranoside (CPRG) for quantification of enzyme activity. The hydrolysis of substrate is measured spectrophotometrically at 550–600 nm.

Luminescence-based assays are finding increased use in chemical and medical diagnostics. A chemiluminescent assay for β-galactosidase using Lumi-Gal 530 (Lumigen, Southfield, MI, USA), wherein chemiluminescence of the product is measured with a luminometer, was evaluated. This assay exhibits advantages over the standard spectrophotometric technique. It is simple and relatively inexpensive and has a 20-fold greater sensitivity [7].

Bioluminogenic substrates with even higher sensitivity have been developed for the determination of enzymes and many different analytes. The sensitivity of CEDIA has been substantially increased by utilization of a highly sensitive substrate for β-galactosidase, based on the release of D-luciferin from 6-*O*-β-galactopyranosyl-luciferin by the action of β-galactosidase. D-Luciferin can be easily quantified in a luminometric assay [8]. The Beta-Glo Assay System (Promega, Madison, WI, USA), is based on the two coupled enzyme reactions and allows for measuring β-galactosidase activity in a homogeneous assay format.

Our goal is to develop a simple, highly sensitive, single-step homogeneous immunoassay platform for application to a luminescence-based ChemChip [4].

Materials and methods

Homogenous immunoassay with spectrophotometric detection in microplate reader

Reagents for the homogeneous immunoassay. CEDIA valproic acid II kit (Catalog No. 100013) was purchased from Microgenics. Reagent 1 (R1) of CEDIA kit contains antianalyte antibody and EA. Reagent 2 (R2) consists of analyte–ED conjugate, antiimmunoglobulin secondary antibody, and substrate CPRG. Both reagents R1 and R2, supplied in lyophilized form, were reconstituted with provided buffer solutions and stored at 4 °C.

Solutions for calibration and standard curves. CEDIA Core TDM Multi-Cal kit (Catalog No. 100007, Microgenics) contained High and Low Calibrators (143.2 μg/ml VPA and 0.1 μg/ml VPA, respectively). Solutions of different VPA concentrations were prepared by dilution of the High Calibrator with 20 mM Hepes, pH 7.5. The concentrations of VPA used in the study (from 0.1 to 144 μg/ml) covered its therapeutic range from 50 to 100 μg/ml VPA.

Spectrophotometric detection of enzyme activity during CEDIA. Optical density (O.D.) of the colorimetric product was recorded using a Microplate Reader Spectra MAX 250 with its parameters being controlled by Soft Max Pro software (Molecular Devices, Sunnyvale, CA, USA). Spectrophotometric assays were carried out in 96-well microplates (Nunc-Immuno Module; No. 120080LE P891) according to the following procedure. The CEDIA reagents (R1 and R2) and VPA samples were equilibrated to 37 °C separately in the Microplate Reader Spectra Max 250 for 8 min. At the time of experiment, the VPA samples were transferred into R1, and immediately thereafter R2 was added to a mixture of R1 and VPA. After quick mixing, the plate was placed into the Microplate Reader. O.D. was recorded at 570 nm as a function of time for nearly 10 min in 22-s intervals at 37 °C.

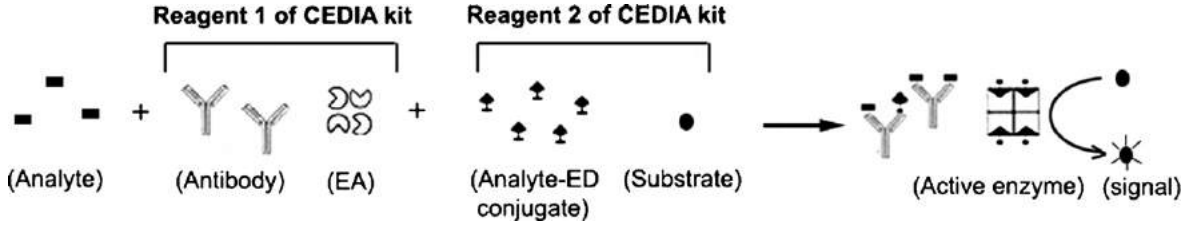

Fig. 1. One-step CEDIA assay. All of the CEDIA reactants are mixed simultaneously in the same vessel. Subsequently, color or luminescence can be measured depending on a signal generation process of substrate added.

Homogenous immunoassay with chemiluminescent detection in luminometer

Chemiluminescent substrate for β-galactosidase. Lumi-Gal 530 is a complete liquid formulation that contains stabilized dioxetane in 2-amino-2-methyl-1-propanol buffer, pH 9.6, and an enhancer system incorporating the fluorescer 5-(*N*-tetradecanoylamino)-fluorescein. This cocktail can be used directly for analysis using CEDIA system, described above. For the experiments with Lumi-Gal 530, R2 of CEDIA kit, without substrate, was kindly provided by Microgenics.

Preparation of β-galactosidase solutions. Escherichia coli β-galactosidase (Sigma–Aldrich) was diluted to 1000 U/ml in deionized water and stored at −70 °C in 10-μl aliquots. Dilutions were made with the pH 7.5 buffer, containing 10 mM Hepes, 1 mM EDTA, and 2 mg/ml bovine serum albumin, immediately prior to assay.

One-step CEDIA with Lumi-Gal 530. Solutions with different concentrations of VPA were prepared by dilution of valproate sodium (Depacon, 500 mg/ml) with 20 mM Hepes, pH 7.5. CEDIA reagents (R1; R2 without substrate), VPA, and Lumi-Gal 530 were incubated at 37 °C in water bath for 10 min. The VPA samples (2 μl) were transferred into R1 (8 μl), and immediately R2 (6 μl) was added to the mixture of R1 and VPA. Then the mixture was transferred to a polystyrene tube (12 × 55 mm; Elkay Products, Shrewsbury, MA, USA) containing Lumi-Gal 530 (25 μl). Luminescent signal was measured using a Luminometer TD 20/20 (Turner Designs, Sunnyvale, CA, USA), at a sensitivity setting of 70.0%, as a function of time at room temperature (RT; about 22 °C).

Luminescent homogenous immunoassay with Beta-Glo Assay System

Luminescent substrate for β-galactosidase. The Beta-Glo Assay System (Promega) consists of two components that are combined to form Beta-Glo Reagent [9]. It is stored at −20 °C and thawed at RT immediately prior to assay. It is recommended by Promega to not reduce the volume of reagent to less than 1:1 ratio with the volume of test solution.

One-step CEDIA with Beta-Glo Assay System. Solutions with different concentrations of VPA were prepared by dilution of valproate sodium (Depacon, 500 mg/ml) with 20 mM Hepes pH 7.5. CEDIA reagents (R1; R2 without substrate), VPA solutions, and Beta-Glo reagent solution were incubated at 37 °C in water bath for 10 min. VPA samples (2 μl) were transferred into R1 (8 μl), and immediately R2 (6 μl) was added to the mixture of R1 and VPA. Then the mixture (16 μl) was transferred to a polystyrene tube containing Beta-Glo reagent solution (16 μl). Luminescent signal was measured using a Luminometer TD 20/20 (Turner Designs), at a sensitivity setting of 70.0%, as a function of time at RT (about 22 °C). The smaller volumes [1 μl CEDIA reagents (0.5 μl R1, 0.375 μl R2, and 0.125 μl VPA) + 1 μl Beta-Glo reagent] were also tested.

Results and discussion

Homogeneous immunoassay with spectrophotometric detection

The CEDIA valproic acid II kit contains the chromogenic substrate CPRG. It is normally used in automated analyzers as a two-step procedure. To simplify the experiment and reduce assay time and volumes and with the aim to apply it to a ChemChip format [4], a one-step assay procedure (Fig. 1) was used in the current study. In a one-step CEDIA all the reactants were mixed together simultaneously, so a separate incubation step between analyte and antibody was omitted. The optical density, dependent on concentration of VPA, was recorded at 570 nm as a function of time. As follows from Fig. 2, O.D. corresponding to a range of measured VPA concentrations could be discerned after 6 min. Calibration curves (Fig. 3) were generated by plotting the slopes,

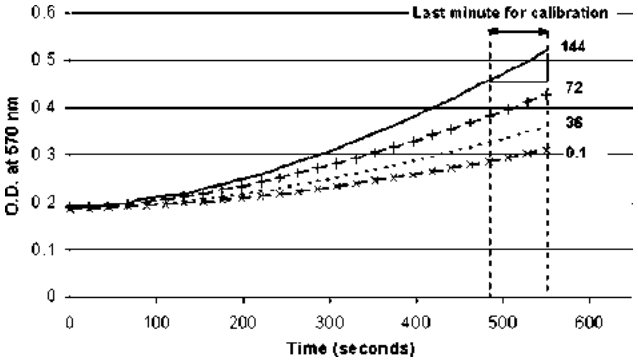

Fig. 2. One-step spectrophotometric assay using the CEDIA kits for VPA. Volumes of CEDIA reagents, R1 (80 μl) + R2 (60 μl), and VPA (20 μl) of different concentrations diluted 1:10. Curves from top to bottom represent VPA initial concentration as 144, 72, 36, and 0.1 μg/ml, respectively.

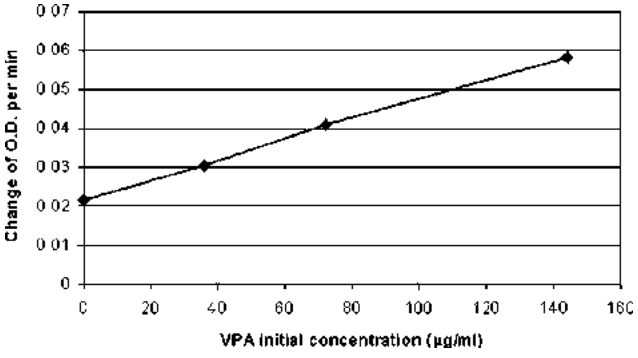

Fig. 3. Calibration curve of one-step CEDIA generated with spectrophotometric substrate. It represents slope of each kinetics curve in the last minute as a function of VPA initial concentrations covering the therapeutic range from 50 to 100 μg VPA per ml.

changes in O.D. of the kinetics curves in the last 60 s, as a function of VPA concentrations.

Homogeneous immunoassay with chemiluminescent detection

Lumi-Gal 530 provided by Lumigen Inc. is a ready to use formulation containing Lumigen GDP (4-methoxy-4-(3-β-D-galactosidephenyl) spiro [1,2-dioxetane-3,2′-adamantane]) for the one-step chemiluminescent detection of β-galactosidase. The reaction of the chemiluminescent substrate Lumigen GDP with active β-galactosidase formed causes cleavage of the galactoside unit resulting in a moderately stable intermediate. The decomposition of this intermediate in alkaline solution generates chemiluminescence.

To determine the range of β-galactosidase concentrations over which the light output would correspond to the enzyme concentration generated by one-step CEDIA, we have carried out experiments with pure enzyme and Lumi-Gal 530 first.

As depicted in Fig. 4, the relative light unit (RLU) numbers, corresponding to the chemiluminescence intensity, are directly proportional to the quantity of β-galactosidase. This range covers the amount of enzyme produced during CEDIA. The optimal conditions for one-step CEDIA with the chemiluminescent substrate were obtained with the following volumes: 16 µl CEDIA reagents + 25 µl Lumi-Gal 530. Using the volume ratio as recommended by the manufacturer's protocol, i.e., Lumi-Gal 530 should not be diluted by more than 10% through addition of enzyme or other reagents (Lumigen), the results obtained were repeatedly inconsistent. One of the plausible reasons for this could be that the CEDIA reagents were diluted by Lumi-Gal 530 to such an extent that reactions involved in CEDIA could not proceed efficiently and in a reproducible manner. Fig. 5 shows that the separation between RLU, corresponding to different concentrations of VPA, could not be distinguished before 15 min after mixing all the reactants. Moreover, a moving average over 10 s to smooth out the kinetic curves had to be applied. Assays using smaller total volumes, i.e., 6.4 µl of CEDIA reagents and 10 µl of Lumi-Gal 530, also produced acceptable values (Fig. 6). Although smaller volumes yielded lower light outputs, these results indicated nevertheless the feasibility of using smaller volumes of the reactants for application to a ChemChip format [4].

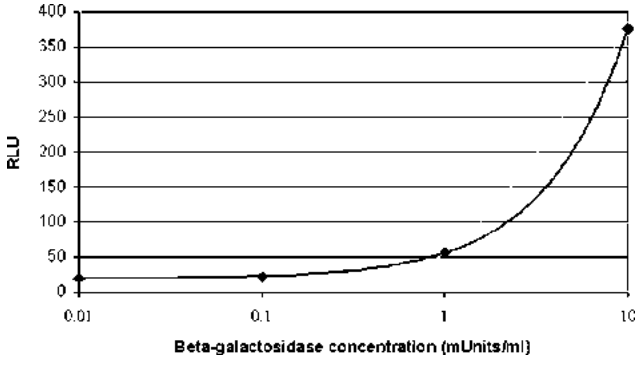

Fig. 4. Determination of the range of chemiluminescent intensity with pure β-galactosidase and the substrate Lumi-Gal 530. Chemiluminescent signal was recorded for 1 h after mixing a 5-µl aliquot of an appropriate dilution of β-galactosidase and 50 µl Lumi-Gal 530.

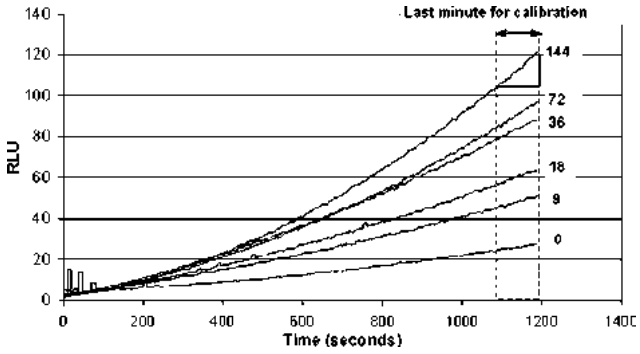

Fig. 5. One-step CEDIA with chemiluminescent substrate Lumi-Gal 530. Volumes of CEDIA reagents, R1 (8 µl) + R2 (6 µl), and VPA (2 µl) of different concentrations + Lumi-Gal 530 (25 µl). For test conditions, see Materials and methods. Detection sensitivity of luminometer was set at 70.0%. Compared to the results in Fig. 4, concentrations of β-galactosidase produced in one-step CEDIA with tested VPA concentrations are estimated to be in the range 0.01–1 mU/ml. Curves from top to bottom represent VPA initial concentration as follows: 144, 72, 36, 18, 9, and 0 µg/ml, respectively. A moving average was applied to obtain the kinetics curves.

Homogeneous immunoassay with bioluminescent detection

The Beta-Glo assay system provides a coupled enzyme reaction system utilizing a luciferin-galactoside

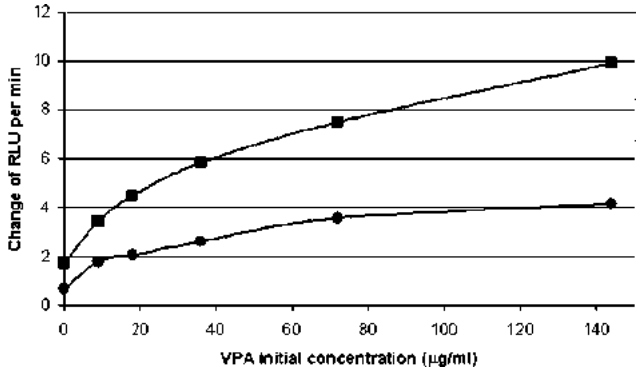

Fig. 6. Calibration curves of one-step CEDIA with Lumi-Gal 530. Large volumes (closed squares): 16 µl CEDIA reagents (8 µl R1, 6 µl R2 and 2 µl VPA) + 25 µl Lumi-Gal 530. Small volumes (closed circles): 6.4 µl CEDIA reagents (3.2 µl R1, 2.4 µl R2, and 0.8 µl VPA) + 10 µl Lumi-Gal 530. They represent slopes of kinetics curves in the last minute (indicated by a bracket) as a function of VPA initial concentration.

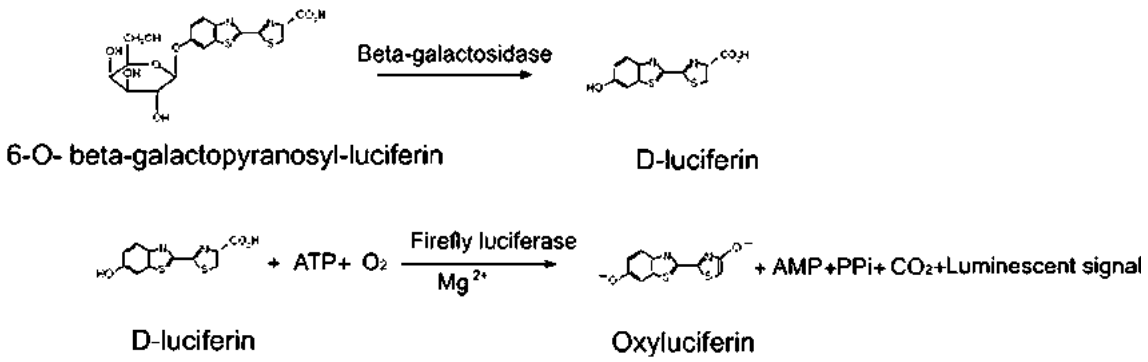

Fig. 7. Summary of the coupled reactions in the Beta-Glo Assay system. In the reaction, 6-*O*-β-galactopyranosyl-luciferin is cleaved by β-galactosidase to yield luciferin, which is then catalyzed by firefly luciferase in the presence of cofactors to yield light.

substrate (6-*O*-β-galactopyranosyl-luciferin). The principle of this assay is presented in Fig. 7. The coupled reactions in the system include luciferin-galactoside (6-*O*-β-galactopyranosyl-luciferin) cleaved by the enzyme with β-galactosidase activity formed during the CEDIA procedure. The luciferin is then used in a firefly luciferase reaction to generate light [9].

It follows from Fig. 8 that one-step CEDIA performed with the Beta-Glo bioluminescent system is much more sensitive than the one with chemiluminescent substrate, Lumi-Gal 530. With the same initial concentration of VPA, Beta-Glo yields about 300 times more light output at the same detection sensitivity. Differences between VPA concentrations can be detected within 4 min, a much shorter time than the one required in the assay with Lumi-Gal 530. The use of Beta-Glo Assay System results in low background; a moving average data process is not needed. Smaller volumes of the CEDIA reagents and of samples can be used with this substrate (Fig. 9).

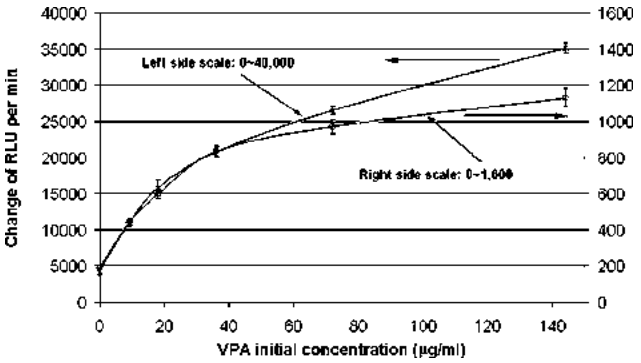

Fig. 9. Calibration curves of one-step CEDIA with Beta-Glo Assay System for two different volumes. Large volumes (cross lines): 16 µl CEDIA reagents (8 µl R1, 6 µl R2, and 2 µl VPA) + 16 µl Beta-Glo reagent. Small volumes (open circles): 1 µl CEDIA reagents (0.5 µl R1, 0.375 µl R2, and 0.125 µl VPA) + 1 µl Beta-Glo reagent. This figure represents slopes of kinetics curves in the last minute as a function of VPA initial concentration. The values obtained with large volumes are within the range of 0–40,000 RLU per min (left side scale), while small volumes yielded signals corresponding to the right side scale (0–1600 RLU per min).

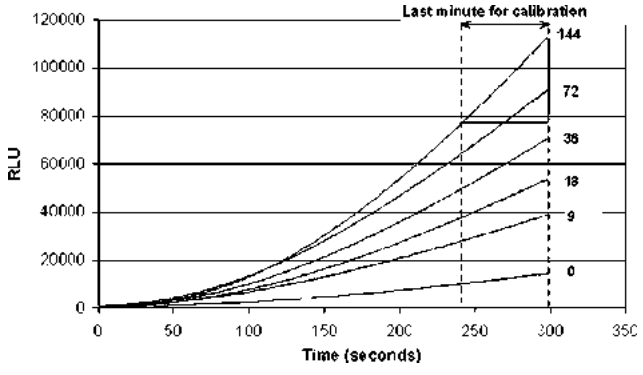

Fig. 8. One-step CEDIA with bioluminescent Beta-Glo Assay System. CEDIA reagents R1 (8 µl) + R2 (6 µl) + VPA (2 µl) of different concentrations + 16 µl Beta-Glo Assay solution. Detection sensitivity at 70.0% was the same as that for Lumi-Gal 530 in Fig. 5. Curves from top to bottom represent VPA initial concentration as follows: 144, 72, 36, 18, 9, and 0 µg/ml, respectively.

Conclusions

Our investigations of one-step CEDIA, using three different signal generation processes, are summarized in Table 1. Much smaller volumes of the reagents for one-step CEDIA are needed with Beta-Glo Assay System to yield significant luminescence signal, compared with colorimetric substrate (CPRG). With the chemiluminescent substrate Lumi-Gal 530, longer time is required to discern RLU differences between different VPA concentrations, and the high noise level requires data processing methods to smooth the data curves.

In summary, one-step CEDIA with the Beta-Glo assay system provides a very sensitive and relatively fast technique for immunochemical detection and quantification of analytes. The enzyme with β-galactosidase activity generated during the CEDIA process catalyzes

Table 1
Comparison of one-step CEDIA performed with spectrophotometric, chemiluminescent, and bioluminescent substrates

Method of detection	Spectrophotometric	Chemiluminescent	Bioluminescent
Substrate	CPRG	Lumi-Gal 530	Beta-Glo Assay System
Detection of signal	Optical density (O.D.) at 570 nm by UV-visible spectrophotometer	Luminescence signal (RLU) detected by luminometer	Luminescence signal (RLU) detected by luminometer
Total volume of test solution: (R1 + R2 + VPA) + appropriate substrate	160 µl	Large volume: 41 µl Small volume: 16.4 µl	Large volume: 32 µl Small volume: 2 µl
Time period to detect differences between VPA concentrations	6 min	15 min	4 min
Change of detected signal in the last recording minutes [a]	0.06 O.D./min	Large volume: 10 RLU/min Small volume: 4 RLU/min	Large volume: 35,000 RLU/min Small volume: 1200 RLU/min
Refer to Figure	Figs. 2 and 3	Figs. 5 and 6	Figs. 8 and 9

[a] The numbers indicate the VPA initial concentration of 144 µg per ml performed with three substrates.

the hydrolytic cleavage of 6-*O*-β-galactopyranosyl-luciferin, coupled to the firefly luciferase reaction, resulting in effective light generation.

The procedure developed in our laboratory permits immunoassay to be carried out simply, in a homogeneous manner, with the CEDIA reagents (available for many analytes from Microgenics) and the Beta-Glo assay system kit for detection (available from Promega). Thanks to very small volumes (1 µl each) of CEDIA reaction mixture and Beta-Glo assay reagent and the efficient light output, this immunoassay procedure lends itself for application to biosensors in a ChemChip format being developed for the point-of-care setting [4].

Acknowledgments

Dr. Sang Il Jeon, visiting professor from Kangnung National University, Kangnung, Korea, worked on simulation of one-step CEDIA [6]. We thank Professor S. Kern for use of his laboratory facilities and equipment. We also express our appreciation to the University of Utah ChemChip group, especially Rupert Davies, Daniel Bartholomeusz, and Jenny Hatch, for assistance and helpful discussions and to Dr. Rueyming Loor, Microgenics, for providing CEDIA reagents, specifically R2 without substrate. This work was supported by NIH Grant RR17329.

References

[1] T. Yokozeki, H. Ueda, R. Arai, W. Mahoney, T. Nagamune, A homogeneous noncompetitive immunoassay for the detection of small haptens, Anal. Chem. 74 (2002) 2500–2504.
[2] D.R. Henderson, S.B. Friedman, J.D. Harris, W.B. Manning, M.A. Zoccoli, CEDIA, a new homogeneous immunoassay system, Clin. Chem. 32 (1986) 1637–1641.
[3] W.A. Coty, in: D. Wild (Ed.), The Immunoassay Handbook, Nature Publisher, New York, 2001, pp. 373–376.
[4] R. Davies, D.A. Bartholomeusz, J.D. Andrade, Personal sensors for the diagnosis and management of metabolic disorders, IEEE Eng. Med. Biol. Mag. 22 (2003) 32–42.
[5] P. Khanna, S.B. Friedman, D.S. Kates, Liquid single reagent for air enzyme complementation assay. US Patent (1991) 5032503.
[6] S.I. Jeon, X. Yang, J.D. Andrade, Modeling of homogeneous cloned enzyme donor immunoassay, Anal. Biochem. 333 (2004) 136–147.
[7] E.G. Beale, E.A. Deeb, R.S. Handley, H. Akhavan-Tafti, A.P. Schaap, A rapid and simple chemiluminescent assay for *Escherichia coli* beta-galactosidase, Biotechniques 12 (1992) 320–323.
[8] R. Geiger, E. Schneider, K. Wallenfels, W. Miska, A new ultrasensitive bioluminogenic enzyme substrate for beta-galactosidase, Biol. Chem. Hoppe. Seyler. 373 (1992) 1187–1191.
[9] R. Hannah, I. Stroke, N. Betz, Beta-Glo® assay system: a luminescent β-galactosidase assay for multiple cell types and media, Cell Notes 6 (2003) 16–18.

Available online at www.sciencedirect.com
ScienceDirect
Analytical Biochemistry 365 (2007) 222–229
ANALYTICAL BIOCHEMISTRY
www.elsevier.com/locate/yabio

An ImmunoChip prototype for simultaneous detection of antiepileptic drugs using an enhanced one-step homogeneous immunoassay

Xiaoyun Yang [a], Jarmila Janatova [a,*], JoEtta M. Juenke [b], Gwendolyn A. McMillin [b,c], Joseph D. Andrade [a,*]

[a] *Department of Bioengineering, University of Utah, Salt Lake City, UT 84112, USA*
[b] *ARUP Institute of Clinical and Experimental Pathology, Salt Lake City, UT 84108, USA*
[c] *Department of Pathology, University of Utah School of Medicine, Salt Lake City, UT 84132, USA*

Received 21 December 2006
Available online 24 March 2007

Abstract

The development and characterization of a one-step homogeneous immunoassay-based multiwell ImmunoChip is reported for the simultaneous detection and quantitation of antiepileptic drugs (AEDs). The assay platform uses a cloned enzyme donor immunoassay (CEDIA) and a Beta-Glo assay system for generation of bioluminescent signal. Results of the one-step CEDIA for three AEDs (carbamazepine, phenytoin, and valproic acid), in the presence of serum, correlate well with the values determined by fluorescence polarization immunoassay. CEDIA intra- and interassay coefficients of variation are less than 10%. A microfabrication process, xurography, was used to produce the multiwell ImmunoChip. Assay reagents were dispensed and lyophilized in a three-layer pattern. The multiwell ImmunoChip prototype was used to detect and quantify AEDs in serum samples containing all three drugs. Luminescent signals generated from each well were recorded with a charge-coupled device (CCD) camera. The assays performed on an ImmunoChip were fast (5 min), requiring only small volumes of both the reagents (<1 μl/well) and the serum sample. The ImmunoChip assay platform described in this article may be well suited for therapeutic monitoring of drugs and metabolites at the point-of-care setting.

Keywords: Homogeneous immunoassay; CEDIA; Bioluminescence; ImmunoChip; Therapeutic drug monitoring; Antiepileptic drugs

The introduction of arrays of immobilized biological compounds in micro-sized spots on a substrate (microarrays) has played an important role in modern biology and medicine [1,2]. Microarrays offer several advantages over conventional analytical devices. They are small, their manufacture can be automated, and only relatively small volumes of sample and assay reagents are required. These features make it possible to miniaturize microarray sensors for application at the point-of-care (POC)[1] setting. The major advantage offered by microarrays is the parallel analysis of multiple analytes.

* Corresponding authors. Fax: +801 585 5361.
E-mail addresses: jarmila.janatova@utah.edu (J. Janatova), jandrade@utahsciencecenter.org (J.D. Andrade).

[1] *Abbreviations used:* POC, point-of-care; CEDIA, cloned enzyme donor immunoassay; AED, antiepileptic drug; VPA, valproic acid; CBZ, carbamazepine; PHT, phenytoin; FPIA, fluorescence polarization immunoassay; TDM, therapeutic drug monitoring; ED, enzyme donor; EA, enzyme acceptor; RT, room temperature; RLU, relative light units; CCD, charge-coupled device; CV, coefficient of variation; HPLC, high-performance liquid chromatography; CBZ-E, carbamazepine-10,11-epoxide; HPPH, 5-(4′-hydroxyphenyl)-5-phenylhydantoin.

0003-2697/$ - see front matter © 2007 Elsevier Inc. All rights reserved.
doi:10.1016/j.ab.2007.03.019

The development of a disposable and quantitative analytical device for the measurement of multiple analytes, such as metabolic markers of chronic diseases, therapeutic drugs, and their pharmacologically active metabolites, in small sample volumes has been under study in our laboratory for several years [3,4]. Such a device, designated as a ChemChip, could be used for the diagnosis and management of clinical conditions at POC and eventually in-home environments. To access analytes not readily measurable by enzyme-based reactions [3], our effort has been extended to the development of a ChemChip, based on an immunological principle, called an ImmunoChip.

Cloned enzyme donor immunoassay (CEDIA) [5], one of a few homogeneous immunoassays available, appeared to be suitable for application to an immunosensor because it uses the competitive binding assay principle without the need for separation steps. During the first phase of an ImmunoChip project, a one-step bioluminescence-based homogeneous immunoassay platform has been developed [6,7], using a CEDIA kit to detect the antiepileptic drug (AED) valproic acid (VPA) in an aqueous matrix, via a luciferin-based, highly sensitive substrate for β-galactosidase [8].

In this article, the optimized luminescence-based one-step CEDIA platform [7] was extended to provide detection and quantitation of three widely used AEDs in serum: VPA, carbamazepine (CBZ), and phenytoin (PHT). Results generated by CEDIA were compared with values obtained by another immunoassay format, fluorescence polarization immunoassay (FPIA) [9].

The main and final objective of the project has been to design and test an ImmunoChip prototype, employing the previously developed immunoassay platform [7], for the simultaneous therapeutic drug monitoring (TDM) of the three AEDs present in small serum sample volumes.

To prototype microstructures for the ImmunoChip, an immunoassay-based biosensor, a novel microfabrication method [10] called xurography, was employed. The one-step CEDIA procedure [7] and monoclonal antibodies specific to each AED were used to simultaneously detect and quantify specific target drugs in the multiwell ImmunoChips.

An immunosensor assay platform, developed and tested in this study with three AEDs, could be extended to other areas of TDM to provide POC monitoring of other therapeutic drugs, their active metabolites, and metabolic markers of chronic diseases.

Materials and methods

Reagents for the luminescence-based homogeneous immunoassay

The CEDIA reagents were a part of the CEDIA kits (Carbamazepine II, Phenytoin II, and Valproic Acid II kits) purchased from Microgenics (Fremont, CA, USA). Commercial R2 reagents were substituted by a special R2 reagent containing only AED–enzyme donor (ED) conjugate and no substrate. Both CEDIA reagents, R1 (anti-AED antibody, enzyme acceptor [EA]) and R2 (AED–ED conjugate), were stored at 4 °C. The Beta-Glo assay system (Promega, Madison, WI, USA) consists of two parts that are combined at the time of assay to form Beta-Glo reagent, which contains biolumigenic substrate. The Beta-Glo reagents were stored at −20 °C and thawed at room temperature (RT, ∼ 22 °C) immediately prior to assay.

Stock solutions of AEDs

CBZ stock solution (420 μg/ml) was prepared by dissolving carbamazepine (Sigma–Aldrich, St. Louis, MO, USA) in ethanol. PHT stock solution (630 μg/ml) was obtained by dissolving phenytoin (Sigma–Aldrich) with acetone. Valproate sodium (Depacon, 500 mg/ml) was diluted with 20 mM Hepes (pH 7.5) to obtain VPA stock solution (3150 μg/ml).

Preparation of AED solutions in normal serum

The stock solution of each of the three AEDs (see above) was diluted sequentially with drug-free serum to yield the final concentrations of each AED as follows (therapeutic range for each drug shown in parentheses): 2.5, 5.0, 10, 15, and 20 μg/ml for CBZ (5–12 μg/ml); 5, 10, 15, 20, and 30 μg/ml for PHT (10–20 μg/ml); and 25, 50, 75, 100, and 150 μg/ml for VPA (50–100 μg/ml). The final concentrations of ethanol and acetone in the final AED solutions were less than 1%.

Analyses of AEDs by one-step CEDIA in the presence of serum

Drug-free serum samples spiked with AEDs were analyzed using the following protocol: CEDIA reagents (R1 and R2), AED solutions, and Beta-Glo reagent were incubated separately in a water bath for 1 min at RT. Each AED solution (0.51 μl) was transferred into R1 (2.56 μl), and immediately R2 (1.93 μl) was added to the mixture of R1 and AED. Then the CEDIA reaction mixture (5 μl) was transferred to a polystyrene tube (12 × 55 mm, Elkay Products, Springfield, NJ, USA) containing freshly prepared Beta-Glo reagent solution (5 μl). Luminescent signal (relative light units [RLU]) was measured as a function of time at RT using a Luminometer TD 20/20 (Turner Designs, Sunnyvale, CA, USA) at a sensitivity setting of 40.2%. The concentrations of all three drugs (CBZ, PHT, and VPA) were measured individually using the procedure described above.

Determination of AED concentrations in serum samples by CEDIA and FPIA

Residual deidentified serum samples from patients, treated with one or more AEDs, were analyzed by the CEDIA procedure (described in the previous paragraph)

and FPIA. The latter was performed at ARUP (Associated and Regional University Pathologists) Laboratories, a Clinical Laboratory Improvement Amendments (CLIA)-certified clinical national reference laboratory (Salt Lake City, UT, USA), according to the manufacturer's instructions. The sources of the reagents for FPIA were as follows: CBZ and VPA (Abbott Laboratories, Abbott Park, IL, USA) and PHT (Seradyn, Indianapolis, IN, USA).

ImmunoChip fabrication

A new rapid prototyping method [10] was used to produce the multi-AED ImmunoChip. A Graphtec FC5100A-75 knife plotter (Graphtec, Santa Ana, CA, USA) was used to cut ImmunoChip patterns (Fig. 1A) in a 180-μm thick adhesive-backed vinyl film (Scotchlite Plus Reflective 680 series, 3 M, St. Paul, MN, USA). The holes were "weeded out" with tweezers, and the "perforated" vinyl film was then transferred to 15-mm square glass cover slips (VWR, West Chester, PA, USA), which were 150 μm thick and became the clear bottom for the 1-μl wells. This prototype of an ImmunoChip consists of 3×3 arrays of 2.5-mm diameter holes spaced 2.0 mm apart.

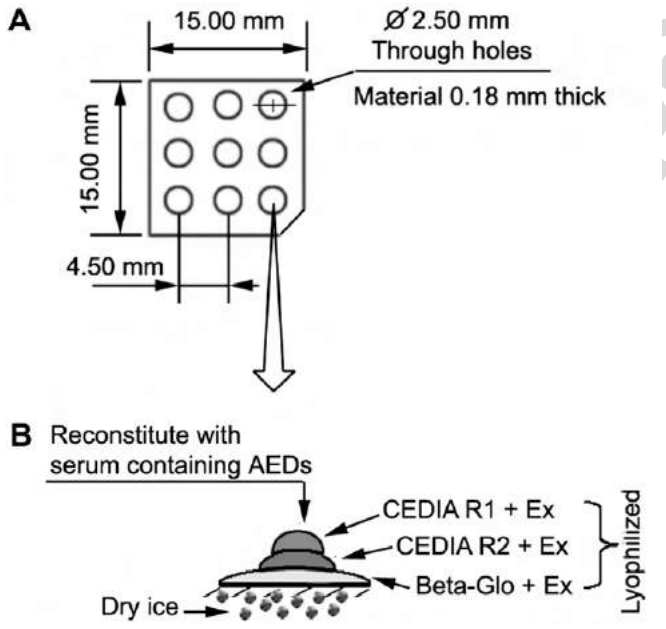

Fig. 1. ImmunoChip design and dispensing of the assay reagents. (A) A 3×3 multiwell ImmunoChip setup and dimensions. (B) Dry ice was placed under the platform (XYZ stage), supporting a number of ImmunoChips, to achieve freezing of the assay reagents as soon as they were dispensed. In each well, the assay's reagents were dispensed in the following order (from bottom to top): (i) Beta-Glo solution with excipients (Ex) (500 nl); (ii) R2, containing AED–ED conjugate and Ex (188 nl); and (iii) R1, consisting of anti-AED antibody and EA and Ex (250 nl). The reagents specific to the three AEDs were dispensed in individual rows (VPA, PHT, and CBZ) in triplicate. ED and EA are two genetically engineered fragments of β-galactosidase that are essential for the CEDIA reaction.

Reagent dispensing and lyophilization

Individual ImmunoChip wells were filled with assay constituents via a computer-controlled XYZ stage with a syringe pump and solenoid dispensing system [11]. To aspirate and dispense multiple reagents, six VHS-M/2 solenoid valves (Lee, Westbrook, CT, USA) were purchased and connected to a computer-controlled syringe pump (P/N 0162573 PSD/2, Hamilton, Reno, NV, USA) fitted with an eight-distribution port valve (P/N 0200018, Hamilton) and a 500-μl syringe (P/N 81247, Hamilton). A LabVIEW program (National Instruments, Austin, TX, USA) was used to control the XYZ stage moving via the computer's serial COM port. The six dispensers were attached to a vertical stepper motor translation stage (VT-80-25-2SM, Phytron, Williston, VT, USA). A dispensing platform that was to hold the ImmunoChips was attached to an XY horizontal stepper motor translation stage (VT-80-150-2SM, Phytron).

To prevent evaporation during dispensing and mixing of the constituents of one-step CEDIA procedure before lyophilization, dry ice was placed under the platform, holding ImmunoChips (Fig. 1B), to freeze a layer of each reagent as soon as it was dispensed. Reagents were delivered into the individual wells and frozen in separate layers sequentially (from the bottom to the top): (i) Beta-Glo solution (500 nl) containing excipients (100 mM sucrose + 50 mM glycine + 10 mM GSH), (ii) R2 (188 nl) with excipients (100 mM sucrose + 50 mM glycine), and (iii) R1 (250 nl) with excipients (100 mM sucrose + 50 mM glycine).

After dispensing, the ImmunoChips with frozen layers of the reagents were placed in the sample chamber of a VirTis Genesis 12 pilot plant lyophilizer (SP Industries, Gardiner, NY, USA) at a shelf temperature of −50 °C. Primary lyophilization was performed in a vacuum at less than 100 mTorr with the condenser chamber cooled to −70 °C for 24 h. The temperature of the shelf chamber was then increased in 25 °C increments every 12 h until it reached 22 °C for the secondary lyophilization stage, which lasted 12 to 24 h.

Sample analysis and ImmunoChip imaging

Serum sample (25 μl) containing all three AEDs was dispensed on the center of the nitrocellulose filter paper (Whatman, Middlesex, UK), which was placed above the wells of the array. Serum sample, applied to the middle, wicked along and through the filter paper and into each well, dissolving the reagents and initiating the CEDIA and bioluminescent reactions.

The bottoms of the ImmunoChips were viewed by placing them on a window above a close-up macro camera lens, which collected the luminescent signals from the individual wells and projected them onto an Andor iXon DV 885 charge-coupled device (CCD, Andor, Belfast, Northern Ireland). The signals were recorded in a

light-tight imaging environment. The luminescent signal for each assay was recorded during a 5-min exposure (CCD temperature = −40 °C, binning = 4 × 4 pixels). Images were analyzed with ImageJ (http://rsb.info.nih.gov/ij) and MatLab (MathWorks, Natick, MA, USA) systems to subtract background noise and integrate the CCD counts across the area of each well for each exposure.

Results and discussion

Performance of one-step CEDIA platform to measure AEDs in serum

Numerous methods have been used to detect and quantify VPA, CBZ, and PHT in serum. These include spectrophotometry [12], gas chromatography [13], high-performance liquid chromatography (HPLC) [14], radioimmunoassay [15], enzyme-linked immunoassay [16], fluorescence polarization immunoassay [9], and tandem liquid chromatography–mass spectrometry [17]. The widespread use of these AEDs as mono- or combined therapy in the management of different seizure types, in combination with well-established therapeutic ranges [18], resulted in a high demand for rapid quantitation of drug concentrations in serum.

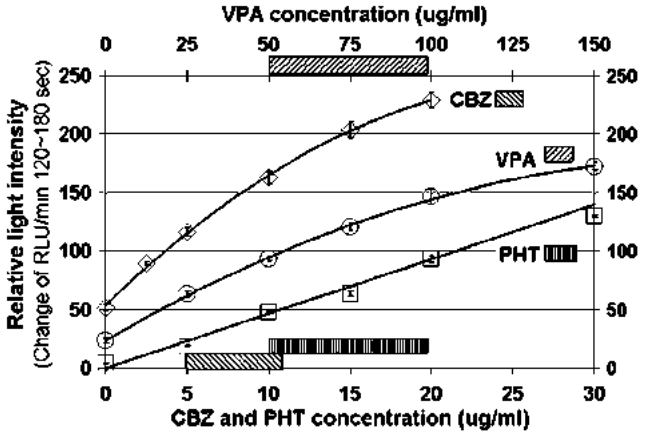

Fig. 2. Determination of VPA, CBZ, and PHT concentrations, in the presence of serum, by one-step CEDIA with Beta-Glo assay system. In this set of experiments, drug-free normal serum was spiked with VPA, CBZ, or PHT as described in Materials and methods. Calibration curves represent slopes of kinetic curves (120–180 s) as a function of AED initial concentration. Crossed bars designate therapeutic ranges of the respective AEDs. Data are based on four replications for each concentration of respective drugs measured (mean ± SD). CBZ (open diamonds) and PHT (open squares) employ the lower x axis, whereas VPA (open circles) uses the upper x axis.

The luminescence-based one-step CEDIA platform [7] provides a sensitive, simple, and relatively fast technique for detection and quantitation of CBZ, PHT, and VPA in the presence of serum. Data generated with increasing concentrations of each drug are shown in Fig. 2 and illustrate how the respective calibration curves may look using this technique. The intra- and interassay imprecision data for measurement of the three AEDs using this one-step CEDIA procedure are summarized in Table 1. Intraassay imprecision was determined by assaying serum samples at six different concentrations of each drug five times in a single day. To define interassay imprecision, serum samples at six different concentrations of each drug were measured on 5 different days over a 2-week period. The highest calculated coefficients of variation (CVs) of intra- and interassay measured in serum samples were 6.9 and 9.3% for CBZ, 5.3 and 9.6% for PHT, and 5.6 and 9.2% for VPA, respectively.

Assays demonstrating intraassay imprecision of 5 to 10% are acceptable for clinical use, according to the Clinical and Laboratory Standards Institute (CLSI) protocols.

Evaluation of luminescence-based one-step CEDIA procedure

Using residual deidentified patient specimens, the results generated with the optimized one-step CEDIA platform were compared with data obtained by FPIA. Results were generated for 10 samples for CBZ and 12 samples for PHT and VPA. Each sample was divided into five aliquots. Every aliquot was tested five times in a single day. Five

Table 1
Intra- and interassay imprecision data from measurements of CBZ, PHT, and VPA by one-step CEDIA in the presence of normal human serum

CBZ			PHT			VPA		
Concentration (μg/ml)	Intraassay CV (%)	Interassay CV (%)	Concentration (μg/ml)	Intraassay CV (%)	Interassay CV (%)	Concentration (μg/ml)	Intraassay CV (%)	Interassay CV (%)
0	5.7	9.3	0	4.5	7.3	0	5.6	5.3
2.5	6.9	5.7	5	4.1	2.4	25	4.3	9.2
5	2.9	6.6	10	1.5	9.6	50	1.7	4.1
10	2.6	1.2	15	3.3	3.1	75	3.0	2.3
15	3.4	8.6	20	5.3	8.6	100	2.1	2.4
20	2.9	4.2	30	1.7	7.2	150	2.9	1.4

Note. Normal serum, on day 0, was spiked with either CBZ, PHT, or VPA stock solution to reach the final concentrations of 0, 2.5, 5.0, 10, 15, and 20 μg/ml for CBZ; 0, 5.0, 10, 15, 20, and 30 μg/ml for PHT; and 0, 25, 50, 75, 100, and 150 μg/ml for VPA. The aliquots of the individual samples, each containing the respective drug at the given concentration, were tested five times in a single day on 6 nonconsecutive days within a 2-week period. $n = 120$ for all three AEDs.

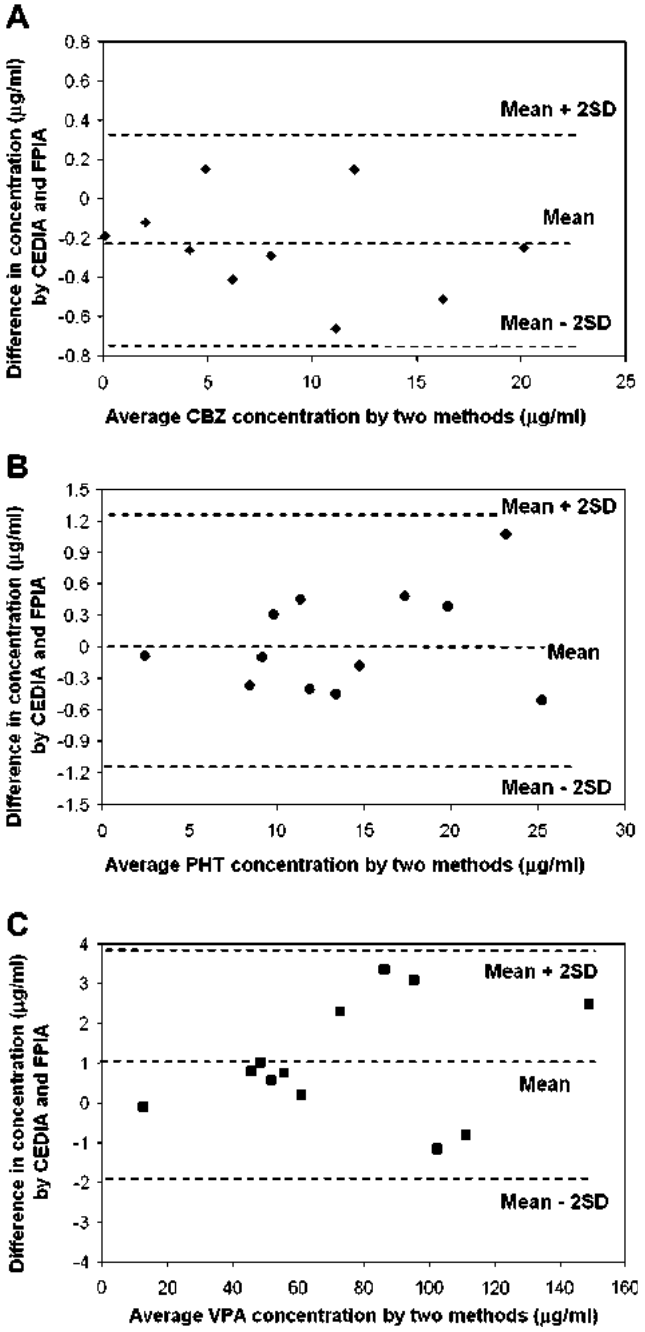

Fig. 3. Difference between the data obtained by one-step CEDIA and FPIA against their means for CBZ (A), PHT (B), and VPA (C). The residual deidentified patients' specimens were analyzed by both the one-step CEDIA procedure and FPIA. The results were evaluated using the Bland–Altman approach [19].

aliquots from the same sample were tested on different days over a 2-week period. Total numbers of tested points were 300 for CBZ (10 samples, five replicates each day, run on 6 days) and 360 each for PHT and VPA.

The Bland–Altman approach [19], based on graphical techniques and simple calculations, was used to describe the correlation of the data obtained by one-step CEDIA and FPIA for measurement of CBZ (Fig. 3A), PHT (Fig. 3B), and VPA (Fig. 3C). Agreement of the values obtained by the two methods can be summarized by calculating the bias, estimated by the mean difference (d) and the standard deviation of the difference (s). If there is no consistent bias, most of the differences are expected to lie between $d - 2s$ and $d + 2s$ and follow a normal distribution. According to these criteria, the results depicted in Fig. 3 demonstrate that the data obtained for the three AEDs by one-step CEDIA agree well with those measured by FPIA.

Specificity of one-step CEDIA for measuring CBZ and PHT

Active metabolites of CBZ and PHT were specifically considered to evaluate the potential for positive bias in results due to the well-recognized potential of these metabolites to cross-react with detection antibodies in immunoassays. Carbamazepine-10,11-epoxide (CBZ-E) is the active metabolite of CBZ, with both having similar structures. Specificity of the one-step CEDIA for measuring CBZ was tested with patient serum specimens containing CBZ and CBZ-E (Table 2). Our results indicate that when the CBZ-E concentration is greater than 10 μg/ml, its cross-reactivity is evident and total CBZ concentrations increase. However, the assay has low cross-reactivity to CBZ-E when this metabolite is present in low concentrations (CBZ-E < 5 μg/ml). Accumulation of CBZ-E is patient specific, so significantly accumulated levels of CBZ-E greater than 5 μg/ml may falsely influence the CBZ results and should be viewed with caution. The main metabolite of PHT, 5-(4′-hydroxyphenyl)-5-phenylhydantoin (HPPH), exhibits a 5% cross-reactivity at its concentration of 500 μg/ml in the CEDIA Phenytoin II assay, as tested at Microgenics. Further evaluation of the specificity and accuracy of the ImmnoChip will require comparison of this method with a chromatographic and/or mass spectrometric methodology.

Simultaneous detection of multiple AEDs using multiwell ImmunoChip

On demonstrating that the one-step CEDIA procedure (i) could quantitatively detect individual AEDs in serum samples (Fig. 2) and (ii) correlates well with a comparison method (Fig. 3), we then investigated the detection of multiple AEDs present in the same serum sample using a multianalyte multiwell ImmunoChip (Fig. 4). Within each row of the three wells (rows from top to bottom in Fig. 1A: (i) VPA, (ii) PHT, and (iii) CBZ), assay reagents specific to a

Table 2
Cross-reactivity detected by one-step CEDIA in patient serum sample during measurement of CBZ in presence of CBZ-E

CBZ (μg/ml)	5	5	5	9	9	9	16	16	16
CBZ-E (μg/ml)	5	10	20	5	10	20	5	10	20
Cross-reactivity (%)[a]	2	12	21	3	8	13	2	4	5

[a] Cross-reactivity (%) = {value of ([CBZ] + [CBZ-E]) − value of [CBZ]}/value of [CBZ] × 100%.

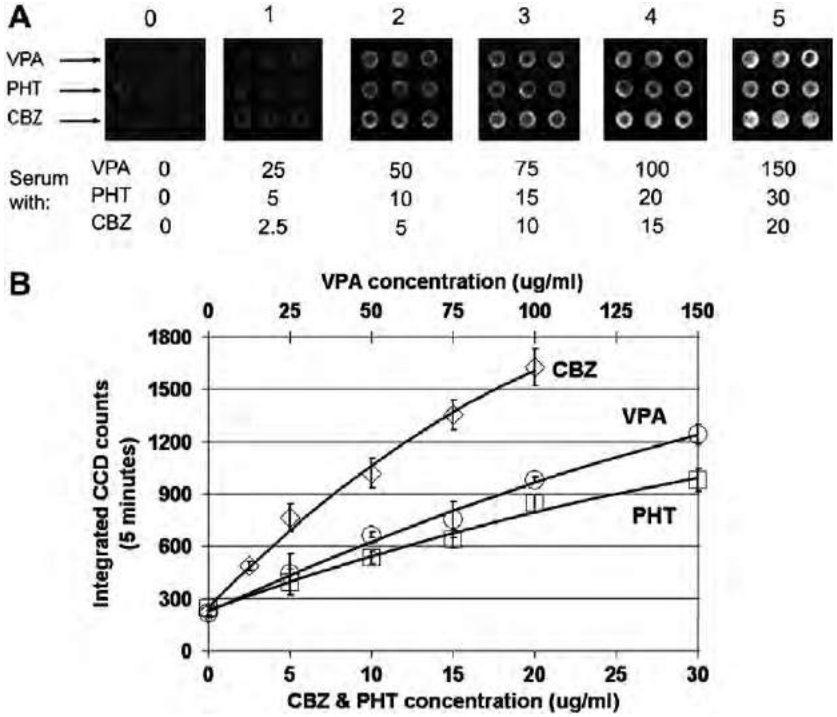

Fig. 4. Simultaneous detection of three AEDs using multiwell ImmunoChips. Serum samples, used in testing the performance of ImmunoChip, were prepared from a drug-free normal serum, to which a mixture of VPA, CBZ, and PHT was added at the concentrations (μg/ml) listed in the table below the CCD images of ImmunoChips. (A) CCD images for VPA, PHT, and CBZ assay performed on ImmunoChips. Serum containing different concentrations of the three AEDs rehydrated the lyophilized reagents (Fig. 1B) in each well and initiated CEDIA and bioluminescence reactions, resulting in luminescent signal. (B) Calibration curves represent integrated CCD counts from 5-min exposures as a function of AED concentrations. CBZ (open diamonds) and PHT (open squares) employ the lower x axis, whereas VPA (open circles) uses the upper x axis.

particular drug were dispensed, as illustrated in Fig. 1B, and lyophilized, as described in Materials and methods.

Serum samples were assayed in triplicate for the presence of the three AEDs using an ImmunoChip. The luminescence patterns that resulted when serum samples containing a mixture of the three AEDs were dispensed over the ImmunoChip through a bonded nitrocellulose filter paper are presented in Fig. 4A. The concentrations (μg/ml) of respective AED in serum samples are listed in the table below each ImmunoChip.

As illustrated in Fig. 4A, assays of AEDs on each ImmunoChip produced different luminescent signal intensities at the appropriate site where particular capture antibodies were dispensed. A comparison of six ImmunoChips (from left to right in Fig. 4A) reveals that the light intensity in each well increases with higher concentrations of the respective drug tested. The calibration curves presented in Fig. 4B demonstrate the feasibility of detection and quantitation of the three AEDs simultaneously in a multi-AED ImmunoChip.

Performance of ImmunoChip prototype

The current study fulfilled one of our major goals. It demonstrated the feasibility to build a multianalyte multiwell immunosensor intended for the TDM at the POC setting. As with each prototype, there were still some limitations identified. Unlike a one-step CEDIA in the fluid phase, an ImmunoChip prototype has had a relatively large CV between different batches. This appears to be due at least partly to the small reagent volumes used in this prototype given that the assay reagents are unlikely to coat each well uniformly and insufficient wetting of the sides may concentrate reagents in that area. This could also contribute to the inhomogeneous signal detected in each well (Fig. 4A). There also may be variations, from batch to batch, with respect to a starting point of the CEDIA and bioluminescent reactions that is assumed to be at the end of the rehydration of lyophilized assay reagents with serum samples. Under the experimental settings used in this study, there was a lapse of approximately 30 s between dispensing serum sample and starting signal recording by CCD camera. The time required for reconstitution, however, depends on the condition of lyophilized reagents such as the shape, homogeneous form, or excipient types and their concentrations used. Taking these factors into consideration, the starting point of reaction taking place in different wells of the same ImmunoChip or wells on different ImmunoChips may have variations, resulting in relatively larger differences of the signal values. To further improve its utility, the ImmunoChip developed and used in this study requires further optimization and testing before it could be made more widely available.

Conclusions

The purpose of this study was to use array technology to make an ImmunoChip for the rapid and simultaneous analysis of multiple AEDs. The luminescence-based one-step CEDIA procedure [7], which serves as the ImmunoChip platform, requires no separation steps, consumes small quantities of reagents and samples, and has a short analysis time with easy handling. This platform provides a precise and relatively fast technique for detection and quantitation of CBZ, PHT, and VPA in serum samples simultaneously. The total analysis time for each serum sample was 30 s for the sample dispensing and 5 min for an exposure to the CCD camera. For each serum sample, three AEDs could be measured in triplicate on one ImmunoChip. CEDIA results, generated using residual patient specimens, correlated well with values obtained by FPIA. In light of the demand for diagnostic assays that can be carried out in small laboratories, doctors' offices, and POC settings, the ImmunoChip opens the door to miniaturized biodiagnostics.

This work has detailed several novel points related to current microarray assays. First, this is one of the first studies to describe the use of a microarray platform to achieve the simultaneous detection of AEDs in serum. Second, the rapid nature of the assay system offers considerable advantages over conventional microarrays that require long incubation times and washing steps. Finally, microfabrication using xurography and noncontact dispensers has the capacity to produce arrays of drugs in small spots. This microfabrication method showed great potential for rapidly prototyping microstructures to perform accurate sample delivery and reagent mixing. In addition, its short processing time and low-cost material requirement make it feasible for high-throughput automated fabrication. This multianalyte ImmunoChip has broad implications for a wide range of substances such as other therapeutic drugs, drugs of abuse, peptide hormones, and metabolic markers of chronic diseases.

Acknowledgments

We thank Rueyming Loor (Microgenics) for providing a special CEDIA R2 reagent without substrate. We also thank Daniel Bartholomeusz for skillful assistance with ImmunoChip fabrication and reagent dispensing system, Steven E. Kern for provision of samples of normal plasma and serum, and Carl T. Wittwer and Scott Sundberg for assistance with the Andor CCD camera. This work was supported by National Institutes of Health (NIH) grant RR17329. Preliminary accounts of this work were presented at the American Association for Clinical Chemistry (AACC) 38th Annual Oak Ridge Conference, April 2006 (San Jose, CA, USA), and the American Chemical Society (ACS) 61st Northwest Regional Meeting, Bioorganic Chemistry and Biosensors I, June 2006 (Reno, NV, USA). This article represents part of Xiaoyun Yang's Ph.D. thesis, "Towards the Development of an ImmunoChip for Therapeutic Monitoring of Antiepileptic Drugs" (University of Utah, 2006).

Appendix A. Supplementary data

Supplementary data associated with this article can be found, in the online version, at doi:10.1016/j.ab.2007.03.019.

References

[1] A. Lueking, M. Horn, H. Eickhoff, K. Bussow, H. Lehrach, G. Walter, Protein microarrays for gene expression and antibody screening, Anal. Biochem. 270 (1999) 103–111.
[2] G. MacBeath, S.L. Schreiber, Printing proteins as microarrays for high-throughput function determination, Science 289 (2000) 1760–1763.
[3] R. Davies, D.A. Bartholomeusz, J.D. Andrade, Personal sensors for the diagnosis and management of metabolic disorders, IEEE Eng. Med. Biol. Mag. 22 (2003) 32–42.
[4] J.D. Andrade, D.A. Bartholomeusz, R. Davies, X. Yang, J. Janatova, Multi-analyte bioluminescence-based disposable ChemChips for home-based applications: Update, in: G.E. Cohn, W.S. Grundfest, D.A. Benaron, T. Vo-Dinh (Eds.), Advanced Biomedical and Clinical Diagnostic Systems IV, Proceedings of SPIE, vol. 6080, 2006, 60800W.
[5] D.R. Henderson, S.B. Friedman, J.D. Harris, W.B. Manning, M.A. Zoccoli, CEDIA, a new homogeneous immunoassay system, Clin. Chem. 32 (1986) 1637–1641.
[6] S.I. Jeon, X. Yang, J.D. Andrade, Modeling of homogeneous cloned enzyme donor immunoassay, Anal. Biochem. 333 (2004) 136–147.
[7] X. Yang, J. Janatova, J.D. Andrade, Homogeneous enzyme immunoassay modified for application to luminescence-based biosensors, Anal. Biochem. 336 (2005) 102–107.
[8] R. Geiger, E. Schneider, K. Wallenfels, W. Miska, A new ultrasensitive bioluminogenic enzyme substrate for β-galactosidase, Biol. Chem. Hoppe-Seyler 373 (1992) 1187–1191.
[9] L.S. Steijns, J. Bouw, J. van der Weide, Evaluation of fluorescence polarization assays for measuring valproic acid, phenytoin, carbamazepine, and phenobarbital in serum, Ther. Drug Monit. 24 (2002) 432–435.
[10] D.A. Bartholomeusz, R.W. Boutte, J.D. Andrade, Xurography: Rapid prototyping of micro-structures using a cutting plotter, IEEE J. Microelectromech. Syst. 14 (2005) 121–131.
[11] D.A. Bartholomeusz, Development of a bioluminescence-based multianalyte biosensor: Fabrication and instrumentation, Ph.D. thesis, University of Utah, 2006.
[12] W.A. Dill, A. Kazenko, L.M. Wolf, A.J. Glazko, Studies on 5,5-diphenylhydantoin (Dilantin) in animals and man, J. Pharmacol. Exp. Ther. 118 (1956) 270–279.
[13] H.J. Kupferberg, Quantitative estimation of diphenylhydantoin, primidone, and phenobarbital in plasma by gas–liquid chromatography, Clin. Chim. Acta 29 (1970) 282–288.
[14] K.M. Patil, S.L. Bodhankar, Simultaneous determination of lamotrigine, phenobarbitone, carbamazepine, and phenytoin in human serum by high-performance liquid chromatography, J. Pharm. Biomed. Anal. 39 (2005) 181–186.
[15] V. Spiehler, L. Sun, D.S. Miyada, S.G. Sarandis, E.R. Walwick, M.W. Klein, D.B. Jordan, B. Jessen, Radioimmunoassay, enzyme immunoassay, spectrophotometry, and gas–liquid chromatography compared for determination of phenobarbital and diphenylhydantoin, Clin. Chem. 22 (1976) 749–753.

[16] D.D. Schottelius, in: J.K. Penry, H. Kutt, C.E. Pippenger (Eds.), Antiepileptic Drugs: Quantitative Analysis and Interpretation, Raven, New York, 1978, pp. 95–108.
[17] H.H. Maurer, Liquid chromatography–mass spectrometry in forensic and clinical toxicology, Anal. Bioanal. Chem. 381 (2005) 110–118.
[18] C.B. Pugh, W.R. Garnett, Current issues in the treatment of epilepsy, Clin. Pharmacol. 10 (1991) 335–358.
[19] J.M. Bland, D.G. Altman, Statistical methods for assessing agreement between two methods of clinical measurement, Lancet 1 (1986) 307–310.

18) V. N. R. Pillai, *Synthesis* **1980**, 1
19) J. A. Barltrop, R. J. Plant, P. Schofield, *J. Chem. Soc. Chem. Commun.* **1966**, 822
20) D. H. Rich, S. K. Gurwara, *J. Chem. Soc. Chem. Commun.* **1973**, 610
21) V. N. R. Pillai, M. Mutter, E. Bayer, *Tetrahedron Lett.* **1979**, 3409
22) W. Stuber, B. Hemmasi, E. Bayer, *Int. J. Pept. Protein Res.* **22**, 277 (1983)
23) E. Bayer, M. Dengler, B. Hemmasi, *Int. J. Pept. Protein Res.* **25**, 178 (1978)
24) P. D. Senter, M. J. Tansey, J. M. Lambert, W. A. Blattler, *Photochem. Photobiol.* **42**, 231 (1985)
25) E. W. Voss, Jr., W. Eschenfeldt, R. T. Root, *Immunochemistry* **13**, 447 (1976)
26) A. H. Adelman, G. Oster, *J. Am. Chem. Soc.* **78**, 3977 (1956)
27) M. Koizumi, Y. Usui, *Mol. Photochem.* **4**, 57 (1972)
28) I. H. Leaver, in: *"Photochemistry of dyed and pigmented polymers"*, ed. by N. S. Allen, McKellar, Applied Science Publ., London 1980, p. 161
29) N. A. Evans, *J. Soc. Dyers Colour.* **86**, 174 (1970)
30) N. A. Evans, *J. Soc. Dyers Colour.* **89**, 332 (1973)
31) T. Watanabe, T. Takizawa, K. Honda, *J. Phys. Chem.* **81**, 1845 (1977)
32) G. Oster, *J. Polym. Sci.* **9**, 553 (1952)

Makromol. Chem. **190**, 69–82 (1989)

Optically controlled ligand delivery, 1

Synthesis of water-soluble copolymers containing photocleavable bonds

Hung-Ren Yen, Jindřich Kopeček, Joseph D. Andrade*

Departments of Material Science and Engineering, and Bioengineering, University of Utah, Salt Lake City, Utah 84112, USA

(Date of receipt: August 7, 1987)

SUMMARY:

To verify the possibility of developing a ligand delivery system which is controlled by light pulses, we synthesized copolymers of *N*-(2-hydroxypropyl)methacrylamide (**1**) containing side-chains terminated in ligands (Boc-Gly, fluorescein, tetramethylrhodamine) bound via photocleavable 2-nitrobenzyl groups. Copolymers in solution were exposed to light of wavelength ≈360 nm which resulted in release of the bound ligands. Depending on the experimental conditions (type of solvent, presence of oxygen) changes in the structure of released fluorochromes were observed (photofading effect). These effects were quantified by determining the binding constants of released modified fluorochromes with monoclonal antifluorescyl antibodies.

Introduction

The specificity of antibody (Ab)-antigen (Ag) interactions and competitive binding reactions using labelled Ag or labelled Ab have permitted the development of immunoassays with very high sensitivity and specificity. Such techniques can detect antigens and haptens at concentrations of 10^{-11} mol·l^{-1} in such complex solutions as blood and serum[1]. However, modern competitive binding immunoassay kits are totally unsuitable for continuous and/or remote measurements.

There is a possibility to use the competitive binding immunoassay principle in fiber optic and thin film wave guide sensors. In this series of papers an effort is made to use evanescent wave excitation and photochemically controlled delivery to develop truly remote, nearly continuous sensors. The development of such sensors requires a number of basic and applied science studies[2], including polymer synthesis and ligand delivery, modulation of Ag-Ab binding constants[3], antibody orientation and immobilization[4], non-specific binding and bio- or blood compatibility.

This communication is focused on one key part of the overall sensor problem: optically controlled release of ligands bound to side-chains of *N*-(2-hydroxypropyl)-methacrylamide (**1**) copolymers via photocleavable 2-nitrobenzyl bonds. Since the structure of copolymers of **1** is variable over a wide range and permits introduction of different reactive units into one polymeric chain[5], it is our strategy to attach these soluble copolymers to functionalized surfaces in the next step of our studies.

0025-116X/89/$03.00

In this first contribution copolymers of **1** containing side-chains terminated in model ligands (Boc-Gly, fluorescein, tetramethylrhodamine) bound via photocleavable 2-nitrobenzyl bonds were synthesized. Photochemical release of ligands induced by exposure to light (wavelength ≈360 nm) was studied and the influence of experimental conditions (type of solvent, presence of oxygen) on the amount of cleavage and change in the structure of released ligands was determined. To detect subtle changes in the structure of released fluorochromes, the association constant of released fluorescein derivatives with monoclonal antifluorescyl antibodies was determined and compared with the values of fluorescein isothiocyanate (**6a**) and the thiourea derivative of fluorescein (**7**).

The photocleavable copolymers were synthesized by a series of polymer analogous reactions starting with the polymeric precursor **3a**, which resulted from the copolymerization of **1** with *N*-methacryloylglycylglycine 4-nitrophenyl ester (**2**). By the reaction of **3a** with an excess of ethylenediamine, copolymer **3b** was obtained, which was transformed into **3c** by condensation with 4-bromomethyl-3-nitrobenzoic acid (**4**). Then, *N-tert*-butoxycarbonylglycine was condensed with **3c** to yield copolymer **3d** from which the *tert*-butoxycarbonyl group was removed and subsequently the resulting **3e** added to 3′, 6′-dihydroxy- or 3′,6′-dimethylaminospiro[phthalide-3,9′-xanthen]-6-yl isothiocyanate (**6a** or **6b**) (fluorescein- or tetramethylrhodamine isothiocyanate), leading to the final products **3f** or **3g**.

Experimental part

Chemicals: N-(2-hydroxypropyl)methacrylamide (**1**) was prepared as previously described[6] (m.p. 69–70 °C). *N*-Methacryloylglycylglycine 4-nitrophenyl ester (**2**) was prepared as described earlier[7] (m.p. 163–164 °C). 2,2′-Azoisobutyronitrile (AIBN) was recrystallized from ethanol. Dimethyl sulfoxide (DMSO) and dimethylformamide (DMF) were purified by distillation under reduced pressure. Other solvents used were freshly distilled. *N-tert*-Butoxycarbonylglycine (Boc-Gly), fluorescein isothiocyanate (**6a**) (from Sigma Chemical Company), and tetramethylrhodamine isothiocyanate (**6b**) (from Serva Company) were used without further purification.

4-Bromomethyl-3-nitrobenzoic acid (**4**): 4-Bromomethylbenzoic acid (11,8 g) was added in portions over 0,5 h to 100 ml of 90% HNO_3 (white, fuming) at −10 °C[8]. The suspension was stirred at −10 °C for an additional 2 h until the solution became clear orange. This solution was poured onto crushed ice. The product was collected by filtration and washed with ice-cold water until the washings were neutral. Drying i. vac. followed by crystallization twice from CH_2Cl_2/hexane gave a pure product; m.p. 134–135 °C. Yield: 7,5 g. (Lit.[8]: m.p. 125–126 °C).

UV: $\varepsilon_{226} = 2{,}23 \cdot 10^4\ l \cdot mol^{-1} \cdot cm^{-1}$ (in CH_3OH).

$C_8H_6BrNO_4$ (260,1)	Calc.	C 36,95	H 2,32	Br. 30,73	N 5,38
	Found	C 37,30	H 2,29	Br 30,8 ± 0,8	N 5,26

N-[3′,6′-Dihydroxyspiro[phthalide-3,9′-xanthen]-6-ylaminothiocarbonyl}glycine (**7**): **6a** (46,7 mg; $1{,}2 \cdot 10^{-4}$ mol) and glycine (45,4 mg; $6{,}0 \cdot 10^{-4}$ mol) were dissolved in 0,5 ml of tetrahydrofuran (THF) and 0,5 ml of distilled water, respectively. The solution of **6a** was slowly dropped into the glycine/water solution with stirring. The pH value of the whole mixture was adjusted to 8,5 by addition of $NaHCO_3$ solution (pH 9). After 24 h at room temperature, the reaction mixture was acidified to pH 3 by addition of 1 N HCl. Solvents were removed on a rotatory evaporator. The rest was dissolved in THF, and a small portion of undissolved

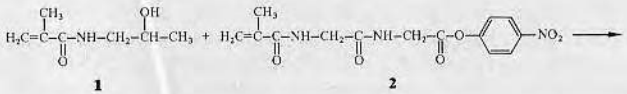

1 **2**

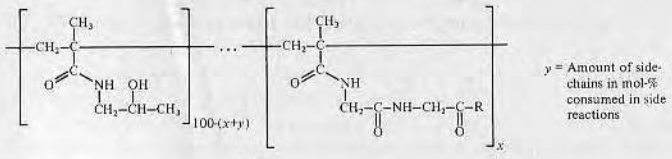

3

	R	x	y
3a	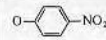	5,2	–
b	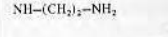	3,9	1,3
c	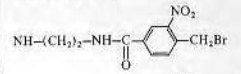	3,7	1,5
d	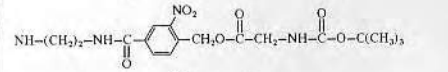	2,6	2,6
e	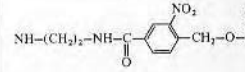	2,6	2,6
f	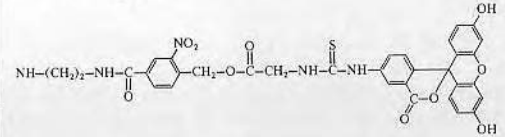	0,9	4,3
g	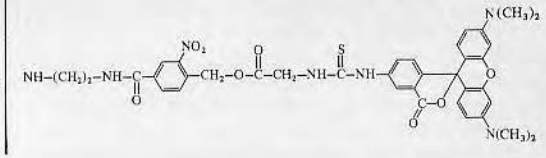	0,6	4,6

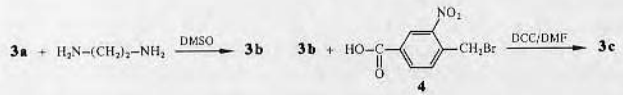

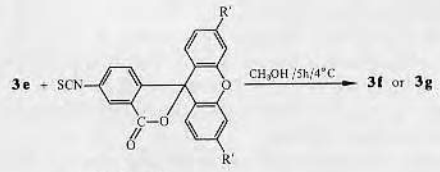

6a: R′ = OH
b: R′ = $N(CH_3)_2$

materials was filtered off. THF was removed under reduced pressure, the rest dissolved in water saturated with ethyl methyl ketone and applied onto a silica gel column (50 × 1,9 cm; eluent: water saturated with ethyl methyl ketone) and the corresponding fraction collected. The product was pure as evaluated by thin-layer chromatography (Silica gel 60 F_{254} from EM Laboratories, Inc.) in water saturated with ethyl methyl ketone (R_F = 0,25).

Antibodies: Monoclonal antifluorescyl antibodies[9] (clone 4-4-20) were a kind gift of Dr. J. Herron and Dr. E. W. Voss, Jr.

Copolymerization: Copolymer **3a** was prepared by radical precipitation copolymerization of **1** with **2** (mole ratio 95:5) in acetone (12,5 wt.-% of monomers: 0,6 wt.-% of AIBN as initiator[10]). The mixture of monomers was poured into a glass ampoule and flushed for 20 min with nitrogen to remove the dissolved oxygen. The ampoule was sealed and copolymerization proceeded at 50 °C for 24 h. The polymer was filtered, washed with a large amount of acetone, then with diethyl ether and dried under reduced pressure. The copolymer was dissolved in methanol and reprecipitated by dropping into a twentyfold excess of acetone, filtered, washed and dried. The content of monomeric units of **2** in copolymer **3a** was calculated to be 5,2 mol-% using the absorption of the nitrophenoxy (ONp) groups (*p*-nitrophenoxy: λ_{max} = 274 nm; ε = 9500 l · mol^{-1} · cm^{-1} in DMSO). Since the λ_{max} of the ONp groups in the monomer and copolymer remained unchanged, it was assumed[7] that the absorption coefficients of the monomer and the monomeric units in the copolymer are identical (the same assumption was made in analyzing the structure of other copolymers). The weight- and number-average molecular weights of copolymer ($\bar{M}_w$ = 27000 $\bar{M}_w/\bar{M}_n$ = 1,3) were estimated (after aminolysis with 1-amino-2-propanol) from the GPC analysis[11] on a Sepharose 4B/6B (1:1) column (90 × 1,6 cm) calibrated with fractions of poly(**1**) (buffer: 0,5 M NaCl + 0,05 M TRIS; pH 7,5).

Polymeranalogous reactions

Synthesis of **3b**: It was synthesized by the reaction of copolymer **3a** (5,2 mol-% of monomeric units of **2**) with an excess of ethylenediamine[12]. Copolymer **3a** (11,3 g, containing 3,9 · 10^{-3} mol of ONp groups) was dissolved in DMSO (120 ml). Ethylenediamine (52 ml; 0,78 mol) was dissolved in 330 ml of DMSO. The solution of copolymer **3a** was dropped slowly into the ethylenediamine solution with vigorous stirring. The reaction was allowed to continue 4 h at room temperature. The reaction mixture was then concentrated to approximately one half of the original volume under reduced pressure and precipitated in an excess of acetone. The copolymer was filtered, washed with acetone, dried and reprecipitated from a DMSO solution into an excess of acetone. Yield: 9,87 g of **3b**, containing 3,9 mol-% of side-chains terminated in NH_2 groups, as determined by reaction with **2** (conversion of Gly-Gly-ONp side-chains: 75%). No change in molecular weight distribution was observed (compared to copolymer **3a**), indicating that the intermolecular crosslinking reaction was negligible.

Synthesis of **3c**: Copolymer **3b** (8,5 g, containing ≈2,3 · 10^{-3} mol of NH_2 groups) was dissolved in 100 ml of DMF. 4-Bromomethyl-3-nitrobenzoic acid (**4**) (2,23 g; 8,58 · 10^{-3} mol) and dicyclohexylcarbodiimide (DCC) (1,77 g; 8,58 · 10^{-3} mol) were dissolved in DMF (105 ml), and the solution was cooled to −10 °C. To the latter the solution of copolymer **3b** was dropped with stirring. The reaction proceeded for 4 h at −10 °C and at 4 °C overnight. Then, the reaction was continued while stirring at room temperature for 24 h. The dicyclohexylurea (DCU) formed was filtered off. The reaction solution was concentrated to one half of its original volume under reduced pressure, a few drops of acetic acid were added to inactivate any remaining DCC and the reaction mixture was refrigerated overnight. The DCU formed was again filtered off and the concentration of the copolymer solution was adjusted and the copolymer precipitated into an excess of acetone. Yield of crude product: 6,8 g. It was twice reprecipitated from methanolic solution into acetone. The copolymer **3c** contains 0,2 mol-% of side-chains terminated in NH_2 groups, i.e. 3,7 mol-% of side-chains are terminated in 4-bromomethyl-3-nitro benzoyl residues (conversion of side-chains: 95%).

Synthesis of **3d**: Copolymer **3d** was synthesized by reaction of copolymer **3c** with Boc-Gly[13]. Copolymer **3c** (1,78 g, containing approximately 4,2 · 10^{-4} mol of side chains terminated in CH_2Br groups) was added to an ethyl acetate (62 ml) solution of Boc-Gly (0,60 g, 3,43 · 10^{-3} mol). To this mixture *N,N*-diisopropylethylamine (0,60 ml; 3,43 · 10^{-3} mol) was added slowly. The whole reaction mixture (suspension) was gently boiled. After reacting 4 days, the suspension was filtered, washed with acetone, and dried under vacuum. The crude product was dissolved in ethanol (12 wt.-% solution) and precipitated into an excess of acetone, filtered, washed and dried under reduced pressure. Yield: 1,54 g. The amount of side-chains terminated in Boc-Gly units (2,6 mol-%) was estimated from the analysis of copolymer **3e**. The conditions used for the removal of Boc protecting groups[13] justify the assumption that all Boc groups were removed. Conversion of side-chains based on this assumption was 70%.

Synthesis of **3e**: Copolymer **3d** (0,50 g) was dissolved in 7 ml of 30 wt.-% HCl/MeOH. After 1 h stirring, the copolymer solution was precipitated into acetone. The copolymer was dissolved in distilled water (5 wt.-% solution), and pH was adjusted to 10 by addition of 1 N NaOH. This solution was dialysed overnight in Visking dialysis tubing against water. The copolymer (0,26 g) was isolated by evaporating the water on a rotary evaporator and reprecipitated from methanolic solution into an excess of acetone. The copolymer contained 2,8 mol-% of side-chains terminated in NH_2 groups, as determined by reaction with **2**. Since 0,2 mol-% of NH_2 groups were present in copolymer **3c**, copolymer **3e** contains 2,6 mol-% of side-chains terminated in glycine residues. Thus, 50% of Gly-Gly-ONp side-chains (copolymer **3a**) were transferred into glycine terminated side-chains.

Synthesis of **3f**: Copolymer **3e** (58,65 mg, containing approximately 1,0 · 10^{-5} mol of NH_2 groups) was dissolved in methanol (1,5 ml) and cooled to 4 °C. To this mixture 4 ml of a solution of **6a** (9,26 mg; 2,3 · 10^{-5} mol) in methanol, precooled to 4 °C, was added slowly with stirring. After reacting 5 h at 4 °C, copolymer **3f** was isolated by gel filtration on Sephadex LH-20 columns (1 × 40 cm; eluent: methanol). The content of side-chains terminated in the fluorochrome (0,9 mol-%) was determined by UV spectrophotometry using the absorption coefficient of **6a** (ε_{494} = 6,8 · 10^4 l · mol^{-1} · cm^{-1}, in potassium phosphate, buffer pH 8). The conversion of the glycine side-chains was 34,6% (i.e. 17,3% based on copolymer **3a**).

To estimate the possibility of the reaction of **6a** with secondary OH groups of the copolymer, poly[*N*-(2-hydroxypropyl)methacrylamide] was incubated with **6a** under the same conditions as above. No binding of **6a** to the polymeric chain was observed as determined by GPC analysis on Sephadex LH-20 columns and UV spectrometry of the polymer fraction.

Synthesis of **3g**: Copolymer **3g** was prepared by reaction of copolymer **3e** with **6b**, using a procedure analogous to the preparation of copolymer **3f**. The mole ratio of NH_2 groups in copolymer **3e** (49,18 mg, containing approximately 8,4 · 10^{-6} mol) to **6b** (4,23 mg; 9,5 · 10^{-6} mol) was 1:1,1. The content of side-chains terminated in the fluorochrome (0,6 mol-%) was determined similarly as for copolymer **3f**. (**6b**: ε_{542} = 2,65 · 10^4 l · mol^{-1} · cm^{-1}, in methanol containing 0,02 vol.-% of DMSO). The conversion of the glycine side-chains was 23% (i.e. 11,5% based on copolymer **3a**).

Analysis of copolymers containing free NH_2 groups

The copolymers were analyzed[7] using reaction with **2**. The respective amount (1 − 2 mg) of the copolymer was dissolved in 0,5 ml of DMSO and mixed with 3 ml of a DMSO solution containing 4 − 6 · 10^{-7} mol of **2**. The reaction was followed spectrophotometrically at 274 nm with a Beckman Model 35 spectrophotometer. After constant absorption was reached, the content of the NH_2 groups in the copolymers was calculated from the conversion of **2**.

Photocleavage

Cleavage of Boc-Gly from copolymer **3d**: The copolymer was dissolved in methanol to form a 1 wt.-% solution and then de-aerated with nitrogen for 30 min. The copolymer solution was irradiated in a quartz cuvette (d = 1 cm) with a LH 150 mercury lamp (Schoeffel Instr. Co.) with max emission at 360 nm for various time periods at room temperature (intensity: 8 mW/cm^2; between lamp and the sample a lens was placed for focusing). After irradiation, 0,17 ml of samples of the reaction mixture were mixed with 0,15 ml of 30 wt.-% HCl/MeOH to remove the Boc-protecting groups from both the released Boc-Gly and the uncleaved side-

chains in copolymer **3d**. After 70 min, approx. 0,2 ml of 5 N NaOH were added to neutralize the mixture. After that the solution was diluted with 0,2 M citrate buffer (pH 5) to a final volume of 1,3 ml. 1 ml of the latter was applied on a Sephadex G-25 column (1 × 42 cm; eluent: citrate buffer), and the high-molecular-weight fraction was collected. The ninhydrin method[14] was used to detect the amount of side-chains terminated in NH_2 groups in this fraction (analysis was done in triplicate). For calibration, both Gly and Boc-Gly were used and gave the same results. The decrease of concentration of NH_2 groups in the copolymer reflected the amount of Boc-Gly released. The structure of Boc-Gly released was qualitatively verified by TLC (Silica gel 60 F254 from EM Laboratories, Inc.) using 1-butanol/acetic acid/water (vol. ratio 3:1:1)[15].

Cleavage of **6a** *and* **6b** *from copolymers* **3f** *and* **3g**, *respectively:* The respective copolymer was dissolved in methanol or distilled water (1 wt.-% solution) and introduced to Pyrex glass ampoules. Two ways of removing dissolved oxygen were used: 1) Bubbling with nitrogen for 60 min, 2) removing oxygen by the freezing-thawing technique. After freezing in liquid nitrogen, the solution was deaerated for 30 min at 10^{-3} mbar. After that the ampoules were flushed with nitrogen and thawed. This procedure was repeated three times. At the last cycle, the ampoules were sealed under vacuo. The solution was then irradiated with a LH 150 mercury lamp (Schoeffel Instr. Co.) at room temperature. After irradiation, the solutions were separated as follows:

Copolymer **3f**: Solutions in methanol were separated on a Sephadex LH-20 column (1 × 40 cm, eluent methanol). Aqueous solutions were separated on a Sephadex G-25 column (1 × 46 cm, eluent water).

Copolymer **3g**: Solutions in methanol were applied directly on a Sephadex LH-20 column (1 × 40 cm; eluent: methanol). Aqueous solutions were evaporated under reduced pressure to dryness, the rest dissolved in methanol and applied on the LH-20 column.

In all cases the high- and low-molecular-weight fractions were collected and analyzed by UV spectrophotometry and the released fluorochrome cleaved from copolymer **3f** characterized by determining its association constant with the monoclonal antifluorescyl antibody.

Determination of antibody (Ab) binding properties of cleaved fluorochromes

The equilibrium association constants (K_a) of monoclonal antifluoresyl antibodies (clone 4-4-20) with fluorescein, thiourea **7** (both synthetic and obtained by photocleavage from copolymer **3f**), were determined using the equilibrium fluorescence quenching assay[16, 17]. The physical basis for this assay is that fluorescence quantum yield of free fluorescein is substantially reduced when specifically bound to antifluorescyl antibody and, therefore, the concentrations of free and bound fluorophores can be determined by monitoring the decrease in fluorescence emission.

Fluorescence measurements of equilibrium fluorescent hapten-antibody interaction were obtained using a spectrofluorimeter equipped with an Ar ion laser (Lexel, Palo Alto, California; model 95). Temperature was regulated with a constant temperature bath that circulated through the fluorometer cuvette chamber. **6a**: excitation 488 nm; emission 530 nm; $[Ab] = 10^{9}$ mol · l^{-1}.

It holds, that

$$K_a = [AbAg]/[Ab][Ag]$$

where K_a is the equilibrium association constant (Ag: antigen).

The fraction of ligand bound (f_b) by antibody was calculated from[16, 17]

$$f_b = Q/Q_{max}$$

where Q and Q_{max} are the fluorescence quenching value and maximum quenching constant, respectively.

The fluorescence quenching value (Q) was determined from fluorescence measurements using the following equation

$$Q = (F_0 - F)/(F_0 - F_{BKG})$$

where F_0 and F are the fluorescence intensities of the reference (buffer + fluorescein) and sample (antibody + fluorescein) solutions, respectively. F_{BKG} is the background intensity of the buffer (50 mmol · l^{-1} potassium phosphate buffer; pH 8,0) and is attributable to Raleigh and/or Raman light scattering.

The maximum quenching constant (Q_{max}) was calculated from fluorescence quenching (Q) and polarization values:

$$Q_{max} = \{1 + F_b[(1/Q) - 1]\}^{-1}$$

where F_b is the fraction of fluorescence intensity due to bound ligand.

Fluorescence polarization was used to determine F_b values as outlined below:

$$F_b = (A - A_f)/(A_b - A_f)$$

where A is the fluorescence anisotropy of the liganded antibody solution, A_f the anisotropy of unbound fluorescein, and A_b the limiting anisotropy of bound fluorescein.

Finally, the values for the equilibrium association constant (K_a) could be determined

$$K_a = f_b/(1 - f_b)(nP_0 - f_b C_0)$$

where n is the antibody valence ($n = 2$), and P_0 and C_0 are the total concentrations of antibody and ligand, respectively.

Results and discussion

The ultimate aim of this series of papers is to develop a ligand delivery system which is modulated or controlled by light pulses delivered via an optical fiber. Generally, the ligand is labelled with a fluorescent dye. The photooptically released fluorescent ligand diffuses to a second nearby optical fiber whose cladding was removed and which contains monoclonal antibody immobilized on the surface. The photoreleased fluorescent ligand competes with the unlabelled ligand in bulk solution for the immobilized monoclonal antibodies. The sensing fiber is illuminated with light at the absorption maximum of the fluorescent dye. The emitted fluorescence is evanescently coupled back into the fiber and directed to a detection system. Such a system would be a remote immunosensor with all the advantages (sensitivity and specificity) of conventional competitive binding immunoassays, but with the further advantage that the measurement can be performed remotely, at will — under optical control.

It is obvious that this is an interdisciplinary approach and several key problems have to be solved step by step. This study has as its main objective to verify the possibility to release a ligand from a polymeric carrier under optical control.

Type of bond between the carrier and ligand

There are many types of photocleavable bonds used in organic synthesis[18]. We have chosen the 2-nitrobenzyl group[19] which is widely used in polymer based peptide synthesis, both in solid[6, 20] and in liquid phases[21–23]. During irradiation (with light

of wavelength ≈ 360 nm) of aromatic nitro compounds which have a C—H bond in the ortho-position, the nitro group is reduced to a nitroso group[19] and an oxygen is inserted into the carbon-hydrogen bond at the ortho-position, followed by a rearrangement to a more stable structure:

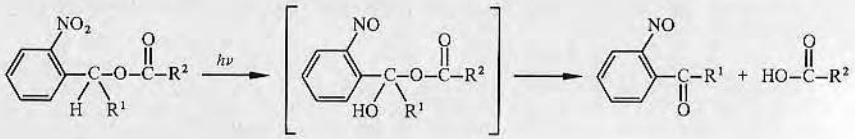

Synthesis of copolymers

Since the 2-nitrobenzyl groups can be cleaved easily when attached both to soluble and unsoluble polymers[18], we have decided to perform this feasibility study on soluble copolymers of **1**. It was believed that in solution both the copolymer structure and the relationship between structure of side-chains and course of photochemical cleavage can be better evaluated.

Polymer analogous reaction of copolymers of **1** were studied in detail[5] and it is possible to synthesize copolymers of **1** which have a fraction of side-chains terminated in ligands bound via cleavable bonds, whereas another fraction of side-chains contains reactive groups (e.g. NH_2) suitable, e.g. for binding these copolymers to functionalized surfaces. Syntheses and characterization of the copolymers **3a – g** are described in the Exptl. part.

The yields of the polymeranalogous reactions are obvious from the content of particular side-chains. They are not maximal obtainable ones, since no effort was undertaken to optimize the reaction conditions of the individual reactions. This effort will be devoted to the copolymer with the optimal structure, which will be used for the development of biosensors. Moreover, we intentionally introduced only small amounts of fluorochromes into copolymers **3f** and **3g** to prevent their interactions (cf. below). In this stage of research, we wanted to demonstrate the possibility of synthesis of copolymers suitable for the controlled photochemical release of the ligand.

Photocleavage of ligands

1. Photochemical release of Boc-Gly from copolymer **3d**

The photocleavage of copolymer **3d** was carried out in methanolic solution in a quartz cuvette in nitrogen atmosphere. After 96 h 84% of Boc-glycine bound via 2-nitrobenzyl groups were released from the polymeric support (Fig. 1). The cleavage appeared to be fast approximately to 50% of ligand released. Similar results were obtained with poly(ethylene glycol) support[15]. In this interval of cleavage the polymer synthesized should be suitable for continuous release of the bound ligand. It is obvious that the rate of release observed may be too slow for the photochemical

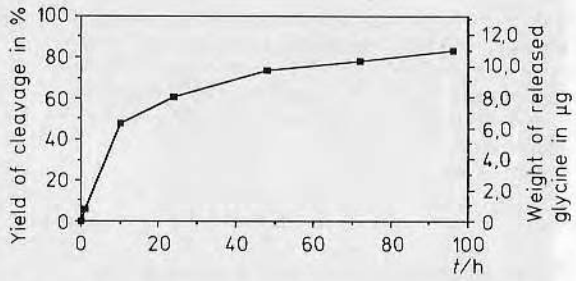

Fig. 1. Cleavage of glycine obtained by photolysis of copolymer **3d** in methanol; λ = 360 nm

delivery of ligands in biosensors. However, using a more potent source of energy, the rate of photochemical release can be substantially increased. Tjoeng et al.[15] observed 98% release of Boc-Leu-Ala-Gly-Val, bound via 2-nitrobenzyl groups to poly(ethylene glycol), supports within 20 h. Senter et al.[24] were able to release pokeweed antiviral protein bound to antibodies via 2-nitrobenzyl bonds in minutes.

Another possibility to increase the yield and rate of the photochemical cleavage is to bind α-substituted 2-nitrobenzyl groups instead of 2-nitrobenzyl groups, to the carboxyl groups of the ligand. The substitution in α-position by phenyl or nitrophenyl groups increases the yield of photochemical cleavage compared to unsubstituted compounds[18].

2. Photochemical cleavage of copolymers **3f** and **3g**

In these copolymers **6a** and **6b** are separated from the photocleavable, bond by a glycine unit. Thus, after photocleavage a glycine modified fluorochrome will be released, *N*-[3′,6′-dihydroxy-(or dimethylamino)spiro[phthalide-3,9′-xanthen]-6-yl-aminothiocarboxyl]glycine (**7**). This should have a minimum effect on their binding constants with antibodies, since it was shown[25] that the amino acid residues attached to the fluorescein molecule in the location used have minimal effect on ligand binding, since the chemical substitution used does not modify the immunocompetent part of the fluorescein molecule. In order to verify this, we have synthesized thiourea **7** and measured the association constant of this compound with antifluorescyl antibodies (Tab. 1).

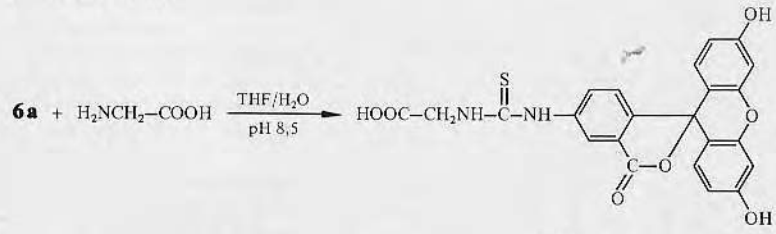

7

Three different reaction conditions were used in the study of the photocleavage of copolymers **3f** and **3g**. a) Methanol was used as solvent and oxygen was removed by bubbling with nitrogen; b) water was used as solvent and oxygen was removed by

Tab. 1. Characterization of the fluorochromes by their association constants K_a with monoclonal antifluorescyl antibodies (clone 4-4-20)

Compound	Condition of photocleavage	$10^{-8} \cdot K_a/(l \cdot mol^{-1})$
Fluorescein	—	50
7 synthesized	—	30
7 released[a)]	H_2O, flushed with N_2	5
	H_2O, freeze and thaw technique	2

[a)] For conditions of photocleavage see Exptl. part.

bubbling with nitrogen; and c) water was used as solvent and the freeze thaw technique to remove oxygen. In all three cases photocleavage took place and glycine modified fluorochromes were released. During photocleavage of copolymer **3f** in case a) major changes in the absorption spectra of the released ligand **7** compared to the free one (Fig. 2) were observed, whereas in cases b) and c) the specra of released and free ligand are similar (Fig. 3). The absorption spectra of **6b** and low-molecular-weight products, separated by column chromatography after photocleavage of copolymer **3g**, are compared in Fig. 4. Only in case c) practically no changes in the UV spectra were observed.

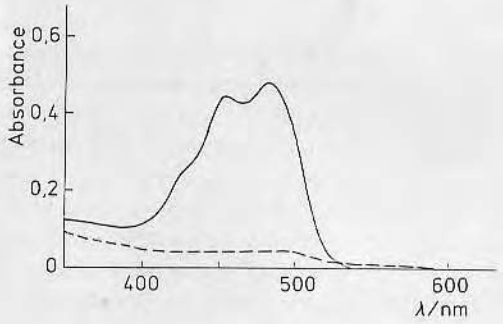

Fig. 2. Comparison of absorption spectra in CH_3OH of free **6a** and modified ligand (**7**) released from copolymer **3f** by photocleavage (λ = 360 nm). (———): free **6a**; (– – –): released modified **7** ligand [reaction condition (a): methanol as solvent and removal of oxygen by bubbling with nitrogen]

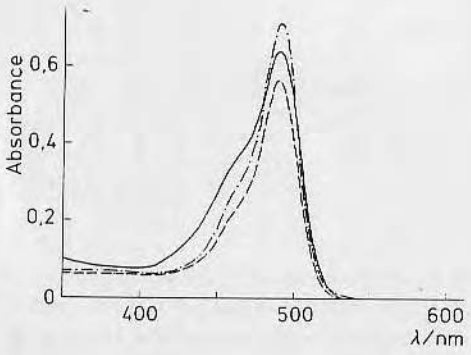

Fig. 3. Comparison of absorption spectra in water of free **6a** and released modified ligands **7** from copolymer **3f** obtained by photocleavage under different conditions (λ = 360 nm). (———): free **6a**; (– · – · –): released modified ligand **7** [reaction condition (b): water as solvent and removal of oxygen by bubbling with nitrogen]; (– – –): released modified ligand **7** [reaction condition (c): water as solvent and freeze thaw technique to remove oxygen]

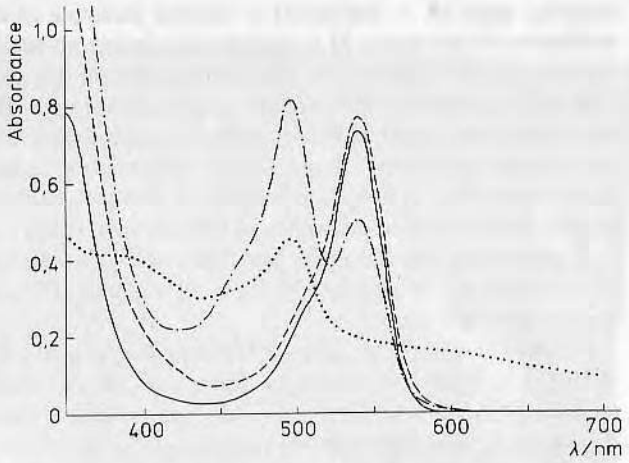

Fig. 4. Comparison of absorption spectra in methanol of free **6b** and released modified ligand *N*-[3′,6′-diethylaminospiro[phtalide-3,9′-xanthen]-6-ylaminothiocarbonyl]glycine from copolymer **3g**, obtained by photocleavage under different conditions (λ = 360 nm). (———): free **6b**; (· · · · · ·): released, glycine modified ligand [reaction condition (a): methanol as solvent and removal of oxygen by bubbling with nitrogen]; (– · – · –): released, glycine modified ligand [reaction condition (b): water as solvent and removal of oxygen by bubbling with nitrogen]; (– – –): released, glycine modified ligand [reaction condition (c): water as solvent and removal of oxygen by freeze thaw technique]

To characterize subtle changes in the structure of released **7** (not detectable by UV spectrophotometry) the association constants (K_a) of released fluorochrome under different photocleavage conditions with monoclonal antifluorescyl antibodies (clone 4-4-20) were compared with the K_a values of fluorescein and synthesized **7** (Tab. 1). The association constants of the released ligands, of fluorescein and of synthesized **7** are within one order of magnitude if the photocleavage was performed in aqueous solution. The very close values of association constants of fluorescein and synthesized **7** with monoclonal antifluorescyl antibodies are in accordance with the results obtained by Voss et al.[25]. Photochemical cleavage of copolymer **3f** carried out under reaction condition (b) showed about 10% of glycine modified fluorochrome released after 96 h. The lower efficiency of cleavage of the latter, compared to the release of Boc-Gly (from copolymer **3d**) is most probably due to the fact that, although the maximal absorbance of fluorescein is located at 492 nm, there still exists mild absorbance around 360 nm. Thus, only part of the energy emitted from the source is available for the excitation of the 2-nitrobenzyl bonds, resulting in the decrease of the quantum yield of their cleavage.

Fluorescein and phthaleins generally, owe their photochemical reactivity to the relatively long life time of the dye triplet[26]. Reactions available to the dye (D) triplet were characterized[27] as D-O; D-R and D-D types, according to whether the primary step involves interactions of the dye triplet with an oxidizing agent (O = oxygen),

reducing agent (R = methanol) or another molecule of dye, respectively. During irradiation of copolymer **3f** in methanolic solution we have observed diminishing of the color of the solution. The absorption spectrum (Fig. 2) is accordingly changed. This is in accordance with the observation that photoreduction to the colorless leuco-dye is one of the principal modes of photodecomposition of phtalein dyes in oxygen-free alcohol solutions[27]. Experiments performed in aqueous solution gave much better results (Fig. 3; Tab. 1) in accordance with the observed stability of phtaleins in oxygen-free aqueous solutions due to reduced possibilities of occurrences of D-O and D-R mechanisms. To reduce the possibility of D-D interactions we have incorporated into copolymers **3f** and **3g** only a small amount of fluorochromes (0,9 and 0,6 mol-%, respectively).

For rhodamines, the key steps in fading appear to involve electron transfer reaction of the long-lived dye triplet to form ion-radicals which undergo irreversible, secondary reactions to form colourless end-products. Besides the colourless leuco dye, which is formed by disproportionation to the semireduced dye radicals[28], other fading products have been identified. Evans[29,30] determined photoproducts of fading of rhodamine B in aqueous solution. The two main photoproducts were shown to be *N,N,N'*-triethylrhodamine and *N,N'*-diethylrhodamine. It was observed[31] that dealkylation is accompanied with a hypsochromic shift of the absorption spectra. Our results (Fig. 4) indicate that under conditions a) and b) the dealkylation reaction could be at least partially responsible for the photofading of the released ligand and to a lower extent of the polymer bound ligand. The latter conclusion is based on the comparison of the UV spectra of the polymer fraction and low-molecular-weight fraction obtained after 96 h of irradiation of copolymer **3g** (Fig. 5). The results show that polymer bound **6b** is much more resistant to photofading compared to the

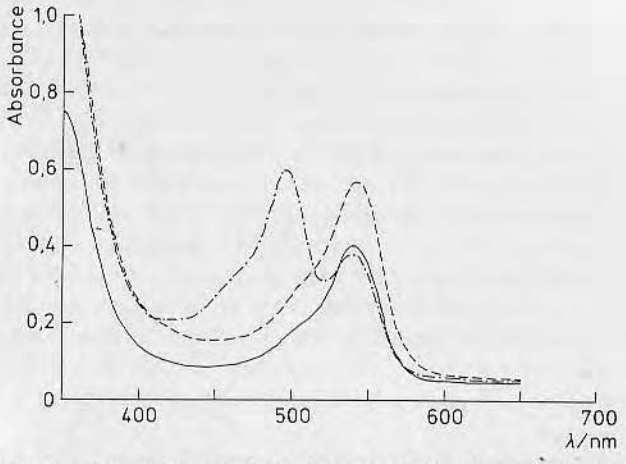

Fig. 5. Comparison of absorption spectra in methanol of copolymer **3g** before and after photocleavage [reaction condition (b): water as solvent and removal of oxygen by bubbling with nitrogen: λ = 360 nm]. (———): Copolymer **3g**; (– – –): high-molecular-weight fraction; (– · – · –): released modified **6b** ligand (low-molecular-weight fraction)

unbound one. Same results were obtained with **6a**, i.e. copolymer **3f** (results not shown). It appears that an increased stability of polymer bound dyes is a general phenomenon. It was shown previously[32] that rose bengal is irreversibly photooxidized in aqueous solutions, whereas when bound to poly(vinylpyrrolidone) the dye resists fading, even when exposed to sun-light for a month.

It can be assumed that when these copolymers will be part of biosensors, the effect of fading should be smaller compared to present experiments, because the photochemical release of the dye (or labelled ligand) will be followed by a fast immunochemical reaction (association with antibody), thus considerably reducing the time when the dye (free or ligand bound) is exposed to irradiation in solution.

From the experiments on the photochemical release of ligands covalently bound to copolymers of **1** it may be concluded that Boc-glycine is stable during irradiation and photocleavage, whereas **6a** and **6b** undergo structural changes in solution. These changes can be minimized by properly adjusting the experimental conditions of photocleavage. Fluorescein derivatives appear to be more stable compared to rhodamine ones. Binding of **6a** or **6b** to water-soluble polymers has a stabilization effect — photofading of polymer bound dyes is minimal.

The work was partially supported by *NSF Grant* ECS-85-02107. We thank Drs. *J. Herron, J.-N. Lin* and *P. Kopečková* for advice and assistance and to Dr. *E. W. Voss, Jr.* and Dr. *J. Herron* for the generous gift of monoclonal antifluorescyl antibodies. J. K. thanks the *Institute of Macromolecular Chemistry, Czechoslovak Academy of Sciences* for leave of absence and the University of Utah for granting a Visiting Professorship.

[1] R. S. Yalow, *Science (Washington, D.C. 1883)* **200**, 1236 (1978)
[2] J.-N. Lin, H. R. Yen, J. Kopeček, J. D. Andrade, J. Herron, Int. Biomaterials Science Workshop on "Future trends of biomedical polymers for diagnostics and therapeutics", Tokyo, Japan, Nov. 1986, Proceedings, p. 45
[3] J. D. Andrade, J.-N. Lin, J. Herron, M. Reichert, J. Kopeček, *Proc. SPIE Int. Soc. Opt. Eng.* **718**, 280 (1986)
[4] J.-N. Lin, J. Herron, J. D. Andrade, M. Brizgys, *IEEE Trans. Biomed. Eng.* **35**, 466 (1988)
[5] J. Kopeček, in: "IUPAC Macromolecules", ed. by H. Benoit and P. Rempp, Pergamon Press, Oxford 1982, p. 305
[6] J. Strohalm, J. Kopeček, *Angew. Makromol. Chem.* **70**, 109 (1978)
[7] P. Rejmanová, J. Labský, J. Kopeček, *Makromol. Chem.* **178**, 2159 (1977)
[8] D. H. Rich, S. K. Gurwara, *J. Am. Chem. Soc.* **97**, 1575 (1975)
[9] D. M. Krantz, E. W. Voss, Jr. *Mol. Immunol.* **18**, 889 (1981)
[10] J. Kopeček, P. Rejmanová, V. Chytrý, *Makromol. Chem.* **182**, 799 (1981)
[11] J. Kopeček, P. Rejmanová, *J. Polym. Chem., Polym. Symp.* **66**, 15 (1979)
[12] J. Kopeček, *Makromol. Chem.* **178**, 2169 (1977)
[13] *"Methoden der Organischen Chemie"* (Houben-Weyl), ed. by E. Müller, vol. 15/1, G. Thieme, Stuttgart 1974, p. 117
[14] S. Moore, W. H. Stein, *J. Biol. Chem.* **176**, 367 (1948)
[15] F. S. Tjoeng, W. Staines, S. St.-Pierre, R. S. Hodges, *Biochim. Biophys. Acta.* **490**, 489 (1977)
[16] R. M. Watt, E. W. Voss, Jr., *Immunochemistry* **15**, 875 (1977)
[17] J. N. Herron, E. W. Voss, Jr., *J. Biochem. Biophys. Methods* **5**, 1 (1981)

Optically Controlled Ligand Delivery. II. Copolymers Containing α-Methylphenacyl Bonds

HUNG-REN YEN, JOSEPH D. ANDRADE, and JINDŘICH KOPEČEK*

Departments of Materials Science and Engineering and of Bioengineering, University of Utah, Salt Lake City, Utah 84112

SYNOPSIS

N-(2-hydroxypropyl)methacrylamide copolymers containing side chains terminated in a model ligand, *N-tert*-butyloxycarbonylglycine (Boc-Gly), bound via photocleavable α-methylphenacyl bonds were synthesized to test the possibility of developing an optically controlled ligand delivery system suitable for sensors. One of the copolymers was further covalently attached to 3-aminopropyl triethoxy silane (APS) coated porous silica beads which were modified with an excess of α,ω-diaminopoly(ethylene oxide), molecular weights 1000 or 5000. The photochemical release of ligand induced by exposure to light in solution and at the solid–liquid interface was studied. The influence of solvent and the length of poly(ethylene oxide) (PEO) spacers on the rate of photocleavage were determined. The hydrolytic stability of the α-methylphenacyl bond in both solution and at the solid–liquid interface were also investigated.

INTRODUCTION

The specificity of antibody (Ab)–antigen (Ag) interactions and competitive binding reactions using labeled Ag or Ab have permitted the development of immunoassays with very high sensitivity and specificity. Although modern competitive binding immunoassay kits are very simple to use, they are totally unsuitable for continuous and/or remote measurements.

There exists a possibility to use the competitive binding immunoassay principle in fiber optics and thin film wave guide sensors.[1] Such sensors will be based on remotely controlled ligand delivery and total internal reflection fluorescence (TIRF) sensing. The development of such sensors requires a number of basic and applied science studies[2] including polymer synthesis, remote ligand delivery,[3] antibody binding, Ag–Ab binding constant regulation,[4] and biocompatibility.

One of the key parts of the overall sensor problem is the optically controlled release of ligands. To investigate this question, we have studied *N*-(2-hydroxypropyl)methacrylamide (HPMA) copolymers containing side chains terminated in ligands bound via photocleavable bonds. Copolymers of HPMA were chosen because their structures permitted introduction of different reactive units into one polymeric chain[5] and, consequently, offer the possibilities to attach ligand-containing copolymers to functionalized surfaces.

In the first paper of this series HPMA copolymers with ligands (Boc-Gly, fluorescein, and tetramethylrhodamine) bound via the 2-nitrobenzyl bond were synthesized and the photocleavage studied.[3] From these experiments, it may be concluded that Boc-Gly is stable during irradiation and photocleavage, whereas fluorescein and tetramethylrhodamine undergo structural changes when in solution. However, all the ligands were stable when attached to HPMA copolymers.

In this communication another photocleavable bond, α-methylphenacyl, was investigated. Copolymers containing side chains terminated in model ligand (Boc-Gly) bound via photocleavable α-methylphenacyl bonds were synthesized. To investigate the photocleavage reaction at the solid–liquid interface, one copolymer was further covalently attached to modified porous silica beads with no spacer

* To whom correspondence should be addressed at the Department of Bioengineering, 2480 MEB.

Journal of Applied Polymer Science, Vol. 43, 1241–1252 (1991)
 CCC 0021-8995/91/071241-12$04.00

or with PEO spacers of different lengths (M_r = 1000 and 5000). Copolymers in solution and at the solid–liquid interface were exposed to light resulting in release of the bound ligand. Depending on the type of solvent and length of PEO spacer, differences in the rate of cleavage were obtained. The hydrolytic stability of the α-methylphenacyl bond in solution and at solid–liquid interfaces was also studied.

METHODS

Chemicals

N-(2-hydroxypropyl)methacrylamide was prepared as previously described (mp 69–70°C).[6] 2,2′-Azoisobutyronitrile (AIBN) was recrystallized from ethanol. Porous silica beads, 3-aminopropyl triethoxy silane (APS) coated, 30–40 mesh, 375 Å pore size, were from Fluka. Glutaraldehyde (Glu), 25% solution in water, E.M. Grade was supplied by Polysciences. Diamines $NH_2-PEO_{1000}-NH_2$ and $NH_2-PEO_{5000}-NH_2$ were a kind gift from Dr. S. Nagaoka (Toray Industries, Inc., Kanagawa, Japan). *N*-succinimidyl-3-(2-pyridyldithio)propionate (SPDP) and *N*-(3-aminopropyl)methacrylamide hydrochloride were from Pharmacia and Kodak, respectively. Dimethylformamide (DMF), dimethyl sulfoxide (DMSO), and aniline were purified by distillation under reduced pressure. Other solvents used were freshly distilled. [^{3}H]-glycine (Amersham) was used without further purification.

Synthesis

Methacrylanilide (1)

Methacrylanilide was prepared according to Ref. 7. The product was crystallized from ethanol, mp 84–85°C (lit.,[7] mp 84–85°C).

ANAL. Calcd for $C_{10}H_{11}NO$ (161.0): C, 74.53%; H, 6.83%; N, 8.69%. Found: C, 74.46%; H, 6.90%; N, 8.60%.

N-[4-(2-Chloropropionyl)phenyl]methacrylamide (2)

Chloropropionyl chloride (66 g, 0.52 mol) was added into the dichloromethane solution (150 mL) of aluminum chloride (84.3 g, 0.63 mol). The reaction proceeded for 10 min under stirring and the solution became dark red. A solution of methacrylanilide (**1**) (30 g, 0.186 mol) and a small amount of hydroquinone in dichloromethane (75 mL) were slowly dropped into the dark red solution. The reaction solution was heated to boiling for 1 h and then hydrolyzed with ice-cold water for 15 min. The dichloromethane layer was collected, dried with magnesium sulfate, and purified with active carbon. The powder residue obtained after removing the dichloromethane was recrystallized twice from acetone/petroleum ether. Yield: 20.5 g, mp 119–120°C.

ANAL. Calcd for $C_{13}H_{14}NClO_2$ (251.5): C, 62.03%; H, 5.57%; N, 5.57%; Cl, 14.12%. Found: C, 61.60%; H, 5.57%; N, 5.36%; Cl, 14.48.

Cesium Salt of [^{3}H]-Boc-Gly (3)

(a) [^{3}H]-Boc-Gly: A mixture of 1.125 g cold glycine (15 mmol) and 1 mCi of [^{3}H]-glycine in 1 mL aqueous solution (specific activity: 19 Ci/mmol) were dissolved in a mixture of dioxane and water (45 mL, vol ratio 2 : 1) and 15 mL of 1*N* NaOH. A dioxane solution of di-*tert*-butyl dicarbonate (3.6 g, 15 mmol) was added into the precooled mixture (4°C). The reaction proceeded under stirring 30 min at 4°C and another 30 min at room temperature. Dioxane and water were rotoevaporated. The residue was dissolved in water and the unreacted di-*tert*-butyl dicarbonate was extracted with ether. The aqueous portion was collected and acidified to pH 2–3 with saturated potassium bisulfate aqueous solution. The crude product ([^{3}H]-Boc-Gly) was extracted twice with ethyl acetate and dried overnight with magnesium sulfate. The next day the magnesium sulfate was filtered off and the dry product (yield: 1.7 g, mp 87°C) was collected by evaporating ethyl acetate.

(b) Cesium salt of [^{3}H]-Boc-Gly: [^{3}H]-Boc-Gly was further reacted with 20% aqueous cesium carbonate (2.94 g, 9 mmol) for 2.5 h. The cesium salt of [^{3}H]-Boc-Gly (**3**) was obtained by removing the water and drying under reduced pressure.

N-{4-[2-(N-Tertbutoxycarbonylglycyloxy)-propionyl]phenyl}methacrylamide (4)

The suspension of **3** (9.8 mmol) in 11.4 mL DMF was added to the DMF solution (1.9 ml) of **2** (0.98 g, 3.9 mmol) with a hydroquinone inhibitor (mole ratio of **2** and **3** = 1 : 2.5). The reaction proceeded for 24 h under stirring at room temperature. A small amount of undissolved powder was filtered off and DMF removed by rotary evaporator. The yellow oil obtained was dissolved in a large amount of ether and the unreacted portion of **3** was extracted with water. The ether portion was collected and put in a freezer for crystallization. The radioactivity of **4** was measured as 0.162 μCi/mg. Yield: 0.36 g, mp 149–150°C. A cold **4** which was sent for elemental anal-

ysis was synthesized by the same method, its elemental analysis was as follows:

ANAL. Calcd for $C_{20}H_{26}N_2O_6$ (390.0): C, 61.54%; H, 6.70%; N, 7.18%. Found: C, 61.69%; H, 6.96%; N, 7.16%.

Copolymerization

Copolymer **5** was prepared by radical precipitation copolymerization of HPMA and **4** (mole ratio 97 : 3) in acetone (12.5 wt % of monomers; 0.6 wt % of AIBN as initiator) at 50°C as previously described.[3,8] The content of monomeric units of **4** in copolymer **5** was calculated to be 2.5 mol % using radioactivity measurement. To perform GPC analysis, a cold copolymer **5** was prepared by the same procedure. The weight- and number-average molecular weights of copolymer **5** (M_w = 100,000; M_w/M_n = 2.8) were estimated from the GPC analysis[9] on a Sepharose 4B/6B (1 : 1) column (90 × 1.6 cm) calibrated with fractions of poly(HPMA) (buffer: 0.5*M* NaCl + 0.05*M* TRIS; pH 8.0).

Copolymer **7** was prepared by radical precipitation copolymerization of HPMA, *N*-(3-aminopropyl)methacrylamide hydrochloride (**6**) and **4** (mole ratio 89.5 : 9 : 1.5) in methanol (12.5 wt % of monomer; 0.6 wt % of AIBN as initiator) as described above. After 24 h at 50°C, the copolymerization was completed and triethylamine was added to transform the hydrochloride into free base. The copolymer solution was precipitated into acetone, reprecipitated, collected, and dried. The content of monomeric units of **4** and **6** was quantified to be 1.4 and 4.7 mol % using radioactivity measurement and the ninhydrin method,[10] respectively. Cold copolymer **7** which was used for molecular-weight determination was prepared the same way. The weight- and number-average molecular weights of copolymer **7** (M_w = 47,000; M_w/M_n = 1.6) were estimated from the GPC analysis.[9]

Modification of Silica Beads

The silica beads were modified according to procedures described in Ref. 11.

Aldehyde Beads:)—APS—GLU—CH=O (9)

One gram of APS coated beads (**8**), containing 14 nmol NH_2/mg, were reacted with 20 mL 2.5% glutaraldehyde (GLU) in borate buffer, pH 8.6 (batch A), or carbonate buffer, pH 9.5 (batch B). The reaction mixture was gently shaken overnight at room temperature, and then washed many times with water, ethanol, ether and dried. No NH_2 groups were detectable on beads by a qualitative test using the ninhydrin method.[10]

Amino Beads:)—APS—GLU—PEO_{1000}—NH_2 (10),)—APS—GLU—PEO_{5000}—NH_2 (11)

One gram of aldehyde beads **9** (batches A and B) were reacted with a large excess of the respective diamine solution: 5 mL 20% NH_2—PEO_{1000}—NH_2 or 4 mL 50% NH_2—PEO_{5000}—NH_2 in sodium carbonate/bicarbonate buffer pH 9.0. Beads were gently shaken overnight and washed thoroughly as described above. The azomethine bond formed was reduced by reaction with 80 mg $NaCNBH_3$ in 3 mL sodium carbonate/bicarbonate buffer pH 9.5. After proper washing and drying the content of NH_2 was determined as described below. No aldehyde groups on beads were detectable after diamine treatment by the reaction with dinitrophenylhydrazine.[12]

Modification of PEO Spacer-Containing Beads: Preparation of)—APS—GLU—PEO_{1000}—GLU—CH=O (12),)—APS—GLU—PEO_{5000}—GLU—CH=O (13)

One gram of NH_2 groups containing beads **10** and **11** (batches A and B), respectively, were treated with 20 mL 2.5% glutaraldehyde by the same procedure as described above. The remaining unreacted NH_2 groups after glutaraldehyde treatment were quantified as described below.

Copolymer-Derivatized Silica Beads:)—APS—GLU—CH_2—NH—Copolymer 7 (14),)—APS—GLU—PEO_{1000}—GLU—CH_2—NH—Copolymer 7 (15), and)—APS—GLU—PEO_{5000}—GLU—CH_2—NH—Copolymer 7 (16)

Five hundred fifty milligrams of beads **9**, **12**, and **13** (batch A), respectively, were treated with excess of the copolymer **7** (500 mg) in DMSO. The suspension was gently shaken overnight at room temperature, and then washed many times with ethanol and methanol. The azomethine bond was further reduced by reaction with 50 mg $NaCNBH_3$ in phosphate/citric buffer, pH 4.5. After proper washing and drying the binding efficiency was quantified as described below.

Nonspecific Adsorption of Copolymer 7 to Silica Beads

To estimate the extent of the nonspecific adsorption of copolymer **7**, beads **8**, **10**, and **11** were incubated with copolymer **7** as described above. Beads with physically adsorbed copolymer **7** were numbered **17**, **18**, and **19**, respectively (see Table II).

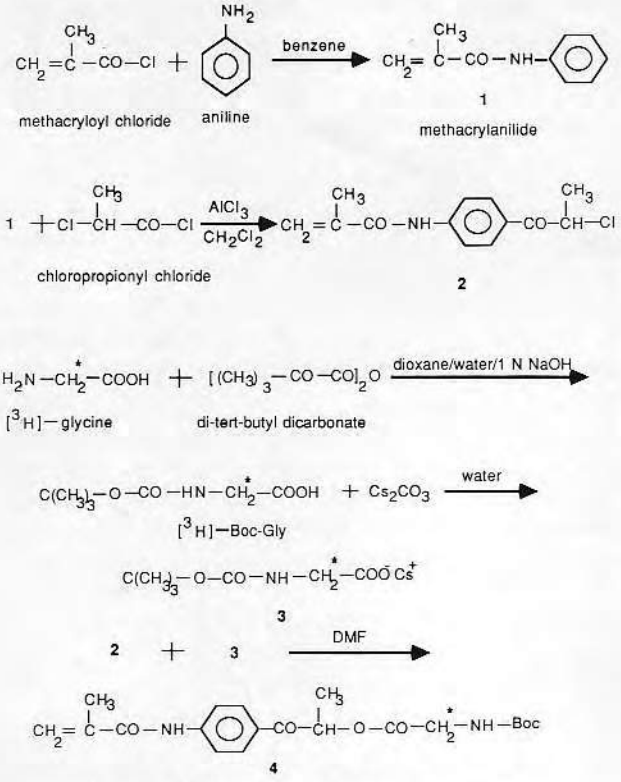

Figure 1 Synthesis of monomers **1–4.**

Analysis of Beads

Determination of NH_2 Groups. The concentration of amino groups on the beads was determined using *N*-succinimidyl-3-(2-pyridyldithio)propionate (SPDP).[13] The beads were treated with an excess of SPDP in the presence of a small amount of 4-dimethylaminopyridine (catalyst). The unreacted reagent was removed by washing, followed by reduction of acylated beads by dithiothreitol (DTT). This results in the release of pyridine-2-thione, whose concentration was determined spectrophotometrically at 343 nm (ϵ = 8080 L/mol cm).

Surface Area of Beads. The specific surface of original APS coated beads was 33.4 m^2/g. All modified beads (batch A) had specific surface in the range from 29 to 31 m^2/g.[11]

Radioactivity Measurement

All ^3H radioactivity measurements were performed with a Beckman LS1801 scintillation counter using biodegradable scintillation cocktail (National Diagnostic, NJ) for photocleavage studies in solution and Ready-Gel cocktail (Beckman) for studies at the solid–liquid interface.

Determination of Radioactivity on Silica Beads

Twenty to thirty milligrams of beads and 0.5 mL 6*N* HCl were put into glass ampoules. The ampoules were sealed and heated at 110°C for 12 h. After cooling the ampoules, the aliquots were transferred to scintillation vials, diluted, neutralized with 6*N* NaOH, and the radioactivity measurement performed.

Hydrolytic Stability

Hydrolytic Stability of Copolymer 5 in Solution

Copolymer **5** was incubated with buffers having different pH's in test tubes at room temperature or 37°C in the dark. After incubation at various time intervals, the copolymer solution (1 wt %) was applied to a PD-10 column (Pharmacia) equilibrated with the buffer. Fractions corresponding to high- and low-molecular-weight substances were pooled and their radioactivities determined. The structure of Boc-Gly released by hydrolysis was verified by TLC (Silica gel 60 F254 from EM Laboratories, Inc.) using 1-butanol/acetic acid/water (vol. ratio 3 : 1 : 1).[14]

Hydrolytic Stability of Copolymer 7-Containing Silica Beads 14

Silica beads (30 mg **14**) and 0.4 ml pH 4.5 citrate/phosphate or pH 7.2 phosphate buffers were incubated in 37°C. The radioactivity of the supernatant was measured at time intervals always before adding fresh buffer. The hydrolytic stability against 50% trifluoroacetic acid (TFA)/CH_2Cl_2 was performed at room temperature similarly as described above.

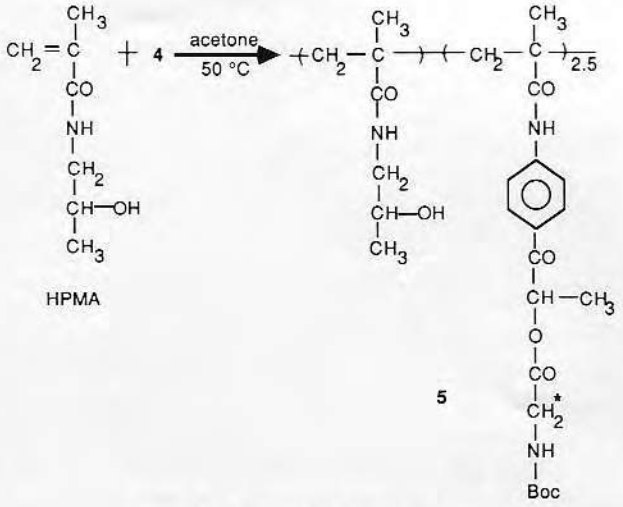

Figure 2 Synthesis of copolymer **5.**

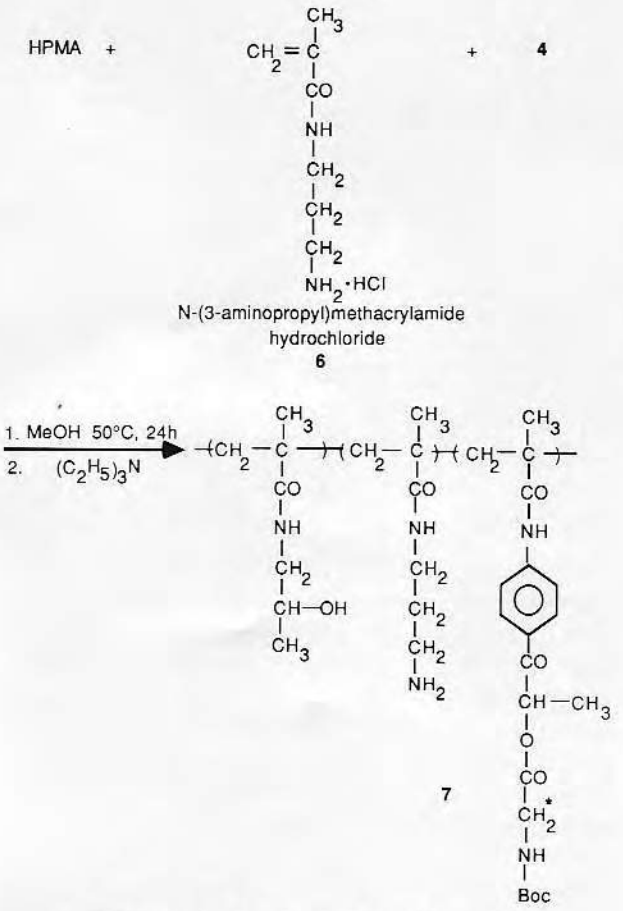

Figure 3 Synthesis of copolymer **7**.

Photocleavage

Photocleavage in Solution

Copolymer **5** was dissolved in methanol or ethanol to form a 1 wt % solution and then deaerated with nitrogen for 30 min. The copolymer solution was irradiated in a quartz cuvette (d = 1 cm) with a LH 150 mercury lamp (200 W, Schoeffel Instr. Co.) with maximal emission at 360 nm for various time periods (intensity: 8 mW/cm^2 at 365 nm; a focusing lens was placed between lamp and the sample). After irradiation, the solution was applied to Sephadex LH-20 column (28 × 1 cm) and the radioactivities of the individual fractions were measured. The decrease of radioactivity in the copolymer reflected the amount of Boc-Gly released (analysis was done in triplicate). The structure of Boc-Gly released was qualitatively verified by TLC.[14]

Photocleavage at the Solid–Liquid Interface

Thirty milligrams of the copolymer **7**-derivatized silica beads (**14**, **15**, and **16**) and 0.5 mL dehydrated ethanol were poured into UV quartz cylindrical cell with Teflon stopper. The cell was attached to a rotator (Clas-Col Co.) with speed 60 rpm, so that during irradiation a centrifugal force gently agitated beads to ensure the same probability of light access to every part of the surface. The cell was irradiated with a LH 150 mercury lamp (200 W, Schoeffel Instr. Co). The emission was first focused by a fused silica lens, then reflected by a dichroic-coating mirror (Oriel Corp.) which reflects only the wavelengths between 260 and 340 nm (the major intense emission peaks are 296 and 312 nm). At chosen time intervals, the supernatant was withdrawn for radioactivity measurement. The increase of radioactivity in the supernatant reflected the amount of photoreleased ligand. Each experiment was performed twice and average data were plotted (the differences between these two sets of data were within 3%). After irradiation, the remaining radioactivities on the silica beads were determined as described above. The mass balance of radioactivity between supernatant and silica bead surfaces were consistent throughout the experiments. Controls were kept in the dark. The Boc-Gly released was qualitatively verified by TLC as described above.[14]

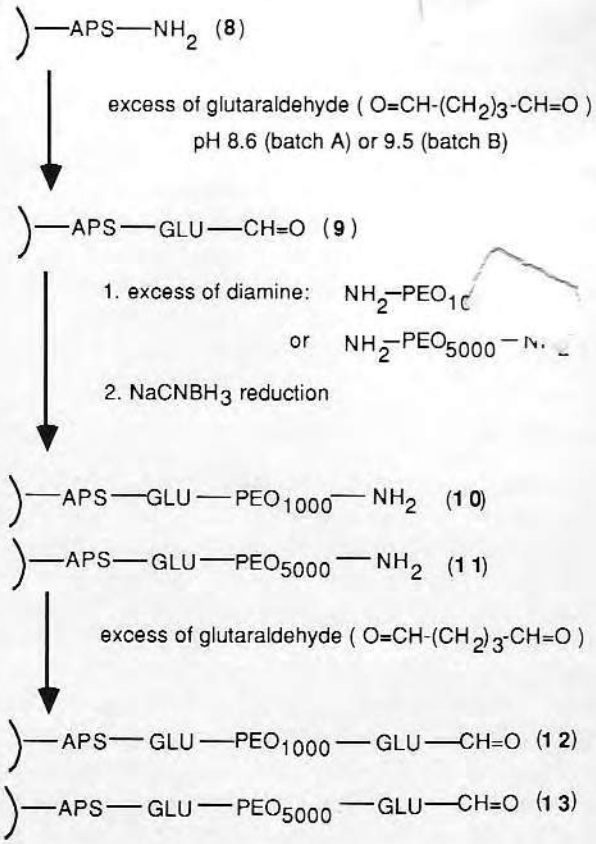

Figure 4 Modification of porous silica beads.

Table I The Content of NH_2 Groups on Silica Beads 8–13

Silica Bead No.	Schematical Structures	Content of Amino Group (NH_2) (nmol/mg) Batch A[a]	Batch B[b]
8	)—APS—NH_2	14	14
9	)—APS—GLU—CH=O	0	0
10	)—APS—GLU—PEO_{1000}—NH_2	9	7
11	)—APS—GLU—PEO_{5000}—NH_2	10	7
12	)—APS—GLU—PEO_{1000}—GLU—CH=O	1	1
13	)—APS—GLU—PEO_{5000}—GLU—CH=O	2	1

[a] These beads were prepared by reacting with glutaraldehyde at pH 8.6.
[b] These beads were prepared by reacting with glutaraldehyde at pH 9.5.

RESULTS

Synthesis of Monomers and Copolymers

The monomer containing Boc-Gly bound via α-methylphenacyl group was synthesized by a series of reactions. By the reaction of methacryloyl chloride with aniline in benzene, methacrylanilide **1** was obtained,[7] which was further reacted with chloropropionyl chloride to yield **2.** An excess amount of the cesium salt of [^{3}H]-*N-tert*-butoxycarbonylglycine (**3**) were then allowed to react with **2** in dimethylformamide to obtain the final product **4** (Fig. 1). The photocleavable copolymer **5** was prepared by copolymerization of HPMA and **4** in acetone (Fig. 2). In order to attach the copolymer to modified silica beads, *N*-(3-aminopropyl)methacrylamide hydrochloride (**6**), a comonomer containing free NH_2 groups, was incorporated into copolymer **7.** The latter was synthesized by copolymerization of HPMA, **4** and **6** in methanol (Fig. 3).

Modification of Silica Beads

The modification of porous silica beads is schematically shown in Figure 4.[11] The APS-coated beads **8** contained 14 nmol/mg of amino groups. After reaction with a large excess of glutaraldehyde, practically all amino groups were converted to aldehyde groups (beads **9**). The latter were modified with a large excess of diamines, NH_2—PEO_{1000}—NH_2 and NH_2—PEO_{5000}—NH_2. The resulting beads **10** and **11** contained 7–10 nmol/mg of terminal amino groups. Due to the incomplete reaction of beads **10** and **11** with excess of glutaraldehyde, the beads **12** and **13** still contained less than 2 nmol/mg of unreacted NH_2 groups on surfaces (Table I). To evaluate the influence of pH on the binding reactions, two procedures were chosen: In batch A the reaction with glutaraldehyde was performed at pH 8.6, whereas in the batch B it was performed at pH 9.5. The content of NH_2 groups on beads **10** and **11** of batch A was 2–3 nmol higher than in batch B (Table I). The surface area of the beads (batch A) did not show any dramatic change during these polymer-analogous reactions.[11]

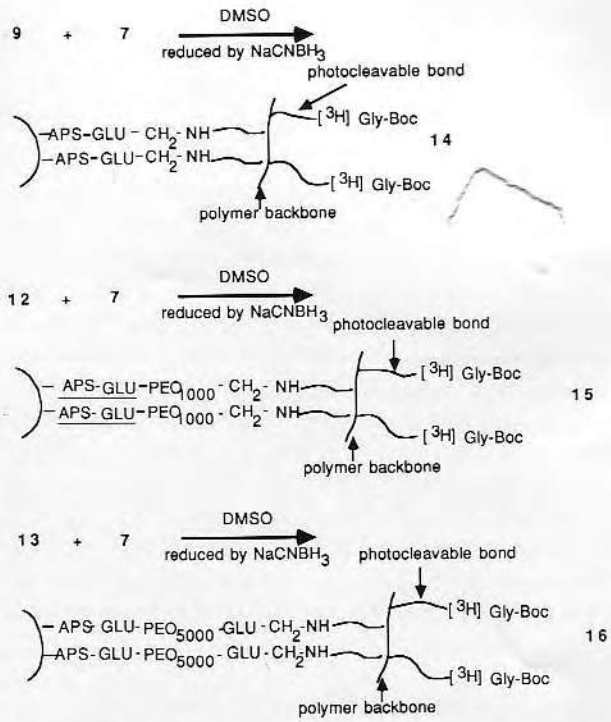

Figure 5 Synthesis and schematic structures of silica beads **14, 15,** and **16.**

Table II The Radioactivities (DPM) and Amounts of Copolymer 7 Bound on Modified Silica Beads 14–19

Beads No.	Radioactivity of Bound Copolymer **7** (DPM/50 mg beads)	Amount of Bound Copolymer **7** (mg/50 mg beads)	Amount of Bound Copolymer **7** (mg/m^2)[a]
14[b]	24,900	1.81	1.21
15[b]	15,400	1.12	0.75
16[b]	10,300	0.75	0.50
17[c]	5700	0.4	0.28
18[c]	1100	0.08	0.06
19[c]	300	0.02	0.01

[a] The specific surface area of 30 m^2/g of bead was used as a basis for calculation.
[b] Covalent attachment to beads **9**, **12**, and **13**, respectively.
[c] Nonspecific adsorption on beads **8**, **10**, and **11**, respectively.

Copolymer-Derivatized Silica Beads

Silica beads **14, 15,** and **16,** containing copolymer **7,** were synthesized by treating silica beads **9, 12,** and **13,** respectively, with copolymer **7.** Their schematic structures are shown in Figure 5. The amounts of copolymer **7** on silica beads **14–16** were quantified by hydrolyzing the beads with 6*N* HCl at 110°C for 12 h, followed by measurement of the radioactivities of the supernatants. The radioactivities and amounts of copolymer bound on silica **14–16** are shown in Table II. To estimate the nonspecific adsorption of copolymer on silica surface, the radioactivities of physically adsorbed copolymer **7** on beads **8, 10,** and **11** were included for comparison. The results suggest that the amounts of covalently bound and of nonspecific adsorption of HPMA copolymer decreased as the length of PEO spacer increased.

Hydrolytic Stability of α-Methylphenacyl Bond

Hydrolytic Stability of α-Methylphenacyl Bond in Solution in the Dark

Table III shows the degree of hydrolysis of α-methylphenacyl bond in copolymer **5** at different pH's. As expected the ester bond (see structure of copolymer **5** in Fig. 2) between [^{3}H]-Boc-glycine and the polymeric backbone was more stable toward hydrolysis under acidic rather than alkaline conditions, yet the extreme instability in pH 7.2 buffer (close to pH of human blood) was somewhat surprising. Copolymer **5** was almost completely hydrolyzed within minutes in more alkaline conditions, i.e., at pH's 9.5 and 10.7. The time course of copolymer **5** hydrolysis at pH 7.0 and 7.2 at 37°C is shown in Figure 6. At pH 7.2, 90% hydrolysis occurred within 10 h.

Hydrolytic Stability of α-Methylphenacyl Bond at the Solid–Liquid Interface in the Dark

The hydrolytic stability of the α-methylphenacyl bond at the solid–liquid interface is shown in Figure 7. Again, as expected, the bond is stable in pH 4.5 and unstable in pH 7.2 at 37°C. However, the rate of hydrolysis at pH 7.2 at the solid–liquid interface was considerably slower when compared to the hydrolysis in solution (compare curve A, Fig. 6 with curve A, Fig. 7; 90% of bonds were hydrolyzed in solution within 10 h, whereas only 30% at the surface). It appears that the surface has a stabilizing effect against hydrolysis. This anchoring bond was completely stable at the solid–liquid interface in 50% TFA/CH_2Cl_2, but it was labile toward hydrolysis in solution (data not shown). This was consistent with previously published data.[15]

Photocleavage

Photocleavage in Solution

The photocleavage of copolymer **5** was carried out in ethanolic and methanolic solutions in a quartz cuvette under nitrogen atmosphere. During irradiation, the Boc-Gly bound via α-methylphenacyl group was released from the polymeric support. The structure of the released ligand (Boc-Gly) was confirmed by TLC.[14] Figure 8 shows the rates of photocleavage release in methanolic and ethanolic solutions (the photocleavage rate of Boc-Gly from HPMA copolymer containing 2-nitrobenzyl group in methanol solution is included for comparison[3]). The rate of photocleavage of the HPMA copolymer containing the

Table III Hydrolytic Stabilities of Copolymer 5 at 37°C at Different pH[a]

pH	% of Hydrolysis
2[b]	< 5
4.5[b]	< 5
7.2[b]	96
9.5	Almost completely hydrolyzed within minutes
10.7	Almost completely hydrolyzed within minutes

[a] Buffers: pH 2—hydrochloric acid/potassium chloride buffer; pH 4.5—citrate/phosphate buffer; pH 7.2—phosphate buffer; pH 9.5 and 10.7—carbonate/bicarbonate buffer.
[b] Incubation for 10 h.

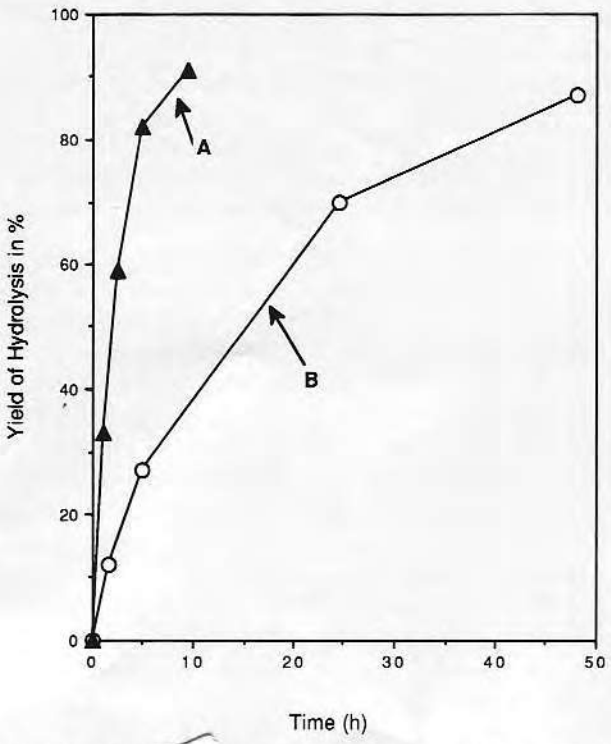

Figure 6 ...dependent hydrolysis of α-methylphenacyl bo... ...olution: (A) in pH 7.2 phosphate buffer at 37°C; (B ... in pH 7.0 phosphate buffer at room temperature.

α-methylphenacyl group in ethanol was faster than in methanol (Fig. 8). The rate of the 2-nitrobenzyl group cleavage in methanol was intermediate between the other two rates.

Photocleavage at Solid–Liquid Interface

The rates of photocleavage of copolymer-derivatized silica beads **14**, **15**, and **16** in ethanol are shown in Figure 9. In all three silica beads the patterns of photocleavage were similar. The half-lives of photolysis of **14**, **15**, and **16** were approximately 12, 8, and 7 h, respectively. Photolysis for all three bead systems proceeded rapidly in the first 2 h, with more than 20% of ligand release in the first hour. The rate of photolysis increased with an increase in the length of the PEO spacer.

DISCUSSION

The ultimate aim of this series of papers is to determine the feasibility of the development of a ligand delivery system which is remotely controlled by light. Basically the ligand, e.g., fluorescein-labeled or radioactive antigen, is coupled via a photolabile bond to a polymer matrix. Irradiation of light of the proper intensity and wavelength results in bond breakage, providing a released ligand, which then competes with circulating ligand for the antibody binding sites on the sensor surface.[2] In this way, an immunosensor that is remote and continuous with sensitivity and specificity can be developed.[16]

Sensors with different geometries can be developed. Their design may be based on two optical fibers, two-plate geometry or capillary-fill devices.[17] Regardless of geometry, fluoroimmunosensors are based on the competitive binding of antigen (or hapten) and an (optically) released fluorescently labeled antigen to an immobilized antibody. The detection of the antigen–antibody reaction at the solid–liquid interface can be performed using total internal reflection fluorescence.[2]

This study, however, focuses on the possibility to release a model ligand (Boc-Gly) bound via α-methylphenacyl bonds to a polymeric carrier under optical control both in solution and at a solid–liquid interface.

Type of Bond between the Carrier and Ligand

There are many types of photocleavable bonds used in organic synthesis.[18] Among these, the α-methyl-

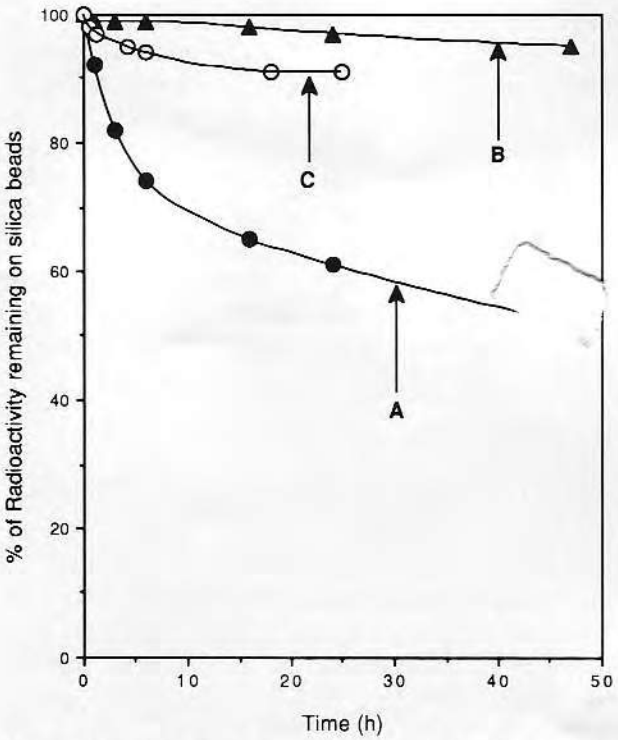

Figure 7 Stability of α-methylphenacyl bonds at solid–liquid interface: (A) in pH 7.2 phosphate buffer at 37°C; (B) in pH 4.5 citrate/phosphate buffer at 37°C; (C) in 50% TFA/CH_2Cl_2 at room temperature.

phenacyl ester bond[19] is of particular interest since it can be readily introduced into polymer matrices.[20] This bond was used as an anchoring linkage between peptide chains and polymer supports in solid and liquid phase peptide synthesis. For example, it was shown that the photolytic rate of tetrapeptide release from a styrene–divinylbenzene copolymer was faster when bound via an α-methylphenacyl bond than when bound via the more frequently used 2-nitrobenzyl bond.[15]

The α-methylphenacyl bond has low-lying excited states because of the interaction of the electrons between the carbonyl group and the phenyl ring. Such interactions render this group photolytically cleavable.[19] The photolytic mechanism is considered to be a simple radical scission of the carbon–oxygen bond.[19] It should be pointed out that the rate of photolytic cleavage of the α-methylphenacyl group is solvent-dependent. The solvents used should behave as hydrogen donors to accelerate the reaction. The photolytic mechanism is shown below[19]:

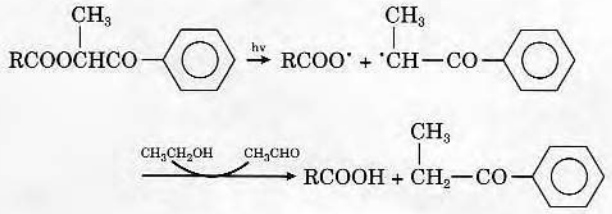

Synthesis

The copolymer **5** used for the photocleavage study in the solution was prepared by copolymerization of HPMA with comonomer **4** containing Boc-Gly bound via an α-methylphenacyl group. To study the photocleavage at a solid–liquid interface a water soluble HPMA copolymer was synthesized which contained additional side chains terminated in NH_2 groups. APS modified porous silica (beads **8**) was used as a solid support. Primary amino groups on its surface (14 nmol/mg) were converted to aldehyde groups by reaction with an excess of glutaraldehyde (beads **9**). Two pH's were used for this reaction, pH 8.6 and 9.5. The resulting beads **9** did not contain any remaining NH_2 groups indicating total conversion. The subsequent reaction was the attachment of α,ω-diaminopoly(ethylene oxide)s. The resulting beads **10** and **11** had a higher content of NH_2 groups when beads **9** were prepared at pH 8.6 (batch A) than those prepared at pH 9.5 (batch B). This indicated that in the latter case part of the aldehyde groups were consumed by polymerization at the surface resulting from aldol condensation.[21–23] Consequently, only silica beads prepared at pH 8.6 (batch A) were used for further investigation.

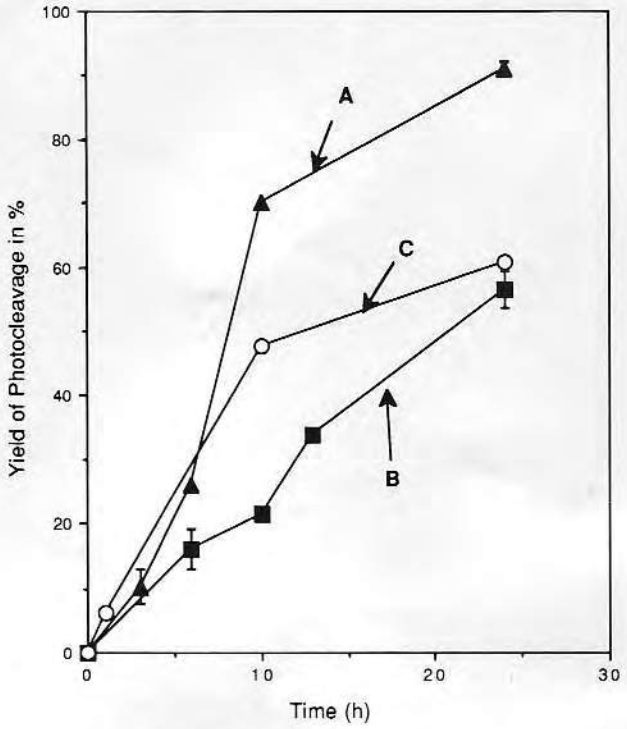

Figure 8 Cleavage of Boc-Gly obtained by photolysis of HPMA copolymers: (A) copolymer 5 in ethanol; (B) copolymer 5 in methanol; (C) HPMA copolymer containing 2-nitrobenzyl group in methanol.[3]

The subsequent reaction (Fig. 4) was again the attachment of glutaraldehyde to beads **10** and **11**. This reaction was not fully complete, resulting beads **12** and **13** contained a small amount of residual NH_2 groups (Table I). The ligand was introduced at the surface by binding of copolymer **7** which contained side chains terminated in NH_2 groups to beads **9, 12,** and **13** containing terminal aldehyde groups (Table II).

The PEO spacer was chosen for this study because it exerts a unique protein-resistant property at solid–liquid interfaces, probably due to its low interfacial free energy with water, unique solution properties and molecular conformation in aqueous solution, hydrophilicity, high surface mobility, and steric stabilization effects.[11,24–26] The results obtained (Table II) demonstrate that the PEO spacer could reduce the nonspecific adsorption of HPMA copolymer **7** on modified silica surfaces. The degree of nonspecific adsorption of HPMA copolymers on silica surface may depend on several factors, e.g., on the density of PEO chains on the surface and on

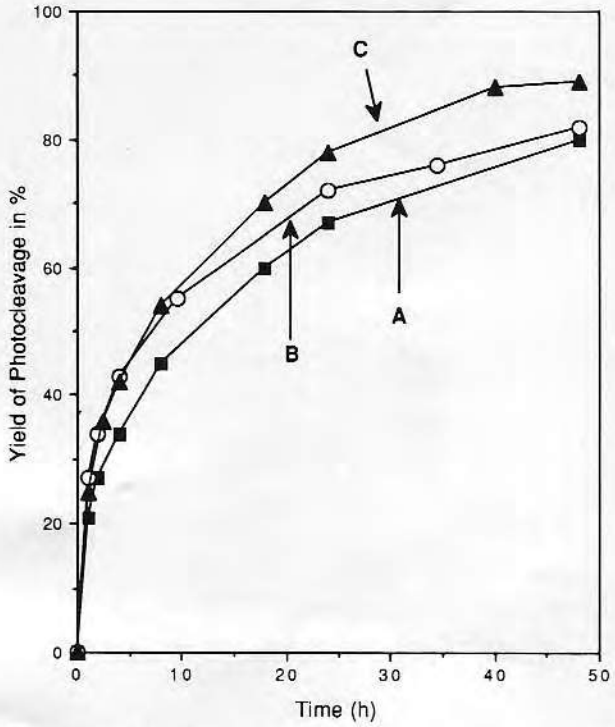

Figure 9 Photocleavage of copolymer **7**-containing silica beads **14** (A), **15** (B), and **16** (C) in ethanol.

their molecular weight. Because of the similar specific surface areas of beads studied,[11] similar content of amino groups at the surface of silica beads **10** and **11** (Table I), and the low possibility for loop formation during PEO attachment (under experimental conditions used), the packing density of PEO chains on surfaces of beads **10** and **11** should be similar. Consequently, the decrease of nonspecific adsorption of copolymer **7**, with increasing length of PEO spacers observed, reflects the molecular weight influence. The amount of covalently bound copolymer **7** on the silica beads also decreased as the length of PEO spacer increased. This is probably due to the lower concentration of free aldehyde groups on silica beads **12** and **13** than on silica beads **9**.

Hydrolytic Stability

During synthesis, the lability of the α-methylphenacyl bond toward acidic conditions was observed in solution. Rapid loss of radioactivity from copolymer backbone (**5**) occurred in 30 wt % HCl/MeOH, 25 and 50% trifluoroacetic acid (TFA)/CH_2Cl_2 at room temperature. The rate of hydrolysis in aqueous solution increased with increasing pH. The increased susceptibility to hydrolysis in alkaline pH's may be due to the polar effect of the carbonyl near the phenyl group[27] and the formation of hydrogen bonds between the acyl oxygen of the ester bond and the hydrogen of amide bond.

On the other hand, when the α-methylphenacyl group was bound at the solid–liquid interface, the surface offered surface-stabilizing effect to improve the resistance to hydrolysis. Wang showed that the α-methylphenacyl ester bond in Z—Lys(Z)—Phe—Phe—Gly—$OCH(CH_3)$—CO—C_6H_4-resin (crosslinked polystyrene beads) was stable against 50% TFA/CH_2Cl_2,[15] and we have observed the same. The surface stabilizing effect is not unexpected. Went et al.[28] studied the hydrolysis of polyacrylamide attached to polystyrene latex particles. The rate of hydrolysis of the former was significantly lower when compared to the rate of polyacrylamide hydrolysis in solution. Apparently, conformational changes of an attached polymer are restricted so that hydrolysis in the regions far from surface is more likely. Consequently, in alkaline solution, due to the concentration of charged carboxylic groups in the peripheral zones of the attached polymer, the repulsion of incoming hydroxyl ions is enhanced, leading to a reduced rate of hydrolysis.[28]

Photocleavage

The photocleavage of copolymer **5** in solution is shown on Figure 8. In both solvents used, methanol and ethanol, the cleavage was fast and approximately linear to 60% of Boc-Gly released. The rate of photocleavage was faster in ethanol than in methanol. During the photocleavage of α-methylphenacyl bond the solvent serves as a hydrogen donor. The differences in the rate of photocleavage can be attributed to the fact that ethanol is a better hydrogen donor. This is consistent with the observation that the rate of photofading of aqueous alcohol solutions of dyes increases with increasing susceptibility of the alcohol towards hydrogen atom abstraction, viz. methanol < ethanol,[29] as well as with the higher chain transfer constant to ethanol than to methanol during polymerization of butyl acrylate.[30]

At the solid–liquid interface the photorelease of Boc-Gly from beads **14**, **15**, and **16** was evaluated in ethanol (Fig. 9). At the onset of photolysis the rate of release was the same. As photolysis continued, the rate of Boc-Gly release was faster for the beads with PEO spacers (beads **15** and **16**) compared to the bead without spacer (bead **14**). The results were similar to the photolytic data obtained with 2-nitrobenzyl photocleavable bonds.[31] The short interval of fast and nearly linear ligand release

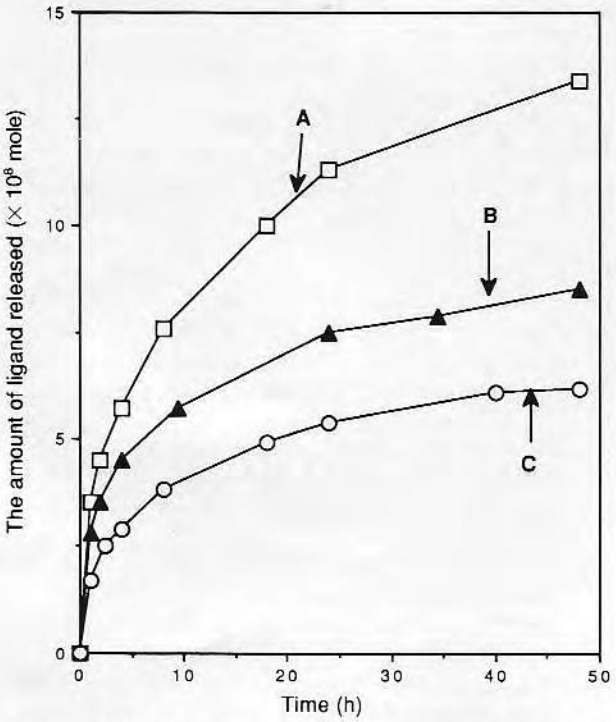

Figure 10 The amount of photoreleased ligand from 50 mg of silica beads **14** (A), **15** (B), and **16** (C) in ethanol.

would be most suitable for ligand delivery applications.

The differences in photolytic rates between **14, 15,** and **16** could be due to the change of microenvironment at the solid–liquid interface, resulting in the change in quantum yield of this photolytic reaction. One possible explanation lies in the flexibility of the PEO spacer.[32,33] The higher mobility of the PEO spacer might make the surface-bound polymer more flexible. Under the photolytic condition, i.e., a nonpolarized light source (medium-pressure mercury lamp), the more mobile polymer would have a higher efficiency of light adsorption and result in a higher photolytic rate.

For developing an optical controlled ligand delivery system several factors, e.g., the amount of photocleavable ligand chemically bound on the surface, nonspecific adsorption, and the rate of photolysis, should be optimized. The capacity of repetitious usage of this system is dependent on the amount of ligand chemically bound on the surface. Nonspecific adsorption can influence the long-term stability of this ligand delivery system due to exposure to different test solutions and body fluids. This problem can be minimized using PEO spacers.[11] The rate of photolysis will influence the operation speed of this delivery system. Figure 10 shows the amount of ligand released vs. time for 50 mg of silica beads **14, 15,** and **16** in ethanol. It showed that the total amount of ligand released decreased with an increase of the length of the PEO spacer, because the amount of ligand which was chemically bound on silica surface decreased (Table II) with the increase of the length of PEO spacer. For silica beads **14,** the amount of ligand loaded on silica surface was the largest, yet the rate of photolysis was lowest and the ability to prevent nonspecific adsorption was poorest. On the other hand, although silica **16** showed the highest rate of photolysis and good capacity for preventing nonspecific adsorption, the amount of ligand chemically bound on surface was the lowest. A simple way to increase load of ligand on surface would be to incorporate a higher mol % of photoreleasable ligand into the copolymer (in this model study, the copolymer **7** contained only 1.4 mol % of side chains terminated with photocleavable ligand).

From the experiments on the photocleavage of α-methylphenacyl bond in solution and at the solid–liquid interface, it may be concluded that in solution the photolysis rate was greater in ethanol than in methanol, perhaps due to the higher hydrogen donor capacity of ethanol. At the solid–liquid interface, the rate of photorelease increased as the length of PEO spacer increased. Although the instability of this bond toward alkaline hydrolysis would limit its application for sensors used *in situ,* it still has the potential to be applied as a ligand delivery system in organic solvents. From another point of view the alkaline hydrolytic property could also be used as a tool for pH-dependent ligand delivery, e.g., in stimuli-sensitive delivery systems, such as hydrogels or liposomes.[34]

The work was partially supported by NSF Grant ECS-85-02107 and by the University of Utah Research Committee. We thank Drs. V. Šubr and P. Kopečková for advice and synthesis assistance and Dr. S. Nagaoka (Toray Industries, Inc., Kanagawa, Japan) for the kind gift of α,ω diaminopoly(ethylene oxide)s.

REFERENCES

1. K. Newby, W. M. Reichert, J. D. Andrade, and R. E. Benner, *Appl. Opti.,* **23,** 1812 (1984).
2. J. D. Andrade, J. Herron, J. N. Lin, H. Yen, J. Kopeček, and P. Kopečková, *Biomaterials,* **9,** 76 (1988).
3. H. R. Yen, J. Kopeček, and J. D. Andrade, *Makromol. Chem.,* **190,** 69 (1989).
4. J. D. Andrade, J.-N. Lin, J. Herron, M. Reichert, and J. Kopeček, *Proc. SPIE Int. Soc. Opt. Eng.,* **718,** 280 (1986).

5. J. Kopeček, in *IUPAC Macromolecules,* H. Benoit and P. Rempp, Eds., Pergamon, Oxford, 1982, p. 305.
6. J. Strohalm and J. Kopeček, *Angew. Makromol. Chem.,* **70,** 109 (1978).
7. G. B. Butler and G. R. Myers, *J. Macromol. Sci. Chem.,* **A5,** 105 (1971).
8. J. Kopeček, P. Rejmanová, and V. Chytrý, *Makromol. Chem.,* **182,** 799 (1981).
9. J. Kopeček and P. Rejmanovà, *J. Polym. Chem. Polym. Symp.,* **66,** 15 (1979).
10. S. Moore and W. H. Stein, *J. Biol. Chem.,* **176,** 367 (1948).
11. P. Kopečkovà, J. Kopeček, and J. D. Andrade, *New Polym. Mater.,* **1,** 289 (1990).
12. F. T. Weiss, in *Determination of Organic Compounds,* P. J. Eiving and I. M. Kolthof, Eds., Wiley, New York, 1970, p. 92.
13. T. T. Ngo, *J. Biochem. Biophys. Methods,* **12,** 349 (1986).
14. F. S. Tjoeng, W. Staines, S. St.-Pierre, and R. S. Hodges, *Biochim. Biophys. Acta,* **490,** 489 (1977).
15. Su-Sun Wang, *J. Org. Chem.,* **41,** 3258 (1976).
16. J. D. Andrade, R. Van Wagenen, D. Gregonis, K. Newby, and J-N. Lin, *IEEE Trans. Electron. Dev.,* **ED-32,** 1175 (1985).
17. R. A. Badley, R. A. L. Drake, I. A. Shanks, A. M. Smith, and P. R. Stephenson, *Phil. Trans. R. Soc. Lond.,* **B316,** 143 (1987).
18. V. N. R. Pillai, *Synthesis,* 1 (1980).
19. J. C. Sheehan and K. Umezawa, *J. Org. Chem.,* **38,** 3771 (1973).
20. T. Mizoguchi, K. Shigezane, and N. Takamura, *Chem. Pharm. Bull.,* **18,** 1465 (1970).
21. F. M. Richard and J. R. Knowles, *J. Mol. Biol.,* **37,** 231–233 (1968).
22. A. H. Korn, S. H. Feairheller, and E. M. Filachione, *J. Mol. Biol.,* **65,** 525 (1972).
23. P. Monsan, *J. Mol. Catal.,* **3,** 371 (1977/1978).
24. J. D. Andrade, *Med. Instrum.,* **7,** 110 (1973).
25. S. Nagaoka, Y. Mori, H. Tanzawa, and S. Nishiumi, in *Polymers as Biomaterials,* S. W. Shalaby, A. S. Hoffman, B. D. Ratner, and T. A. Horbett, Eds., Plenum, New York, 1984, p. 361.
26. D. W. J. Osmond, B. Vincent, and F. A. Waite, *Colloid Polym. Sci.,* **253,** 676 (1983).
27. C. K. Ingold, *Structure and Mechanism in Organic Chemistry,* 2nd ed., Cornell University Press, Ithaca, NY, 1969, p. 1131.
28. P. M. Went, R. Evans, and D. H. Napper, *J. Polym. Sci. Symp.,* **49,** 159 (1975).
29. M. Imamura and M. Koizumi, *Bull. Chem. Soc. Japan,* **29,** 899 (1956).
30. U. S. Nandi, M. Singh, and P. V. T. Raghuram, *Makromol. Chem.,* **183,** 1467 (1982).
31. H. R. Yen, J. D. Andrade, and J. Kopeček, *Polymer,* to appear.
32. H. Hommel, A. P. Legrand, J. Lecourtier, and J. Desbarres, *Eur. Polym. J.,* **15,** 993 (1979).
33. S. Nagaoka, *Trans. Am. Soc. Intern. Organs,* **10,** 76 (1988).
34. A. Kusumi, S. Nakahama, and K. Yamaguchi, *Chem. Lett. (Jpn.),* 433 (1989).

Received August 16, 1990
Accepted January 3, 1991

Optically controlled ligand delivery: 3. Photocleavage of 2-nitrobenzyl bonds at solid–liquid interfaces

Hung-Ren Homer Yen, Joseph D. Andrade and Jindřich Kopeček*
Departments of Material Science and Engineering, and Bioengineering, University of Utah, Salt Lake City, Utah 84112, USA
(Received 20 December 1990; revised 5 April 1991; accepted 17 April 1991)

Optically controlled ligand delivery systems would be useful for the design and development of biosensors. We synthesized a *N*-(2-hydroxypropyl)methacrylamide (HPMA) copolymer containing sidechains terminated in model ligand (Boc–Gly), bound via photocleavable 2-nitrobenzyl bonds. To study photocleavage at solid–liquid interfaces, the HPMA copolymer was covalently attached to 3-aminopropyl triethoxy silane (APS)-coated porous silica beads, which were modified with α,ω-diaminopoly(ethylene oxide) of molecular weight 1000 or 5000. The influence of the poly(ethylene oxide) (PEO) spacer on the rate of photolysis and on the minimization of non-specific adsorption was determined. The results show that the photolytic rates are faster for copolymer-derivatized silicas with PEO spacers compared to that without spacer and that the PEO spacer reduces the non-specific adsorption of HPMA copolymer on the silica surface.

(Keywords: ligand delivery; optical control; 2-nitrobenzyl bonds)

INTRODUCTION

The combination of the specificity of antibody–antigen (Ab–Ag) interactions and sensitivity of competitive binding assays using labelled Ag or labelled Ab can be applied to the development of biosensors[1]. Such fibre-optic, or waveguide-based sensors could be used in a continuous or semicontinuous mode[1]. One type of sensor is based on remotely controlled ligand delivery and total internal reflection fluorescence (t.i.r.f.) sensing[2].

This series of papers focuses on one key part of this sensor research: optical ligand delivery[3,4]. In the first paper HPMA copolymers with ligands (Boc–Gly, fluorescein and tetramethylrhodamine) bound via 2-nitrobenzyl bonds were synthesized and their photocleavage in solution studied[3]. The second paper focused on the synthesis of HPMA copolymer-derivatized silica beads with ligand, Boc–Gly, bound via the α-methylphenacyl group and on the study of their photocleavage, both in solution and at the solid–liquid interface[4].

Silica was used as a solid support because of its optical properties; especially its high optical transmission, low fluorescence and relatively high refractive index. The last of these permits the use of total internal reflection optics as a means to excite fluorescence on the solution side of the solid–liquid interface without exciting bulk fluorescence in the solution phase[5,6].

In this paper we present a HPMA copolymer containing sidechains terminated in model ligand (Boc–Gly) bound via 2-nitrobenzyl groups. This copolymer was used to study the photocleavage reaction at the solid–liquid interface. Copolymers at the solid (silica beads)–liquid interface were exposed to light, resulting in release of the bound ligand. The dependence of the rate of cleavage on the presence of the PEO spacer was determined.

* Correspondence should be addressed to: J. Kopeček, Department of Bioengineering, 2480 MEB, University of Utah, Salt Lake City, Utah 84112, USA

EXPERIMENTAL

Materials

Porous silica beads, 3-aminopropyl triethoxy silane (APS)-coated, 30–40 mesh, 37.5 nm pore size, were obtained from Fluka. Glutaraldehyde (GLU), 25% solution in water, E.M. Grade, was supplied by Polysciences. Diamines: NH_2–PEO_{1000}–NH_2 and NH_2–PEO_{5000}–NH_2 were a kind gift from Dr S. Nagaoka (Toray Industries, Inc., Kanagawa, Japan).

Synthesis

N-(2-Hydroxypropyl)methacrylamide (HPMA) was prepared as described previously, melting point 69–70°C (reference 7, melting point 69–70°C). 4-[N-(tert-Butoxycarbonyl)glycyloxymethyl]-3-nitrobenzoic acid was prepared by a series of reactions as described previously, melting point 163–164°C (reference 8, melting point 159–160°C).

Copolymer **1** (*Figure 1*) was prepared by radical copolymerization of HPMA and N-(3-aminopropyl)-methacrylamide hydrochloride (mole ratio 85:15) in methanol (12.5 wt% of monomer, 0.6 wt% of AIBN as initiator) as described previously[3,4,9]. The content of monomeric units of N-(3-aminopropyl)methacrylamide was found to be 8.7 mol% by using the ninhydrin method[10]. The weight- and number-average molecular weights of copolymer **8** ($M_w = 51\,000$, $M_w/M_n = 1.6$) were estimated from the g.p.c. analysis on Sepharose 4B/6B[11].

Copolymer **2** (*Figure 2*) was prepared by polymer-analogous reaction of copolymer **1** with 4-[N-(tert-butoxycarbonyl)glycyloxymethyl]-3-nitrobenzoic acid by

0032-3861/92/081763-05

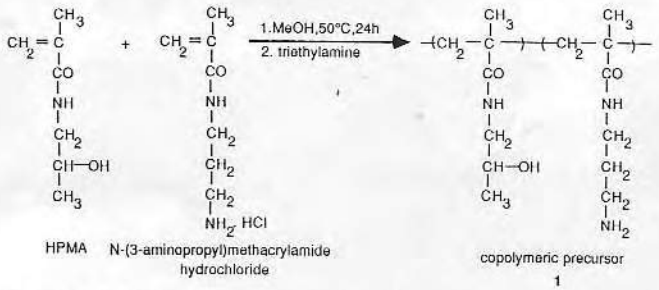

Figure 1 The preparation of copolymer **1**

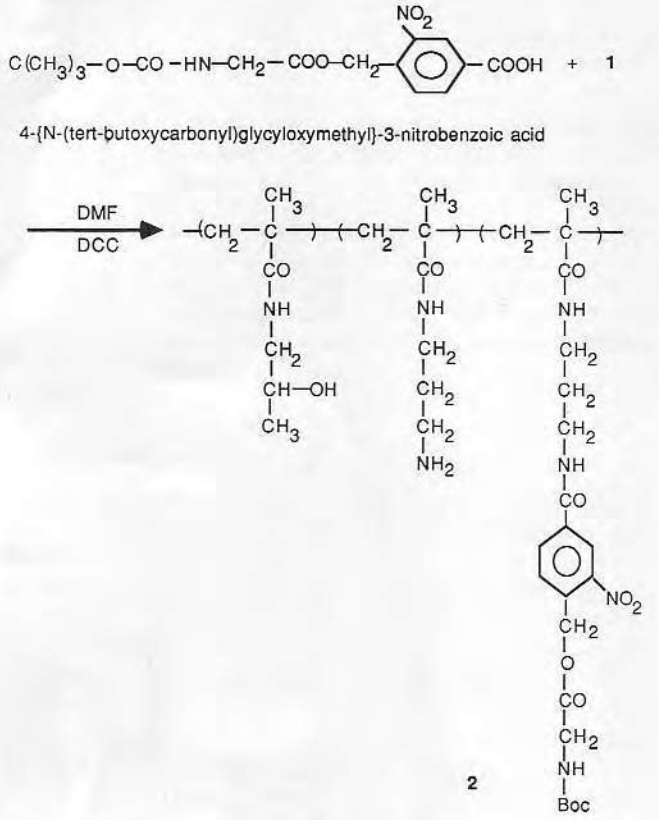

Figure 2 The preparation of copolymer **2**

using the dicyclohexylcarbodiimide (DCC) method[3]. The content of remaining sidechains containing free amino groups in copolymer **2** was calculated to be 5.0 mol% by using the ninhydrin method[10]. Consequently, 3.7 mol% of sidechains in copolymer **2** were terminated with Boc–Gly bound via 2-nitrobenzyl groups.

Modification of silica beads

The silica beads were modified according to procedures previously described[4,12] (*Figure 3*). The concentration of amino groups on the modified beads (**3–8**) was determined by using N-succinimidyl-3-(2-pyridyldithio)-propionate (SPDP)[13].

Preparation of copolymer-derivatized silica beads:)–APS–GLU(glutaraldehyde)–CH_2–NH–copolymer **2** (**9**),)–APS–GLU–PEO_{1000}–GLU–CH_2–NH–copolymer **2** (**10**) and)–APS–GLU–PEO_{5000}–GLU–CH_2–NH–copolymer **2** (**11**).

Beads **4**, **7** and **8** (250 mg) were treated with excess of copolymer **2** (125 mg) in DMSO. The azomethine bond (–CH=N–) was further reduced by reaction with 50 mg $NaCNBH_3$ in pH 4.5 citrate/phosphate buffer. At the end of reduction, the beads were further soaked in pH 4.5 buffer under shaking. After two days of soaking, the beads were dried and the binding efficiency was quantified by the use of amino-acid analysis.

Non-specific adsorption of copolymer **2** *to silica beads*

To estimate the extent of the non-specific adsorption of copolymer **2**, beads **3**, **5** and **6** were incubated with copolymer **2**, as described above. Beads with physically adsorbed copolymer **2** were numbered **12**, **13** and **14**, respectively.

Quantification of the surface-bound copolymer on silica surface

The amount of surface-bound (by covalent or physical bonds) copolymer **2** on silica beads was quantified by amino-acid analysis. During the hydrolysis procedure, the Boc group of the Boc–Gly bound to the copolymer **2** was removed by acidolysis and the glycine obtained could be quantified by high-pressure liquid chromatography (h.p.l.c.). Hydrolysis was performed according to Scotchler *et al.*[14]. All analyses were performed on a 1084 A Liquid Chromatograph (Hewlett–Packard) by using a Beckman Column No. 235330 (4.6 mm × 15 cm), Model Ultrasphere (5 μm diameter beads).

Photocleavage

Thirty milligrams of copolymer-**2**-derivatized silica beads (**9**, **10** and **11**) and 0.5 ml pH 7.2 PBS buffer or 0.5 ml pH 4.5 citrate/phosphate buffer were poured into

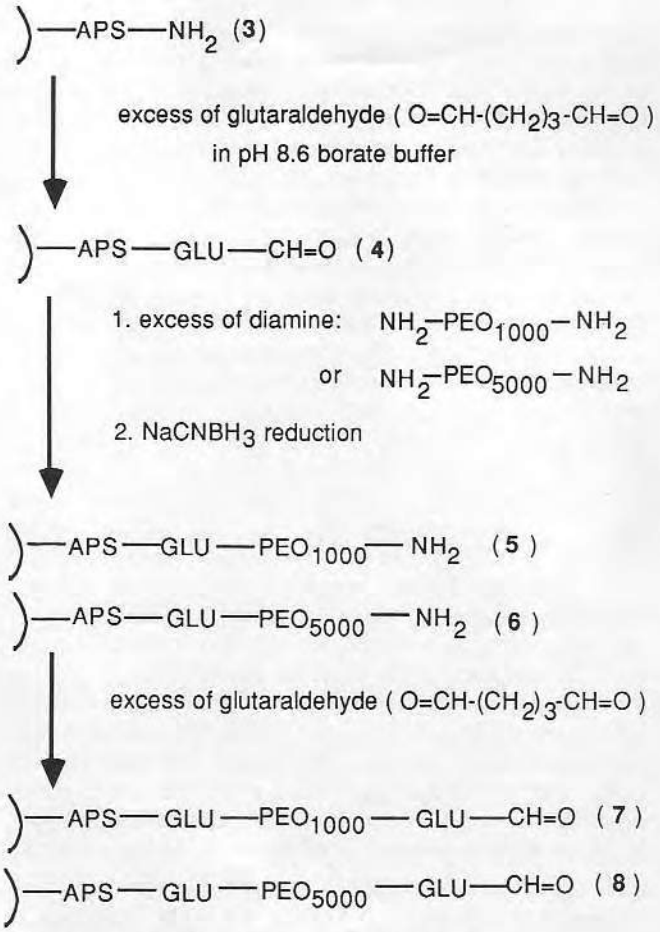

Figure 3 Modification of porous silica beads **3–8**

Table 1 The properties of the modified silica beads **3–8**

Silica beads[a] No.	Schematic structures	Content of amino groups (NH_2) (nmol mg^{-1})	Specific surface area ($m^2\ g^{-1}$)
3	)–APS–NH_2	14	33.4
4	)–APS–GLU–CH=O	0	–
5	)–APS–GLU–PEO_{1000}–NH_2	9	29.4
6	)–APS–GLU–PEO_{5000}–NH_2	10	31.0
7	)–APS–GLU–PEO_{1000}–GLU–CH=O	1	–
8	)–APS–GLU–PEO_{5000}–GLU–CH=O	2	30.6

[a]For experimental details see reference 4. Reaction with glutaraldehyde was performed at pH 8.6

a u.v. quartz cylindrical cell with Teflon stopper. The cell was attached to a rotator (Clas-Col Co.) and a speed of 60 rev min^{-1} was used, so that during irradiation a centrifugal force gently agitated the beads to ensure even light access. The cell was irradiated with an LH 150 mercury lamp (200 W, Schoeffel Instr. Co). The light was first focused by a fused silica lens, then reflected by a dichroic-coating mirror (Oriel Corp.), which reflected only the wavelengths between 260 nm and 340 nm (the major intense emission peaks are 296 nm and 312 nm). At chosen time intervals, the supernatant was withdrawn and the beads were washed with water, ethanol, ether and dried. Then the beads were analysed by using amino-acid analysis. The decrease of the amount of surface-bound glycine after irradiation reflected the amount of photo-released ligand. Controls were kept in the dark.

RESULTS

Synthesis

To prepare the copolymer suitable for ligand delivery system, a HPMA and *N*-(3-aminopropyl)methacrylamide hydrochloride copolymer precursor **1** (*Figure 1*) was synthesized. Copolymer **2** (*Figure 2*), containing side-chains with 2-nitrobenzyl bonds, was prepared by reacting copolymer **1** with 4-[N-(tert-butoxycarbonyl)-glycyloxymethyl]-3-nitrobenzoic acid using the DCC method. The remaining free amino groups of copolymer **2** could be further reacted with the functionalized silica surface, i.e. silica beads with terminal aldehyde groups.

Modification of silica

The modification of porous silica beads is shown schematically in *Figure 3*, and their properties are given in *Table 1*[4,12]. The APS-coated beads **3** contained 14 nmol mg^{-1} of amino groups. After reaction with glutaraldehyde, practically all amino groups were converted to aldehyde groups (beads **4**). The latter were modified with PEO diamines. The resulting beads **5** and **6** contained 9 and 10 nmol mg^{-1} of terminal amino groups, respectively. Owing to the incomplete reaction of beads **5** and **6** with glutaraldehyde, beads **7** and **8** still contained less than 2 nmol mg^{-1} of unreacted amino groups on surfaces (*Table 1*). The surface areas of the beads did not show any dramatic change during these polymer-analogous reactions (*Table 1*).

Copolymer-derivatized silica beads

Silica beads **9**, **10** and **11** were synthesized by reacting copolymer **2** with silica beads **4**, **7** and **8**, respectively. The amounts of copolymer **2** on silica beads **9**, **10** and **11** were quantified by hydrolysing the beads with propionic/hydrochloric acid (50:50, v/v) for 1 h, followed by amino-acid analysis. The amounts of Boc–Gly bound on silica **9**, **10** and **11** are shown in *Table 2*. To estimate the non-specific adsorption of copolymer on the silica surface, the amounts of physically adsorbed copolymer **2** on silica beads **3**, **5** and **6** were included for comparison. The amounts of non-specific adsorption of HPMA copolymer were very limited. The results suggest that the amounts of covalently bound and of adsorbed HPMA copolymer decreased as the length (molecular weight) of the PEO spacer increased.

Table 2 The amounts of Boc–Gly bound on modified silica beads **9–14**

Beads No.	Amount of bound Boc–Gly	
	nmol per 50 mg of beads	nmol per m^2[a]
9[b]	267	178
10[b]	164	109
11[b]	128	85
12[c]	16	11
13[c]	10	7
14[c]	6	4

[a]The specific surface area of 30 $m^2\ g^{-1}$ of beads was used as a basis for calculation
[b]Covalent attachment to beads **4**, **7** and **8**, respectively
[c]Non-specific adsorption on beads **3**, **5** and **6**, respectively

Photocleavage

The rates of photocleavage of copolymer-derivatized silica beads **9**, **10** and **11** in pH 4.5 citrate/phosphate buffer are shown in *Figure 4*. In all three silica beads the patterns of photocleavage were similar. The half-lives of photolysis of **9**, **10** and **11** were approximately 2, 1 and 1 h, respectively. The rates of photolysis are similar for both beads with PEO_{1000} and PEO_{5000} spacers and faster than those of beads without PEO spacer. Photolysis for all three bead systems proceeded rapidly in the first hour, with more than 35% of ligand released.

The photolytic yield after 5 h irradiation for silica beads **9**, **10** and **11** in pH 7.2 PBS buffer were 78%, 87% and 85%, respectively (results not shown). These results were almost the same as the data obtained in pH 4.5 citrate/phosphate buffer (77%, 85% and 86% for silica **9**, **10** and **11**, respectively).

DISCUSSION

Immunoassays for clinical medicine often use the competitive binding principle[15], which requires the availability

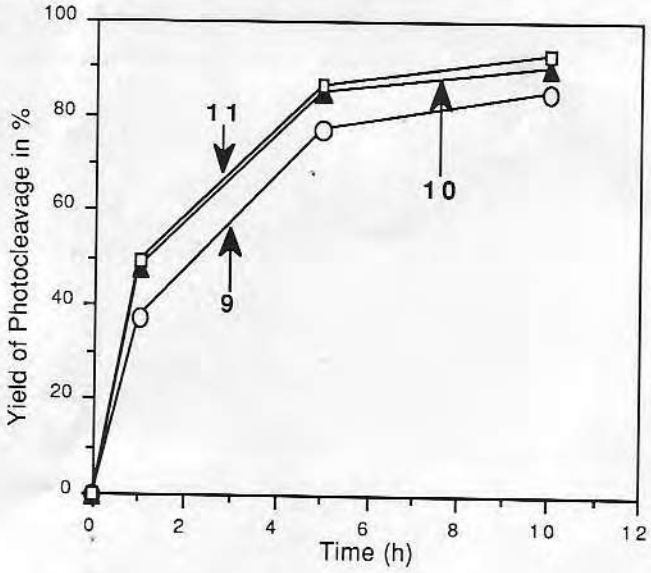

Figure 4 Photocleavage of copolymer-2-derivatized silica beads **9**, **10** and **11** in pH 4.5 citrate/phosphate buffer

of a labelled competing reagent with identical binding properties to the analyte. As our approach to remote sensing is optical, we have chosen to develop an on-demand, optically based, reagent delivery technology. Basically the ligand, e.g. fluorescein-labelled or radioisotope-labelled antigen, is coupled via a photolabile bond to a polymer matrix. Exposure to light of the proper intensity and wavelength results in bond breakage, providing released ligand, which then competes with circulating ligand for the antibody binding sites on the sensor surface[2]. In this way, an immunosensor that is remote and continuous can be developed[16].

This study focuses on means of releasing a model ligand (Boc–Gly) at the solid–liquid interface under optical control. Boc–Gly was attached to a surface-bound polymeric carrier via 2-nitrobenzyl bonds.

Type of bond between the carrier and ligand

The 2-nitrobenzyl group[17] is widely used in polymer-based peptide synthesis, both in solid[18] and in liquid phases[19–21], and in light-flash physiology[22–24] (the application of the light-flash technique to photosensitive molecules to study how intracellular messengers act). During irradiation of aromatic nitro compounds, which have a C–H bond in the *ortho*-position, the nitro group is reduced to a nitroso group[17] and an oxygen is inserted into the C–H bond at the *ortho*-position, followed by rearrangement to a more stable structure.

Copolymer-derivatized silica beads

PEO spacers were chosen for this study because PEO has a unique protein-resistant property at solid–liquid interfaces, probably due to its low interfacial free energy with water, unique solution properties and molecular conformation in aqueous solution, hydrophilicity, high surface mobility and steric stabilization effects[12,25–27]. The results (*Table 2*) demonstrate that the PEO spacer reduces the non-specific adsorption of HPMA copolymer **2** on modified silica surfaces. The degree of non-specific adsorption of HPMA copolymer on silica surfaces may be dependent on several factors, e.g. on the density of PEO chains on the surface and on their molecular weight. Because of the similar specific surface areas of beads studied (*Table 1*), similar content of amino groups at the surface of silica beads **5** and **6** (*Table 1*), and the low possibility for loop formation during PEO attachment (under experimental conditions used)[4,12], the packing density of PEO chains on surfaces of beads **5** and **6** should be similar. Consequently, the decrease of non-specific adsorption of copolymer **2** with increasing length of PEO spacers, reflects the molecular weight influence. The amount of covalently bound copolymer **2** on the silica beads also decreased as the length of PEO spacer increased. This is probably due to the lower concentration of free aldehyde groups on silica beads **7** and **8** than on silica beads **4**.

Photocleavage at the solid–liquid interface

At the solid–liquid interface the photorelease of Boc–Gly from beads **9**, **10** and **11** was evaluated in pH 7.2 PBS buffer and pH 4.5 citrate/phosphate buffer (*Figure 4*). The photolytic rates in pH 4.5 and pH 7.2 buffers were almost the same (5 h irradiation). The rates of photolysis for **10** and **11** (with PEO spacer) were similar, but were distinctly higher compared with **9** (without PEO spacer). These results are consistent with our previous data using photocleavable α-methylphenacyl bonds[4]. The differences in photolytic rates could be due to the change of microenvironment at the solid–liquid interface, resulting in a change in quantum yield of this photolytic reaction[4]. One possible explanation is related to the flexibility of the PEO spacer[28,29]. The higher mobility of the PEO spacer might make the surface-bound polymer more flexible. Under the photolytic condition, i.e. a non-polarized light source, the more mobile polymer would have a higher efficiency of light absorption and result in a higher photolytic rate. The short interval of fast and nearly linear ligand release (the first hour of irradiation) would be most suitable for ligand delivery applications.

Several factors should be optimized for the development of an optically controlled ligand delivery system: the amount of photocleavable ligand chemically bound on the surface; minimization of non-specific adsorption; and the rate of photolysis[4]. For silica beads **9**, the amount of ligand loaded on the silica surface was the largest, yet the rate of photolysis was lowest and the ability to prevent non-specific adsorption was poorest. On the other hand, although silica **11** showed the highest rate of photolysis and good capacity for preventing non-specific adsorption, the amount of ligand chemically bound on the surface was the lowest.

CONCLUSIONS

The amino-acid analysis method was successfully applied to quantify surface-bound amino-acid ligand and the rate of photolysis at the solid–liquid interface. This method can be potentially extended as a general analytical tool to monitor the photocleavage patterns for peptide ligands.

The amount of covalently bound HPMA copolymer or ligand, i.e. Boc–Gly, on the silica surface decreases as the length of PEO spacer increases.

The PEO spacer reduces the non-specific adsorption of HPMA copolymer on the modified silica surface.

The photolytic rates of 2-nitrobenzyl bonds are faster

for copolymer-derivatized silicas with PEO spacers than for those without spacers.

It appears that the amount of photocleavable ligand chemically bound on the surface, minimization of non-specific adsorption and the photolytic rate are three major factors to be optimized before developing a ligand-delivery-system-based biosensor.

ACKNOWLEDGEMENTS

This work was partly supported by NSF Grant ECS-85-02107 and by the University of Utah Research Committee. We thank Dr P. Kopečková for advice and assistance with synthesis, Dr S. Nagaoka (Toray Industries, Inc., Kanagawa, Japan) for the kind gift of α,ω-diaminopoly-(ethylene oxide)s, and Dr S. Oscarsson and Ms Y.-G. Yan for their assistance in amino-acid analysis.

REFERENCES

1 Newby, K., Reichert, W. M., Andrade, J. D. and Benner, R. E. *Appl. Optics* 1984, **23**, 1812
2 Andrade, J. D., Herron, J., Lin, J. N., Yen, H., Kopeček, J. and Kopečková, P. *Biomaterials* 1988, **9**, 76
3 Yen, H. R., Kopeček, J. and Andrade, J. D. *Makromol. Chem.* 1989, **190**, 69
4 Yen, H. R., Andrade, J. D. and Kopeček, J. *J. Appl. Polym. Sci.* 1991, **43**, 1241
5 Hlady, V., Reinecke, D. R. and Andrade, J. D. *J. Coll. Interface Sci.* 1986, **111**, 555
6 Andrade, J. D., Lin, J.-N., Hlady, V., Herron, J., Christensen, D. and Kopeček, J. 'Biosensor Technology' (Ed. R. P. Buck, W. E. Hatfield, M. Umana and E. F. Bowden), Marcel Dekker, 1990, p. 219
7 Strohalm, J. and Kopeček, J. *Angew. Makromol. Chem.* 1978, **70**, 109
8 Hemmasi, B., Stuber, W. and Bayer, E. *Hoppe-Seyler's Z. Physiol. Chem.* 1982, **363**, 701
9 Kopeček, J., Rejmanová, P. and Chytrý, V. *Makromol. Chem.* 1981, **182**, 799
10 Moore, S. and Stein, W. H. *J. Biol. Chem.* 1948, **176**, 367
11 Kopeček, J. and Rejmanová, P. *J. Polym. Chem., Polym. Symp.* 1979, **66**, 15
12 Kopečková, P., Kopeček, J. and Andrade, J. D. *New Polym. Mater.* 1990, **1**, 289
13 Ngo, T. T. *J. Biochem. Biophys. Methods* 1986, **12**, 349
14 Scotchler, J., Lozier, R. and Robinson, A. B. *J. Org. Chem.* 1970, **35**, 3151
15 Davis, T. D., Vanderveen, R. L. and Nienhuis, M. 'Applied Clinical Pharmacokinetics' (Ed. D. Mungall), Raven Press, NY, 1983, p. 79
16 Andrade, J. D., Van Wagenen, R. A., Gregonis, D. E., Newby, K. and Lin, J. N. *IEEE Trans. Electron Devices* 1985, ED-**32**(7), 1175
17 Baltrop, J. A., Plant, P. J. and Schofield, P. *J. Chem. Soc. Chem. Commun.* 1966, 822
18 Rich, D. H. and Gurwara, S. K. *J. Chem. Soc. Chem. Commun.* 1973, 610
19 Pillai, V. N. R., Mutter, M. and Bayer, E. *Tetrahedron Lett.* 1979, 3409
20 Stuber, W., Hemmasi, B. and Bayer, E. *Int. J. Peptide Protein Res.* 1983, **22**, 277
21 Bayer, E., Dengler, M. and Hemmasi, B. *Int. J. Peptide Protein Res.* 1978, **25**, 178
22 Kaplan, J. H., Forbush, B. and Hoffman, J. F. *Biochemistry* 1978, **17**, 1929
23 Engels, J. and Reidys, R. *Experentia Basel* 1978, **34**, 14
24 Gurney, A. M. and Lester, H. A. *Physiol. Rev.* 1987, **67**(2), 583
25 Andrade, J. D. *Med. Instrum.* 1973, **7**, 110
26 Nagaoka, S., Mori, Y., Tanzawa, H. and Nishiumi, S. 'Polymers as Biomaterials' (Ed. S. W. Shalaby, A. S. Hoffman, B. D. Ratner and T. A. Horbett), Plenum Press, New York, 1984, p. 361
27 Osmond, D. W. J., Vincent, B. and Waite, F. A. *Colloid Polym. Sci.* 1983, **253**, 676
28 Hommel, H., Legrand, A. P., Lecourtier, J. and Desbarres, J. *Eur. Polym. J.* 1979, **15**, 993
29 Nagaoka, S. *Trans. Am. Soc. Intern. Organs* 1988, **10**, 76

Development of Fiber Optic Fluoroimmunoassay: Proximal vs. Distal End Collection Geometries of a Fiber Sensor

D.E.Yoshida, J.T.Ives, W.M.Reichert,
D.A.Ghristensen, and J.D.Andrade

University of Utah
Department of Electrical Engineering and Bioengineering
and Center for Sensor Technology
Salt Lake City, Utah 84112

Abstract

Evanescent fiber optic sensors are being developed for remote in situ immunoassay. The evanescently excited fluorescence can be collected from either the proximal or distal end of the sensing fiber. The tradeoffs between the two directions of collection are investigated to determine the efficiency of fluorescence detection. Tetramethylrhodamine was used as the fluorescent standard with excitation by the 514.5nm line of an argon laser. A comparison of the two collection geometries demonstrated that although the distal end collection had a higher background, similar fluorescence concentrations were detected. The immunoassay technique was demonstrated with the specific binding of tetramethylrhodamine-conjugated goat anti-human immunoglobulin G (αH-IgG) to preadsorbed H-IgG on the sensor surface. A detection limit of 14nmole/L was measured. Future improvements and disadvantages of the current optical system are discussed, as well as the importance of quantifying the protein concentration in terms of the fluorescence.

1. Introduction

Evanescent fiber optic sensors are based on the principle of total internal reflection (TIR). TIR occurs when a light beam originating in the optically denser (higher refractive index, n_1) medium hits the interface between two transparent media at an angle of reflection larger than the critical angle θ_c given by

$$\theta c = \sin^{-1}(n_2/n_1) \qquad (1)$$

During TIR, an evanescent wave is generated at the interface which decays exponentially into the optically less dense (lower refractive index, n_2) medium. The depth of penetration of the evanescent wave is approximately a third of a wavelength ($\lambda/3 \approx 1500$Å). Evanescent fields are used in fiber optic immunosensors to obtain a surface sensitive signal. In addition, the theory of reciprocity predicts that only evanescently excited fluorescence will back couple into the fiber core and propagate as a guided mode. This back coupling mechanism separates the evanescently excited fluorescence from the bulk solution fluorescence excited by scattered light.[1]

Fluoroimmunosensors based on optical fibers[2,3,4] can potentially use the evanescent surface sensitivity for in situ monitoring because a separation step is not required. Other advantages of optical fiber fluoroimmunosensors include remote detection, small size, immunity to electromagnetic interference, lack of electrical connections in the sensing area, and relatively low cost.

For an optical fiber immunosensor with the sensing region located in the fiber midsection, the back coupled fluorescence signal propagates in both directions along the optical fiber and can be collected from either the proximal (excitation incoupling) or the distal end of the fiber sensor. However, these two collection methods have several differences, such as optical system alignment, number of optical components, and elastic light background. This report presents results on characterization of the two collection methods.

Also presented are the preliminary results from the specific binding of goat anti-human immunoglobulin G (αH-IgG) to human IgG (H-IgG) adsorbed on the quartz fiber optic core. Based on these experiments and the potential in vivo application of fiber optic fluoroimmunosensors, improvements in the system design are proposed.

2. Methods

The midsection of a 600 μm optical fiber (Quartz Products) is used as the sensor. The buffer and cladding are mechanically stripped from a 3cm long midsection, then immersed in 85°C chromic acid to remove any cladding residues on the fiber core. The sensor is placed in a cylindrical flow cell to allow the introduction of solutions. The flow cell consists of two Teflon endcaps sealing the ends of a glass capillary tube (0.125" inner diameter). The fiber fits through the center of the endcaps with Teflon sealing gaskets.

Various concentrations of tetramethylrhodamine (TMR, Molecular Probes, Inc.) and tetramethylrhodamine isothiocyanate-conjugated (MRITC) αH-IgG (Sigma Chemicals) in phosphate buffered saline (PBS, pH=7.4) are prepared for the proximal vs. distal comparison and the protein experiment, respectively. The absorbance from different concentrations of TMR was measured on a Beckman spectrophotometer (Model 35). A general measure of the degree of conjugation developed by Brandtzaeg[5] was used to estimate the degree of labeling and protein concentration.

The 514.5nm light from an argon laser (Lexel Model 95) is reflected by a dichroic filter (Newport Corp.), then focused by lens (L_1) into the optic fiber for proximal end collection (Figure 2a). For the distal end collection, the laser light is focused into the optic fiber by a microscope objective (Figure 2b). The back coupled fluorescence collected from either the distal or proximal end of the fiber is first collimated by L_1, then passes through the dichroic and 514.5nm blocking filter (Pomfret), and focused by lens (L_2) into the monochromator (Instrument SA, Inc. HR-640). The output is detected by a photomultiplier tube (Hamamatsu R585) and photon counting instrumentation (EG&G Ortec).

The same experimental procedure and dye solutions were used for the two collection geometries. First, the signal at the emission maximum of TMR (570nm) was obtained with PBS in the flow cell. Next, the lowest concentration (10^{-10}M) of TMR was injected into the flow cell, and the fluorescence was measured when the intensity reached a steady state. The dye solution was then flushed with PBS until a stable baseline was maintained. The next dye concentration was then introduced and the sequence repeated. In these experiments, the concentration of the injected dye solutions was increased from the most dilute to the most concentrated (10^{-10}-10^{-3}M).

The specific binding of different concentrations (0.002-0.526mg/ml) of MRITC-conjugated αH-IgG to H-IgG adsorbed to the sensor surface is also monitored at 570nm. These experiments were performed with the proximal end collection geometry.

First, the emission signal was obtained with PBS in the flow cell, then a concentrated solution of H-IgG (0.5mg/ml) was introduced. The unlabeled H-IgG was allowed to adsorbed onto the sensor for 3 hours, then was flushed with PBS. The lowest concentration of MRITC-conjugated αH-IgG was allowed to bind to H-IgG until the fluorescence emission reached a steady state plateau (approximately 20 minutes). The αH-IgG solution was then flushed with PBS, and after about 30 minutes the signal reached a stable minimum. The next concentration of labeled αH-IgG was then injected into the flow cell. This procedure was continued with increasing concentrations of MRITC-conjugated αH-IgG.

3. Results and Discussions

3.1. Proximal vs. Distal End Fluorescence Detection

Figure 3 represents the fluorescence detected from the distal and proximal end collection geometries normalized by the background counts. The absolute intensity of the distal collection was four times the background intensity of the proximal collection. However, the normalized intensities (fluorescence/background) of the two designs are virtually identical. This result agrees with the theoretical prediction that back coupled light has an equal probability of propagating in either direction. The detection limit of the sensor to TMR was 10^{-7}M.

Although the two collection geometries had nearly identical sensitivities, the proximal end collection geometry was used in the subsequent protein experiments. The proximal end collection geometry requires fewer optical components and has a lower background signal. The background signal in the proximal geometry is primarily from back scattered laser light, as opposed to the distal configuration which points the laser light directly into the collection optics. A lower background signal may allow simpler optical components with less rejection capabilities to be used.

The sensitivity of our system can be improved by matching the numerical aperture of the collection optics more closely with the optical fiber and using filters with higher rejection. In vivo operation of the fiber optic fluoroimmunosensor would be complicated by the intrinsic biological fluorescence of serum. Experiments have been conducted with longer wavelength lasers and dyes (emission at longer wavelengths) to minimize the intrinsic fluorescence. Current fiber optic immunosensors are generally only single use devices. Various chemical methods to modify the sensor surface and thereby create a reusable sensor are being investigated.[6]

This system is relatively large and expensive, and ultimately sensor systems should be compact, inexpensive, and easily operated. A step toward the miniaturization of the system could consist of a smaller fiber optic spectrometer, a lamp as the excitation source, and a fiber optic 50/50 beam splitter. Although not shown in this report, we have begun work on a smaller fluoroimmunosensor using a fused fiber optic coupler and a Guided Wave, Inc. fiber optic spectrometer.

3.2. Specific Binding of Proteins

The specific binding of MRITC-conjugated αH-IgG to H-IgG adsorbed on the sensor surface is shown in Figure 4. The sensor surface was close to saturation at the highest concentration of 0.53mg/ml of labeled αH-IgG. Reinecke.[7] observed the same saturation concentration of αH-IgG. The data are also represented as binding curves

of the different concentrations of labeled αH-IgG (Figure 5). Each curve exhibits two major components: 1) a rapid increase in signal due to the specific binding of the labeled αH-IgG and 2) a steady state plateau. Figure 5 also shows the detection limit of the sensor to be 14nmole/L of αH-IgG, similar results using fluorescein labeled αH-IgG has been reported by Sutherland et al.[8]

A method of quantitation must be developed in order to analyze the fluorescence from the specific binding of proteins. The depth of penetration of the evanescent field is approximately 1500Å, while the protein layer thickness is only 200Å. This indicates that some of the bulk solution is being excited evanescently and back coupling into the fiber. Therefore, the protein layer and the evanescent excited bulk fluorescence must be separated to accurately measure the protein concentration.

4. Conclusions

The sensitivity of the fiber optic sensor to detect fluorescence was found to be similar for both proximal and distal end collection. However, proximal end collection has the advantages of a lower background signal and a simpler, more compact design. Preliminary results demonstrated the sensor's ability to detect the specific binding of proteins with a detection limit of 14nmole/L. Improvements in the optical system and advances in surface chemistry should lead to a fiber optic fluoroimmunosensor for remote continuous in situ monitoring. Determining the surface concentration of adsorbed molecules will require further work in signal quantitation.

5. Acknowledgements

Funding for this project was provided by a seed grant from the Center for Sensor Technology and a Biomedical Research grant from the Whitaker Foundation. The authors would also like to thank J.N. Lin and P.A. Suci for helpful discussions and technical assistance.

---

1. C.K.Carniglia, L.Mandel, and K.H.Drexhage, J. Opt. Soc. Am., 62, 479, 1972.
2. T.Hirschfeld, U.S. patent 4,447,546, 8 May 1984.
3. R.M.Sutherland, C.Dahne, J.F.Place, and A.S.Ringrose, Clinical Chemistry, 30, 1533, 1984.
4. W.F.Love and R.E.Slovacek, paper presented at OFS '86, Tokyo, Japan, Oct.1986.
5. P.Brandtzaeg, Scand. J. Immunol., 2, 278, 1973.
6. J.D. Andrade, J-N. Lin, J.N. Herron, W.M. Reichert and J. Kopecek, SPIE vol. 718, 280, 1986.
7. D.R.Reinecke, Master's Thesis, University of Utah, 1985.
8. R.M.Sutherland, see note 3.

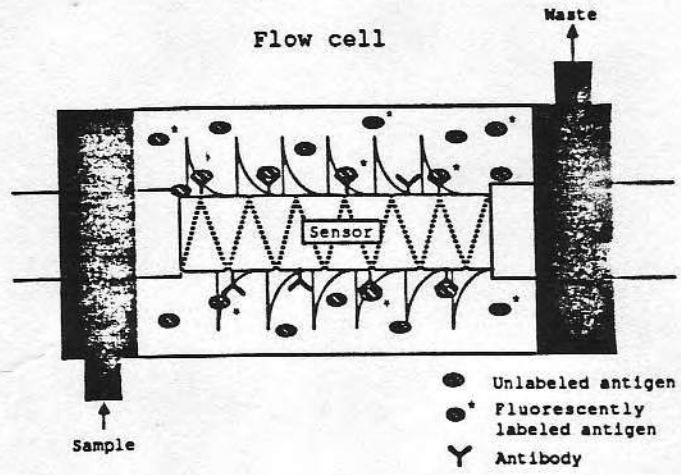

Figure 1. Illustration of evanescent excitation of the fluorescently labeled antigens specifically bound to the antibodies immobilized on the sensor surface.

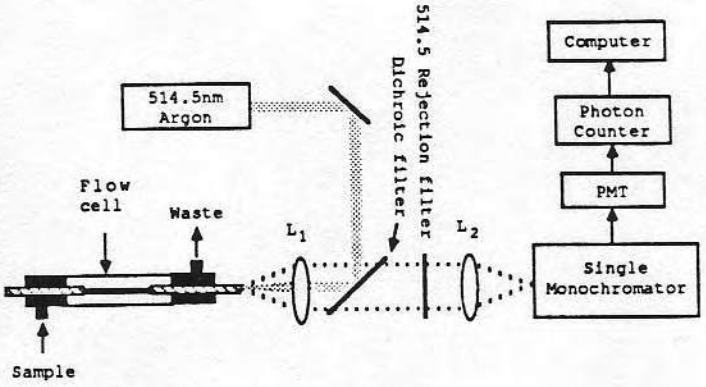

(a) Proximal End Collection

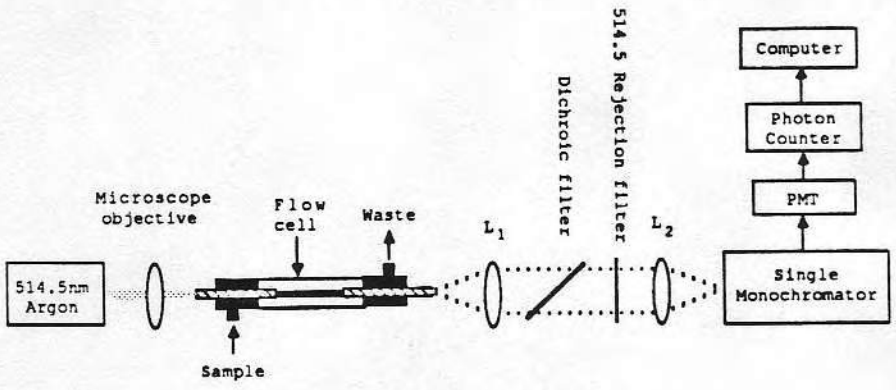

(b) Distal End Collection

Figure 2. Diagram of the fiber optic system with flow cell and coupling optics (L_1 and L_2 are lenses) for (a) proximal end collection and (b) distal end collection of fluorescence.

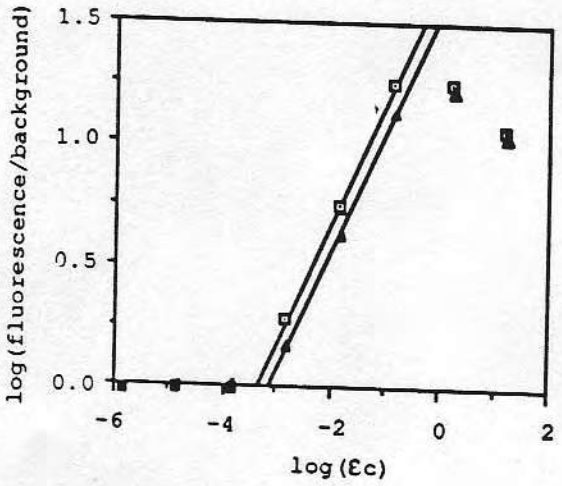

Figure 3. Different concentrations of TMR collected from the distal (■) and proximal (▲) end of the fiber optic sensor, where ε is the molar extinction coefficient and c is concentration.

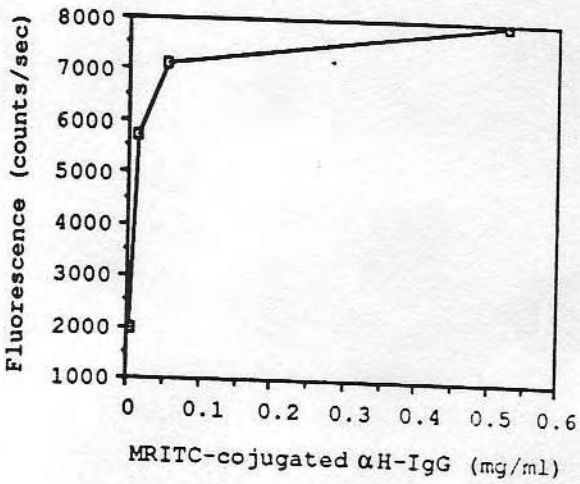

Figure 4. Protein isotherm representing the specific binding of different concentrations of anti-human IgG (αH-IgG) to IgG adsorbed on the sensor. The surface was saturated at .53mg/ml of labeled proteins, shown by the plateau of the signal.

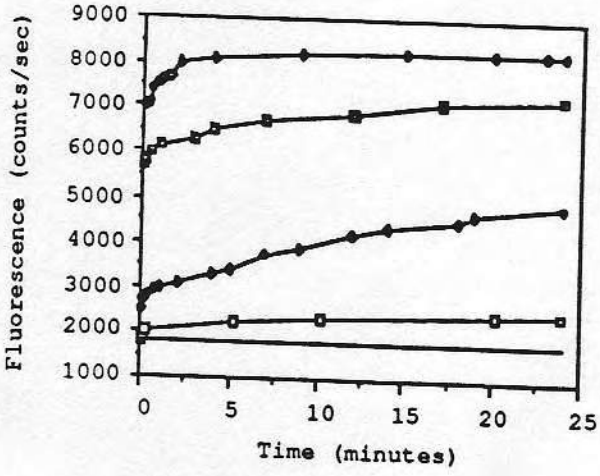

Figure 5. Fluorescence detection of MRITC-labeled α H-IgG binding to IgG adsorbed on the sensor. The detection limit is .002mg/ml (-□-) above the background counts from PBS (—). The other concentrations are .011mg/ml (-◆-), .053mg/ml (-■-), and .53mg/ml (-◆-).

σ–α Transformation, αPhase Transition And Schmitt Trigger Model Of Proteins At Interfaces

Y. Q. Zhang[1], J. D. Andrade[2]

[1]Department of Physics
University of Utah
Salt Lake City, Utah84112

[2]Departments of Bioengineering and Materials Science, Center for Biopolymers at Interfaces
University of Utah
Salt Lake City, Utah84112

Running title: Transformations of Proteins at Interfaces

Correspondence should be addressed to J. D. Andrade

Summary

A transformation(σ–α transformation) is suggested to connect the surface tension of proteins at solution-air interfaces and the stability coefficient α of proteins. Phase transitions are found in the α–time diagrams of three model proteins: Ribonuclease-A, Myoglobin and Cytochrome-c. A general step-by-step picture is proposed for the conformational change of proteins at the interfaces. The Schmitt Trigger model is proposed to simulate the conformational change of proteins at the interfaces. Both the fluctuation and the molecular machine points of view are stressed to understand the behavior of proteins at the interfaces.

1. Introduction

The conformations of macromolecules change in response to changes in the environment, for example, changes in temperature, pH, ion concentration, organic solutes[1] and interfaces[2]. The dynamics of the changes of proteins has been studied extensively. In principle both quantum mechanics and statistical mechanics are needed to determine the conformational changes of proteins. Different simulations including mechanical models[3], energy minimization methods[4], Monte Carlo procedures[5] and diffusion-collision models[6] have been developed. Some important observations such as protein domains[7], intermediates[8], conformational fluctuation[9] and defects[10] of proteins have been reported. Other novel descriptions of protein behavior include the proteinquake[11] and molecular machine[12] concepts.

Proteins, in one aspect, are rigid and static. This has been proven by the analyses of the experimental data from x-ray crystallography[13]. One approach to proteins in theory is the point of view of the molecular machine [2][12][14]. Proteins are taken to be machines, which can do work and transform energy form one form to another form. They can be carriers and transport materials from one site to another site.

In another aspect, fluorescence quenching[10][15] and relaxation[16], NMR[17] and phosphorescence[18] show a rather fluctuating, dynamic picture. The fluctuation of proteins has been shown to be very important to understand the function of proteins, for example , the action of enzymes[12].

In fact both factors are important to understand the structures and functions of proteins. We will show in this paper a mechanism which incorporates both of these factors to understand the behavior of proteins at interfaces.

The behavior of proteins at interfaces is important both in theory and in application[19]-[21]. Experiments clearly show time-dependent conformational changes of some proteins at the air

solution interface. These experimental data shows a complicated behavior of protein conformational changes at the interfaces.

In this paper we apply the $\sigma-\alpha$ transformation to study the conformational stability of proteins at the interfaces, where σ stands for the surface tension and α is a parameter which reflects the stability of proteins(we will show this later). Experiments show that α is a step function instead of a continuous function of time, and we will call this an α phase transition. In order to explain the α phase transition we propose a Schmitt Trigger model to describe the evolution of the conformations of proteins on the interfaces. Especially we will point out that both aspects of proteins, i.e., the fluctuation and the molecular machine, are important in understanding proteins' behavior at the interface.

2. $\sigma-\alpha$ Transformation

The stable conformations of proteins in the bulk solution are not necessary the stable conformations at the interfaces. In fact proteins generally will adjust their conformations in the process of adsorption onto the interfaces. This is proved by surface tension experiments of protein solutions[20]-[21],[24]. It is also possible that proteins may have some backbone and secondary middle metastable conformational states during their evolution from the initial conformational state to the final stable conformational state at the interface[22].

It is important to find out the relationship between the surface tension of a molecular solution and the conformations of molecules at the interfaces. There has been some work on this[23] but only very simple molecules were considered. It turns out to be very difficult to deal with macromolecules such as proteins theoretically. Any semiempirical study would be valuable at this stage.

We propose a $\sigma-\alpha$ transformation, which is given by (1), to set up a relationship between the surface tension σ and the stability of

the conformations of proteins at the interfaces. This transformation will be applied only for situations where there are no backbone middle metastable states.

$$\alpha = -\frac{d[\ \ln(\frac{\sigma-\sigma_2}{\sigma_1-\sigma_2})\ ]}{dt} \qquad (1)$$

where σ is the surface tension corresponding to time t, σ_1 and σ_2 are the initial and final surface tensions of the protein solution, α is a new parameter, which has the dimension of 1/sec. α is the decay constant of the initial conformation of the protein on the interface under some special condition[22]. Although in general it is not exactly the decay constant, it is still reasonable to take it as a parameter which measures the stability of the protein. So this transformation connects the surface tensions of protein solutions and the stabilities of proteins at the interface. We will call α "the stability coefficient" in this paper. The larger the stability coefficient, the more unstable the protein. If the stability coefficient equals zero, the protein is stable and will stay in the initial conformation unchanged.

We adopt the experimental data obtained by Wei, et al[19]. Three proteins are analysed by this method. The results are shown in Fig(1),(4) and (7). The vertical axis in Fig(2), (5) and (8) are $\ln[(\sigma-\sigma_2)/(\sigma_1-\sigma_2)]$. So the minus of the slope of these figures give us the stability coefficient of the corresponding proteins. The resulting α–t diagrams are given in Fig(3),(6) and (9).

The results strongly suggest how the proteins change at the solution-air interface. MYG(Myoglobin, Fig[1]-[3])is the most simple one. It adjusts its conformation gradually at the air-MYG solution surface(within the time period of the experiments). CYT-c(Cytochrome-c, Fig[4]-[6]) changes in a more complex way. It first changes its conformation very slowly until t=4.5 hours and then changes its conformation dramatically up to t=5.7 hours. And after that time it stops changing abruptly. RNASE(Ribonuclease-A, Fig[7]-[9]) is similar to CYT-c but requires more steps to complete its change. Analyses of the data obtained by Tornberg's group[20][21] give similar results. The strong similarities among these several

proteins suggest that this step by step mechanism could be a common characteristic of the evolution of proteins at interfaces. We may view this step-by-step process as the existence of secondary middle metastable states. As time goes on, the free energy of the protein increases and, once it exceeds the local barrier, it is extremely unstable and decays into the next local well. This process is expressed schematically in Fig(10). We propose that these middle metastable states are secondary structural metastable middle states. That is, these several proteins only adjust their secondary structures to lower their surface energy instead of changing their backbone structures, which is studied in detail in [22].

We propose a Schmitt Trigger model[25] to simulate this step-by-step conformational change of proteins at interface.

3. Schmitt Trigger model of the conformational change of proteins

Proteins are molecular machines. It transduces the quantities it senses in some definite fashion. What we observe in experiments is the outputs, or the products, of this protein molecular machine. We propose a Schmitt Trigger model can apply to the stability coefficient α. Fig(11) shows the common Schmitt Trigger circuit. R_1 and R_2 are the resistance of the proteins to the conformational change. OP AMP is an amplifier for the stability coefficient. If there is a perturbation of the stability of the protein, this amplifier, which is installed in the protein and in fact determined by the protein itself, will amplify this perturbation. As in Fig(11), the protein self-connects in such a way that it becomes a self feed back system. This protein Schmitt Trigger can only output two values of the stability coefficients, α_0 or 0. If the input is higher than α_1, then the output is α_0; if the input is lower than α_2, the output is 0. In analogy to the electronic Schmitt Trigger, α_0, α_1 and α_2 are connected by the following formulae:

$$\alpha_1 = R\alpha_0 + \alpha_r \qquad (2)$$

$$\alpha_2 = \alpha_r \qquad (3)$$

where $R = R_1/(R_1 + R_2)$; α_r is the reference stability coefficient. All these parameters α_r, α_1, α_2 and R are defined by the native structure and interactions of proteins. For a given environmental condition and a given protein, they are constants. Fig(12) shows how this mechanism works.

Of course in reality both CYT-c and RNASE show that real proteins are not ideal two value Schmitt Triggers. But as an approximation we suggest that these proteins can be treated as 2-valued Schmitt Trigger, at least with respect to their interfacial properties. By adding an integration circuit it is easy to realize a more-than-two-value Schmitt Trigger.

Due to the fluctuation of the free energy of proteins at the interface, there is a fluctuation in the stability coefficient α. It is easy to obtain(by integrating (1), notice α is constant section by section):

$$\Delta\alpha = -f(t)\,\Delta\sigma \qquad (4)$$

$$f(t) = \frac{1}{c(t)}\frac{\exp(\alpha t)}{t} \qquad (5)$$

where c(t) is the integral constant. It is a step function of time.

Because the interface contains more than one components(PBS is the background solution in the experiments), so the surface tension does not equal to the surface free energy. But their fluctuations are expected to have the same order. Then we have:

$$\Delta\sigma = \sqrt{kC_v}\,T \qquad (6)$$

where k is the Boltzman constant; T is the temperature of the

environment, which will be taken as the room temperature; C_v is the specific heat of the protein. So $\Delta\sigma$ is approximately constant.

Both when t is around 0 and ∞ the fluctuation of the stability coefficient equals ∞. For infinitely large fluctuational input the proteins cannot follow the change so the stability of the protein will just stay in the value which is determined before the infinitely high fluctuation. We postulate the following conditions for the effective response of the protein:

$$\Delta\alpha - \alpha_1 - \alpha_2 \tag{7}$$

and

$$\alpha \sim \alpha_2 \sim \alpha_r \tag{8}$$

Given the outputs α in Fig[13], f(t) is calculated and given in Fig[14] (notice in Fig[14] the vertical axis is ln(f(t))). It is easy to see that the fluctuation of the surface tension is nearly a constant and is very small , the fluctuation of the stability coefficient increases with time and rapidly approaches infinity. The protein trigger machine has response only when α satisfies (8) and (9). A more careful study about α_1, α_2 and R is under way.

4. Discussion

We have shown a mechanism as to how the fluctuation aspect of a physical quantity couples with the static and deterministic aspect of proteins to determine conformational change at interfaces. Without the fluctuation in the free energy of proteins, there would be no fluctuation in the stability coefficient and it would not be possible for the protein to jump from one state to another. On the other hand, if the protein were not a self-controlled molecular machine, the protein would have no specific response. So both fluctuation and molecular machine points of view are necessary to understand proteins.

5. Figure Captions

Fig(1). The surface tension-time data for a Myoglobin solution(from Ref[19]).
Fig(2). $\ln[(\sigma-\sigma_2)/(\sigma_1-\sigma_2)]$-time diagram of Fig(1).
Fig(3). Stability coefficient-time diagram of Myoglobin at the Myoglobin solution-air interface(from Fig(1,2) and equation(1)).
Fig(4). The surface tension-time data for a Cytochrome-c solution(from Ref[19]).
Fig(5). $\ln[(\sigma-\sigma_2)/(\sigma_1-\sigma_2)]$-time diagram of Fig(4).
Fig(6). Stability coefficient-time diagram of Fig(4,5) and equation(1).
Fig(7). The surface tension-time data of a Ribonuclease-A solution(from Ref[19]).
Fig(8). $\ln[(\sigma-\sigma_2)/(\sigma_1-\sigma_2)]$-time diagram of Fig(7).
Fig(9). Stability coefficient-time diagram of Ribonuclease-A at the Ribonuclease-A solution-air interface(from Fig(7,8) and equation(1).
Fig(10). The explanation of the step-by-step picture of the conformational change of proteins at the interfaces by the existence of the secondary structural middle metastable conformational states.
Fig(11). Schmitt Trigger electronic circuit model(from any electronics textbook).
Fig(12). The working principle of the Schmitt Trigger.
Fig(13). A theoretical ideal output of the stability coefficient with respect to the time.
Fig(14). f(t)-time diagram corresponding to the output of Fig[13]; f(t) is defined by (5).

6. References

[1] For a general review, see Charis Ghelis and Jeannine Yon, Protein Folding, Academic Press, New York, 1982.

[2] Andrade, J.D. , Hlady, .V., Herron, J. and Lin, J-N(1988), Proteins at Interfaces: Principles Relativant To Protein-based Devices.

[3] Ptitsyn, O.B., and Rashin, A.A.(1975), Biophys. Chem. 3, 1-20

[4] Levinthal,C.(1966), Sci. Am. 214, 642-652

[5] Tanaka,S., and Scheraga,H.A.(1975), Proc. Natl. Acad. Sci. U.S.A. 72. 3802-3806.

[6] Karplus, M., and Weaver, D.L.(1976), Nature(London)260, 404-406

[7] Schiffer, M., Girling, R.L., Ely, K.R., and Edmunson, A.B. (1973), Biochemistry 12, 4620-4631.

[8] Frauenfelder, H., Parak, F., and Young, R.D.(1988), Ann. Rev. Biophys. Chem. 1988. 17:451-479

[9] Sternberg, M.J.E., Grace, D.E.P., and Phillips, D.C. (1979). J.Mol. Biol. 130, 231-253.

[10] Lakowicz, J.R., and Weber, G. (1973)Biochemistry. 12, 4171-4179

[11] Ansari, A., Berendzen J., Bownw, S.F., Frauenfelder, H., Iben. I.E.T., Sauke, T.B., Shyamsunder, E., and Young, R.D. (1985) Proc. Natl. Acad. Sci. USA Vol.82, 5000-5004.

[12] Welch, G.R., The Fluctuating Enzyme, John Wiley & Sons, New York, 1986

[13] Richards, F.M.(1974) J. Mol. Biol. 82, 1-14.

[14] Blumenfeld, L.A., Physics of Bioenergetic Processes, Springer, Heidelberg, 1983.

[15] Eftink, M.R. and Ghiron, C.A.(1975) Proc. Natl. Acad. Sci. USA 72, 3290-3294.

[16] Grinvald, A., and Sternberg, I.Z. (1974) Biochemistry 13, 5170-5178.

[17] Allerhand, A. at el, (1971) J. Am. Chem. Soc. 93, 544-546.

[18] Saviotti, M.L., and Galley, W.C. (1974) Proc. Natl. Acad. Sci. USA 71, 4154, 4158.

[19] Wei, A-P, Herron, J., and Andrade, J.D. (1988) , in preparation.

[20] Tornberg, E., and Lunch, G.(1979) J. Colloid. Interfaces. Sci, 79, No.1, 76-84.

[21] Tornberg, E. (1978) J. Collloid. Interfaces. Sci. 64, No.3, 391-402.

[22] Zhang, Y.Q., and Andrade, J.D, in preparation.

[23] Croxton, C.A., Statistical Mechanics of Liquid Surfaces, John Wiley & Sons, New York, 1980.

[24] Graham, D.E. and Phillips, M.C.(1979) J. Colloid. Interfaces. Sci.70, No.3,403-414.

[25] see any electronics textbook.

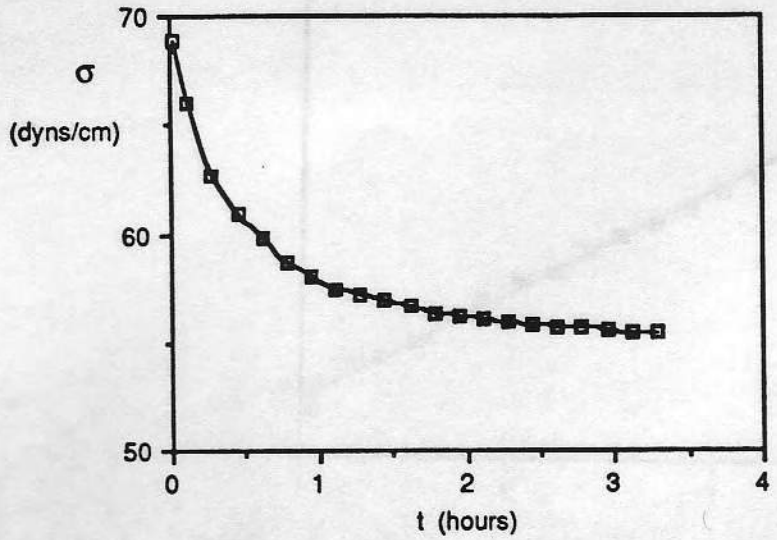

Fig.1

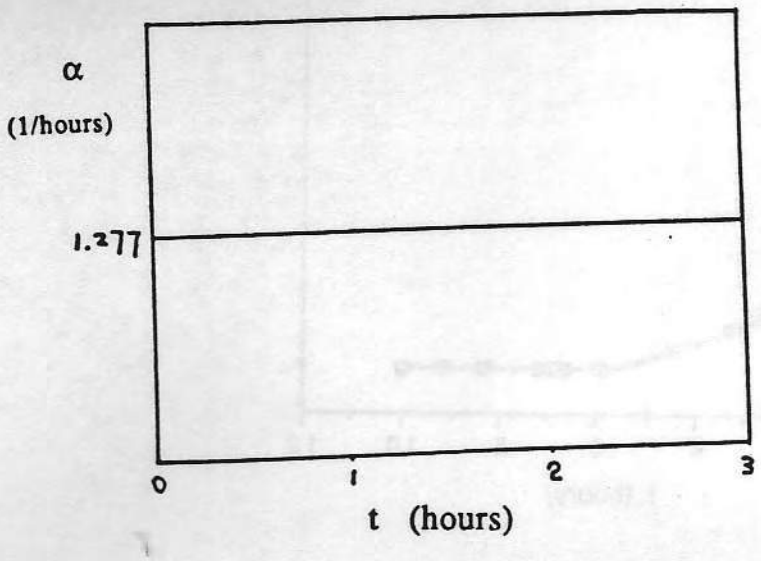

Fig.3

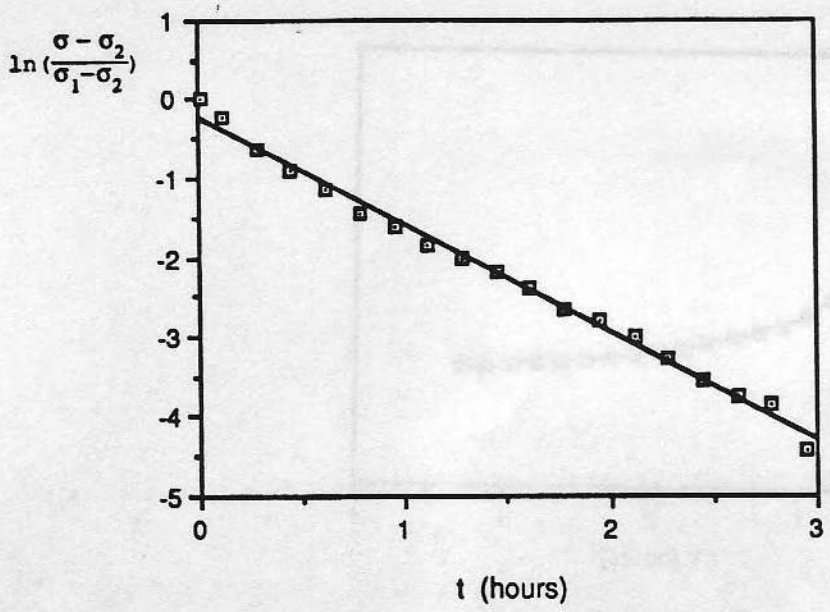
$\ln\left(\frac{\sigma-\sigma_2}{\sigma_1-\sigma_2}\right)$
1
0
-1
-2
-3
-4
-5
0
1
2
3
t (hours)

Fig.2

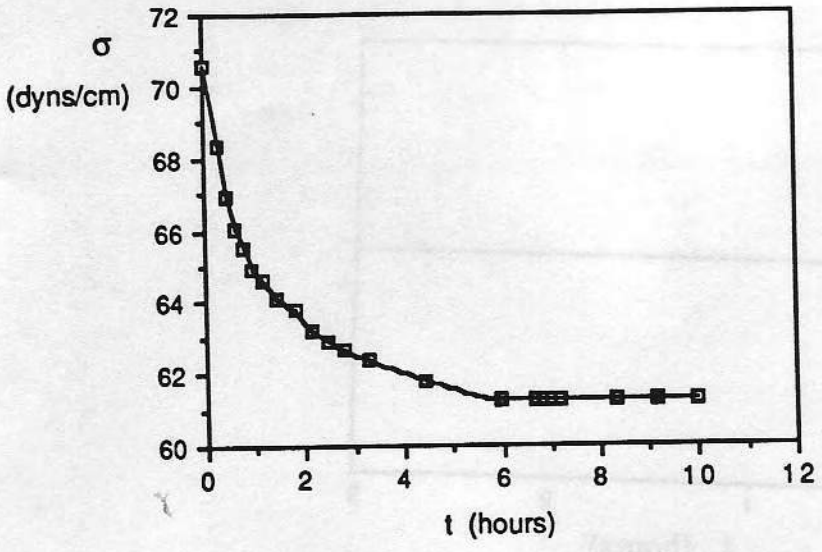
σ
(dyns/cm)
72
70
68
66
64
62
60
0
2
4
6
8
10
12
t (hours)

Fig.4

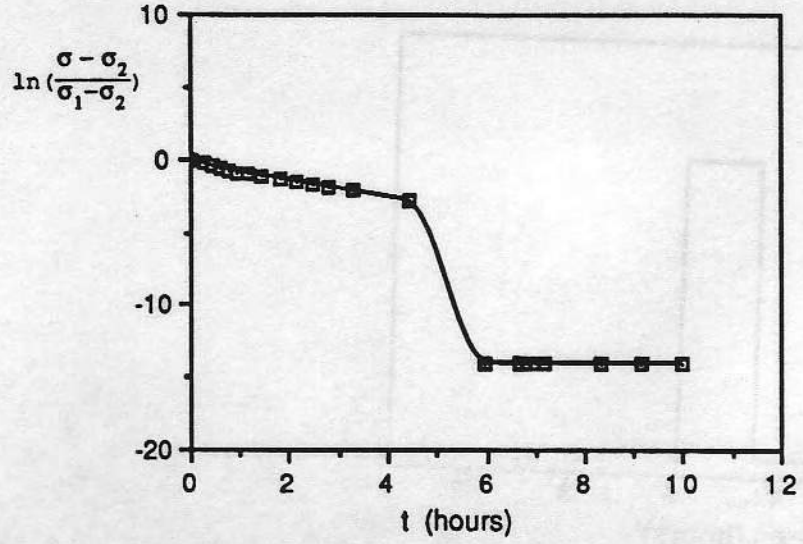
10
0
-10
-20
0
2
4
6
8
10
12
t (hours)

Fig.5

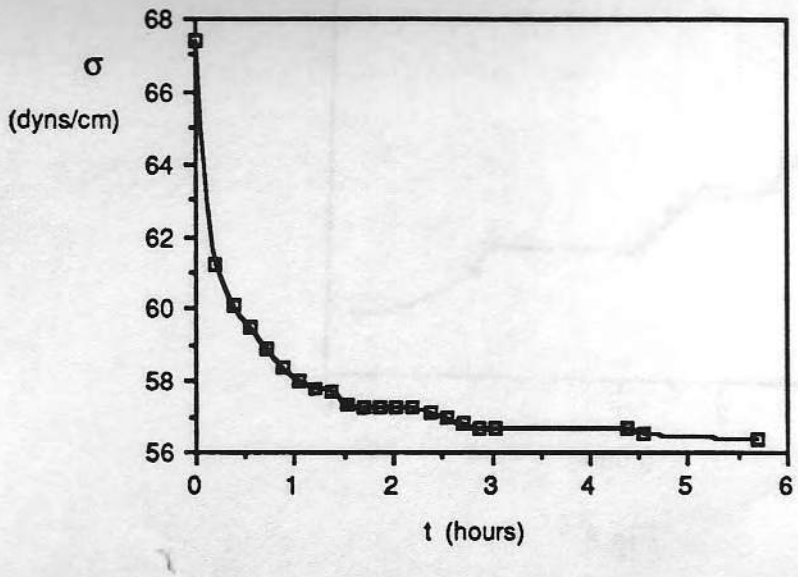
σ
(dyns/cm)
68
66
64
62
60
58
56
0
1
2
3
4
5
6
t (hours)

Fig.7

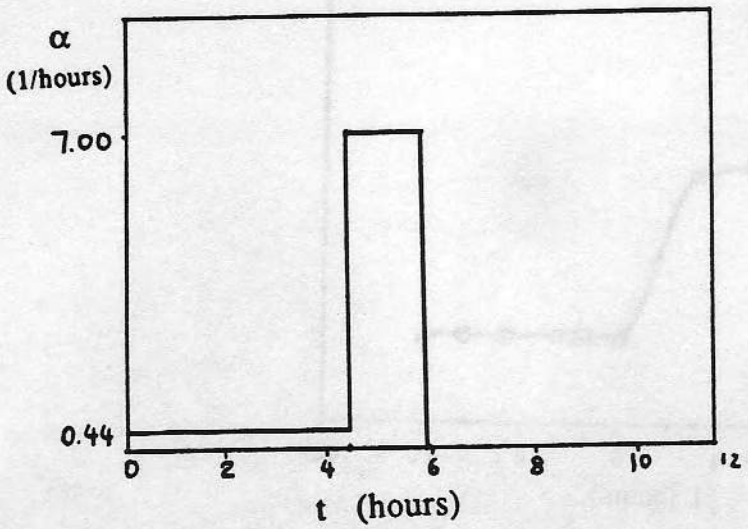
α
(1/hours)
7.00
0.44
0
2
4
6
8
10
12
t (hours)

Fig.6

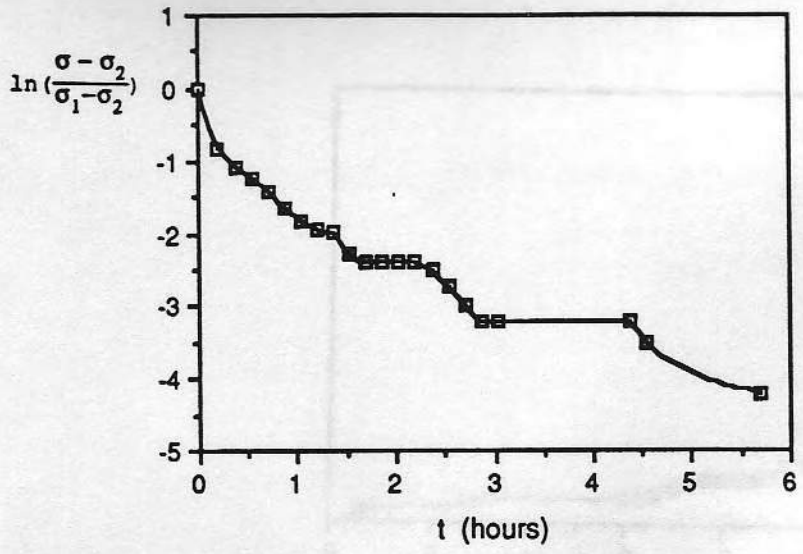
ln((σ − σ2)/(σ1 − σ2))
1
0
-1
-2
-3
-4
-5
0
1
2
3
4
5
6
t (hours)

Fig.8

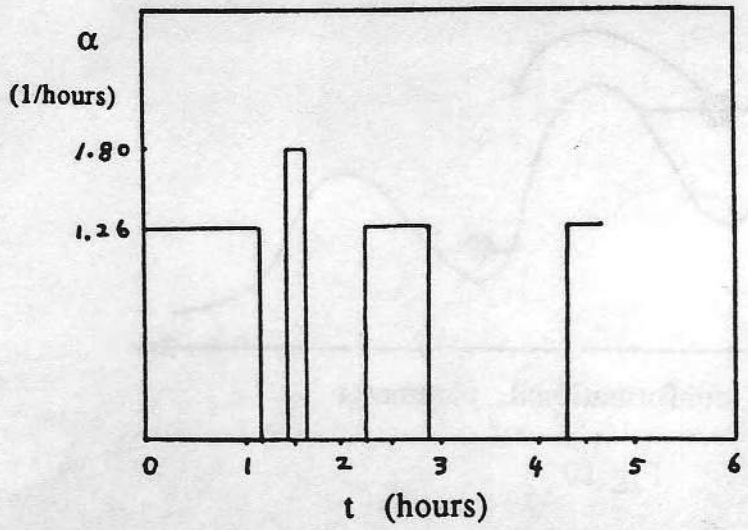
α
(1/hours)
1.80
1.26
0
1
2
3
4
5
6
t (hours)

Fig.9

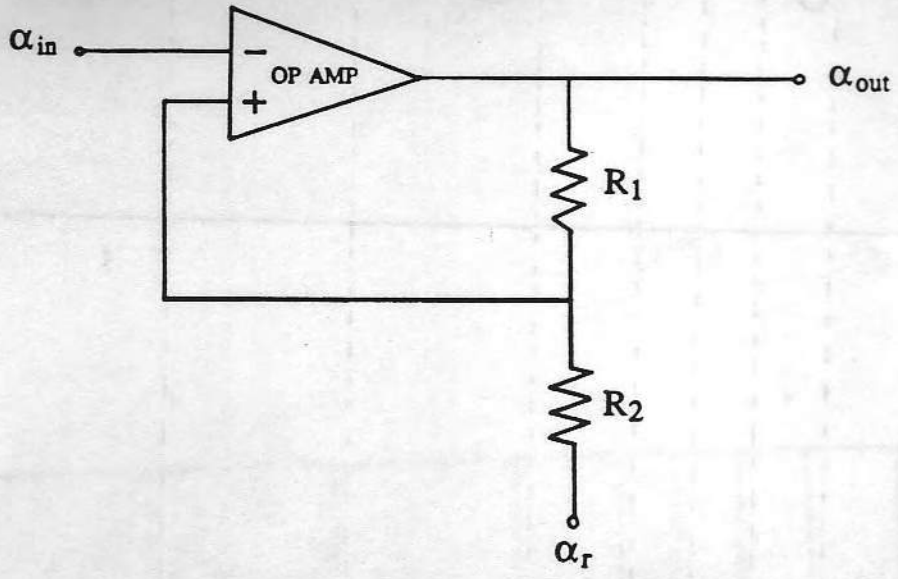
α_{in}
OP AMP
α_{out}
R_1
R_2
α_r

Fig.11

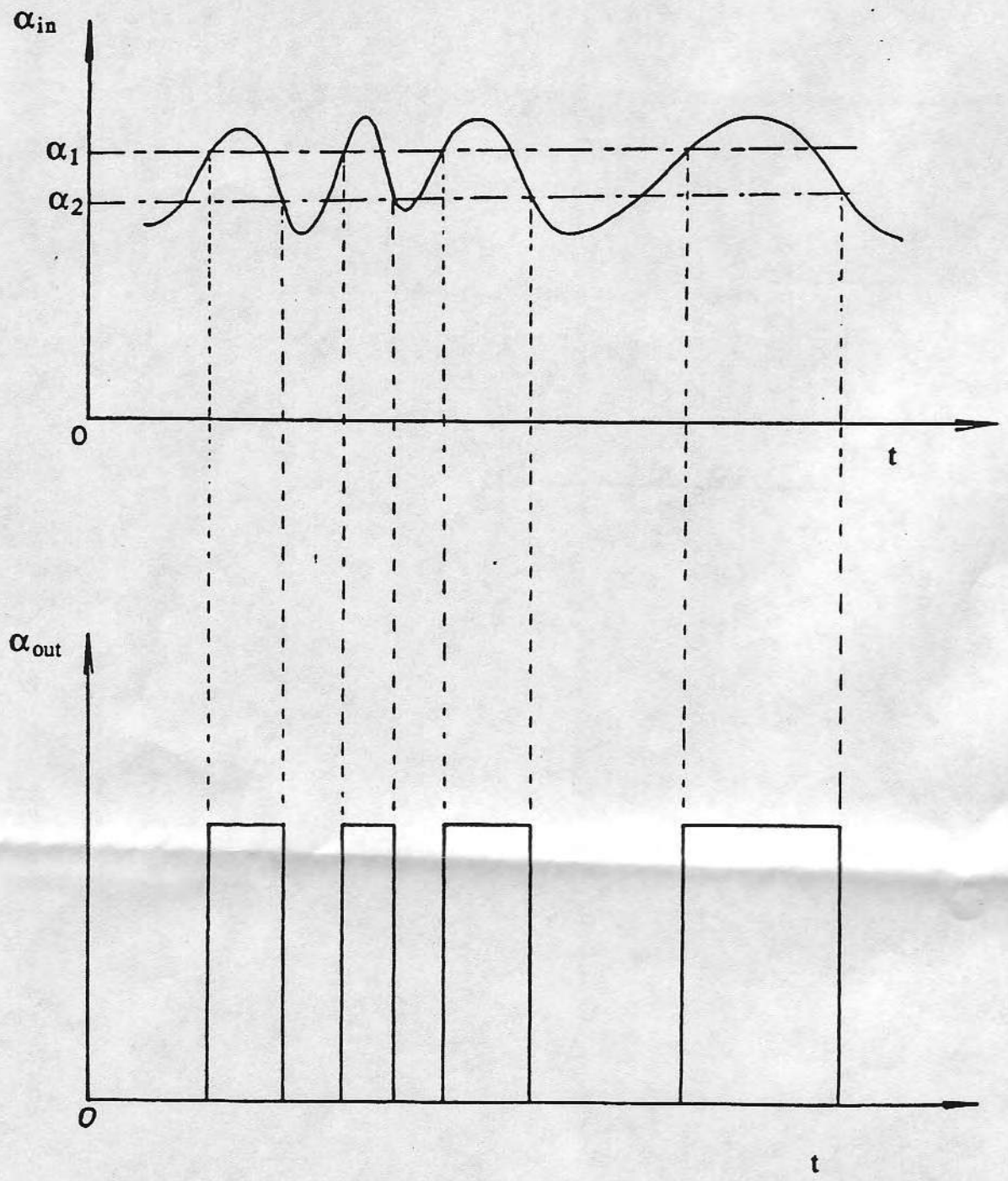

Fig.12

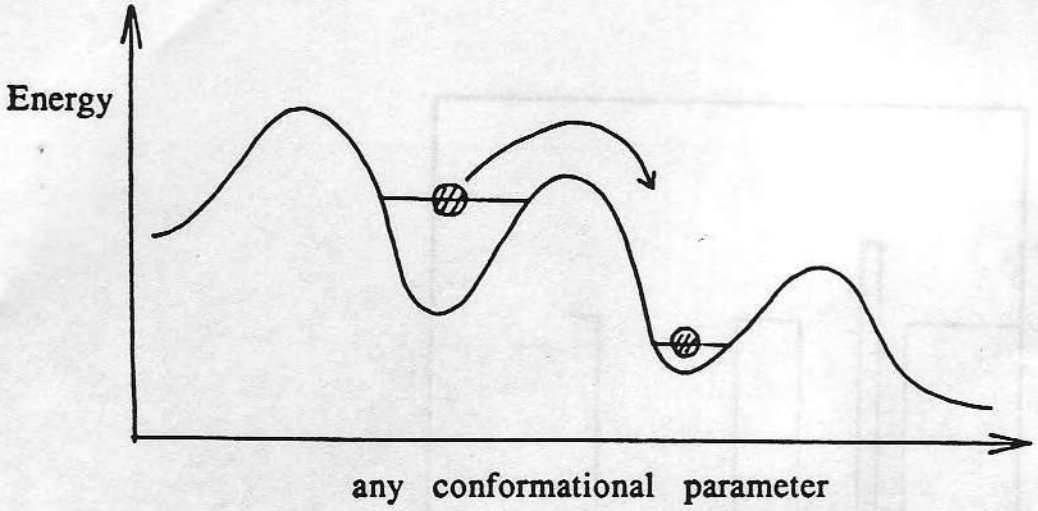
Energy
any conformational parameter

Fig.10

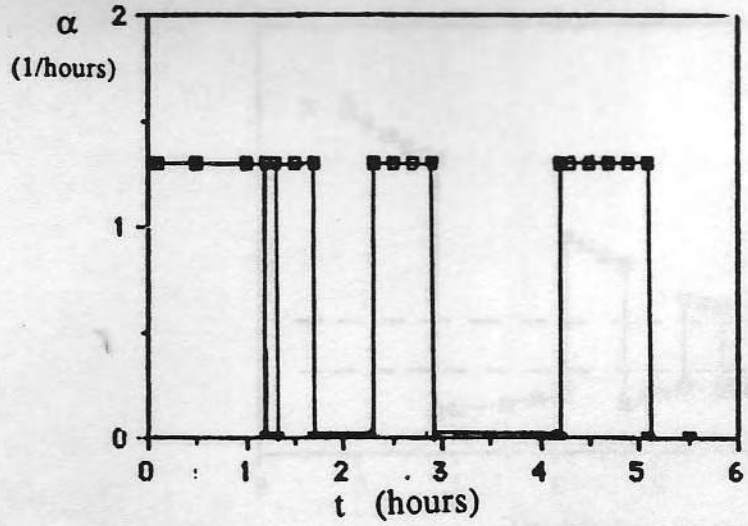
α
(1/hours)
2
1
0
0 : 1 2 . 3 4 5 6
t (hours)

Fig.13

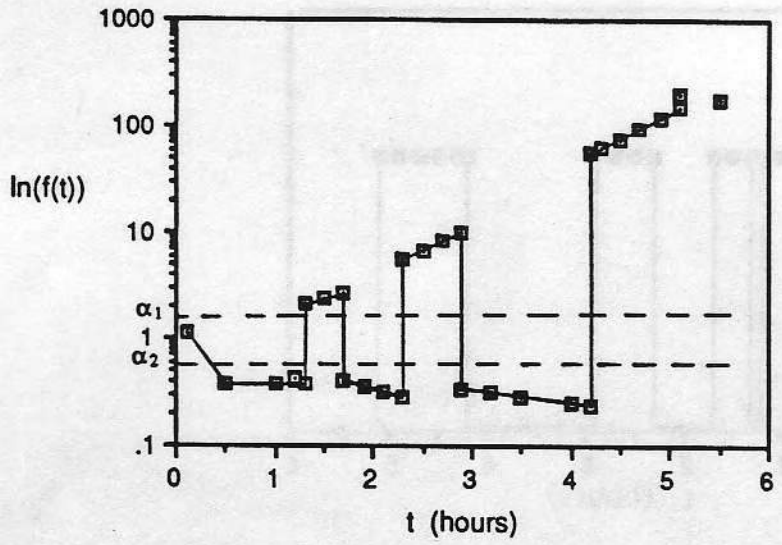

Fig.14

FIRST CLINICAL APPLICATION OF TRANSARTERIAL CLOSED-CHEST LEFT VENTRICULAR (TaCLV) BYPASS

H. H. J. Zwart, A. Kralios, C. S. Kwan-Gett, D. K. Backman,
J. L. Foote, J. D. Andrade, F. M. Calton*, F. Schoonmaker*, and W. J. Kolff

A technique for substitution of left ventricular function without thoracotomy has been developed[1]. Blood is removed from the left ventricle with a flexible cannula which is inserted via the right carotid (animals) or axillary (man) artery (Figure 1). The blood is returned into the arterial vascular bed through a femoral artery. The method is called Transarterial Closed-Chest Left Ventricular (TaCLV) Bypass.

EQUIPMENT† AND OPERATION

The equipment used initially has been described in detail previously[1]. The cannula (1 in Figure 2) to remove blood from the left ventricle is specially fabricated from polyurethane (Estane, 5701 F 1, Goodrich) and reinforced with glass-fiber (Owens-Corning). It is flexible, the wall-thickness is only 0.2-0.4 mm., it is stiff enough to be inserted without a stylet, and once in the body it softens and adapts to the geometry of the arterial system.

The blood circuit (Figure 2) consists of a 6' long 1/2" I.D. 3/4" O.D. silastic tube with 2 1/2-3/8" connectors (Bentley Sales, Inc., Norwalk, Conn.) at each end. The tube is mounted in a roller pump (Travenol 5 M 6002). At the inflow part (2 in Figure 2), the tube is connected to the left ventricular cannula with a 1/2" O.D. 3/8" I.D., 3 cm. long silastic tube. This short piece of thin-walled tubing (3 in Figure 2) is attached to the cannula during insertion and indicates when the cannula tip enters the left ventricle; the barely visible pulsations of the tubing become vigorous. Once it is a part of the circuit the same tube indicates the amount of suction applied to the cannula base by the roller pump. The pump should be slowed down as soon as the tubing starts to collapse. At the outflow part (4 in Figure 2), the tube is connected to a blood return cannula (5 in Figure 2). In between pump and blood return cannulae, the silastic tube of the circuit is interrupted by a silastic thin-walled reservoir (6 in Figure 2). The reservoir serves to trap air and to depulsate the roller pump so that a non-pulsatile flow is produced through the blood return cannula. Three silastic side lines are attached to the reservoir, one for removal of air, the other for perfusion of the right arm or leg, in case collateral circulation beyond the cannulation sides is insufficient.

Recently equipment has been fabricated with which blood return can be pulsed. The pulsations can be counterphased to those of the natural heart. Pulsatile blood return is produced with a rigid cylinder, covered on the inside with a natural latex sleeve (7 in Figure 2 and Figure 1a). The cylinder is to be shoved over the reservoir. If compressed air is forced in between cylinder and latex sleeve, it causes the latter to collapse and the reservoir to be squeezed. The resulting pulsations can be programmed in between natural heart beats by applying the pressure to the cylinder synchronously with the EKG using an R-wave detector with proper delay and duration settings (Figure 3).

The blood circuit has a priming volume of 300 ml. The blood is in contact with silastic (tubing, reservoir), polyurethane (cannula), and polycarbonate (connectors). These materials can be treated[2] so that systemic heparinization is not necessary. Preliminary experiments on sheep, where TaCLV-Bypass, using a heparin treated circuit, was applied without administration of heparin to the animal, were promising; the sheep survived but there were some small clots around the connectors. In addition, the inner surface of the circuit is coated with albumin because there is evidence[3] that this will decrease platelet adhesion to the surface and probably decrease hemolysis as well. It is sufficient to add some 25 mg. of albumin to the priming volume.

COMPILED DATA FROM ANIMAL EXPERIMENTS (18 DOGS, 42 SHEEP)

1. With TaCLV-Bypass the left ventricle can be effectively emptied without thoracotomy, the circulation being maintained by a pump outside the body (Figure 3).
2. The maximum flow (blood, hematocrit 23%, temp. 22°C.) through the system is 6.2 L./min. In vitro, the highest flow obtained in a sheep was 5.3 L./min.
3. The circulation can be maintained during ventricular fibrillation for periods up to 14 hr.[4,5]. Under these circumstances the pressure in the left ventricle is kept around atmospheric.

---

*By invitation.

†Equipment can be obtained through our Laboratory.

From the Division of Artificial Organs, Department of Surgery, University of Utah College of Medicine, Salt Lake City, Utah.

Work in this laboratory is supported by the N.I.H., and N.H.I., and this work in particular by the Max C. Fleischman Foundation, Number 2101.

4. With a little practice, cannulation of the left ventricle with the wide bore cannula can be mastered without the aid of electronic or X-ray equipment. If a pressure catheter is present in the left ventricle, the outflow cannula can be easily inserted using the catheter as a guide.
5. The aortic valve is competent during and after the bypass.
6. Coronary flow is not impaired by left ventricular cannulation[1,6].
7. Deep shock, produced in 5 closed-chest dogs by embolizing the left coronary artery with plastic microspheres, could be restored, and in 4 cases the heart recovered - 2 long-term survivals were obtained[7].
8. Six sheep survived 4 hr. and 2 sheep, 24 hr. of bypass uneventfully. The maximum plasma hemoglobin value obtained was 23 mg.%[8].
9. Four sheep survived a one hour period of ventricular fibrillation; one of these animals gave birth to 2 healthy lambs 2 months later. In the latter sheep, a specially treated blood circuit was used. Heparin was not supplied to the animal.
10. Damage inflicted by the cannula consists of subendocardial hemorrhages, but they are small and usually absent.

CLINICAL EXPERIENCE (TWO CASES BY MARCH, 1970)

Patient 1. We were called to apply TaCLV-Bypass on a 62-year old man with a myocardial infarction. During the preceding 10 hr. his blood pressure was around 80/50 mm.Hg. There was mild venous congestion, slight cyanosis, and the patient complained of angina and shortness of breath. The EKG revealed sinus tachycardia with occasional premature ventricular contractions and slight nonspecific ST-T changes. Physical examination suggested enlargement of the heart and slight pulmonary edema. Urine production had been 150 ml. during the last 6 hr., during which time he had been given diuretics. The EKG later showed a complete atrioventricular block and 2 hr. before mechanical assistance was applied, ventricular fibrillation occurred. After successful defibrillation the systolic pressure was not obtainable or at times was between 50 and 80 mm.Hg. The patient was unconscious, the skin was cold and clammy, there was pulmonary edema on physical examination, and cyanosis notwithstanding assisted intratracheal respiration. Medical treatment did not improve the condition.

We accepted the patient for TaCLV-Bypass, it took 30 min. to perform the necessary cannulations; a cannula inserted into the left ventricle via the right axillary artery and one inserted into the right femoral artery. The patient was heparinized with 2 mg./Kg. body weight and additional doses were given as necessary to keep the clotting time around 25 min. Medical treatment was continued as necessary. The mean bypass flow (Figure 4) gradually decreased from 3.9 L./min. during the first hour to values around 3.3 L./min. after 4-9 hr. of bypass (range 2.2 - 5.8). The flow could be increased by supplying intravenous fluids. The blood pressure (Figure 4), measured with an intra-arterial catheter, increased during the first 4 hr. of bypass to values around 80/60 mm.Hg, then it decreased, whereafter it increased again, and after 8 hr. it was around 90/65 mm. Hg. Occasionally, especially during the first 4 hr. of bypass, there were no pulsations visible on the arterial pressure tracing (Figure 5) indicating that the bypass was complete. The right atrial pressure, measured with a catheter which was inserted after 6 hr., was around 10 cm. H_2O initially but tended to decrease despite the administration of fluids.

The urine production (Figure 6) was 190 m. during the first hr. of bypass, thereafter it decreased gradually to around 50 ml./hr. Large amounts of fluids were supplied, especially after 4 hr. of bypass. The bypass flow and arterial pressure increased after fluid administration but only for a short time. The hematocrit, 63% initially, decreased to 43% after 4 hr. of bypass and to a minimum of 21% after 10 hr. A total amount of 3000 ml. of blood was given to the patient. The pH (Figure 7) was usually within normal range; 528 mEq. of $NaHCO_3$ were supplied. The pCO_2 was most often between 45-50 mm. Hg. The arterial oxygen saturation was too low initially (74-85%) but after 6 hr. of bypass it increased to normal values (over 90%). The plasma was clear throughout the procedure and the electrolytes were within the normal range towards the end of the pumping period. The temperature, measured in the rectum, increased to 101° F.

The patient regained consciousness after 2 hr. of bypass. The rales disappeared gradually from the lungs and the skin became warm and pink. Respiration was assisted with pure oxygen or a mixture of oxygen and air throughout the procedure. Blood loss and pooling were suspected because of the large amounts of fluids that had to be supplied in order to keep up bypass flow and arterial and right atrial pressure. It is estimated that 1000 ml. of blood were lost from the wounds during the entire period of bypass. During the 7th hr. of bypass, a small amount of blood was lost with the urine; however, no other bleeding site could be detected and there was normal peristalsis over the abdomen. The EKG was not much different from that obtained at admission. The circulation in the right arm was like that in the rest of the body. In the right leg circulation became inadequate after 6 hr. but it could be restored by additional perfusion with a side line from the arterial reservoir.

After 9 hr. of bypass the pump was switched off for one hour in an attempt to wean the patient from the assist. The blood pressure fell during the second half of this hour, while right atrial pressure, the EKG, arterial oxygen saturation, and urine production did not change significantly. The bypass was applied for 2 more hours, during which period urine production increased. During the last hour of bypass the blood pressure fell again.

It was decided to discontinue the bypass because blood loss was suspected. The cannulas were removed and the heparin was neutralized with protamine sulfate. The patient remained in the same condition during the next 3 hr., producing some 100 ml. of urine each hour. Thereafter urine production decreased and finally ceased after 3 more hours. Eight hours after the bypass had been discontinued, large amounts of blood were lost per rectum, ventricular fibrillation occurred, defibrillation was unsuccessful, and the patient died.

At autopsy there was generalized arteriosclerosis, the right coronary and the anterior descending branch of the left coronary artery were found to be occluded, and there was massive infarction of the anterior wall and the interventricular septum. No damage was observed that could have been caused by the cannula. The occlusion in the right coronary artery was fresh and could have been removed surgically. Sclerotic plaques were present in the aorta but there was no damage to the aortic wall. Large amounts of blood had accumulated in the gastrointestinal tract. The mucosa of the stomach and the bowel showed congestion but no bleeding site could be detected.

Patient 2. A 52 year old man was admitted in deep shock. There was no history of heart disease; poisoning was suspected. The EKG showed no remarkable abnormalities. The arterial pressure could not be measured but after insertion of a catheter, a reading of 20 mm. Hg was found. The right atrial pressure, measured with a catheter was 45 mm. Hg. Medical treatment did not improve the condition. The patient was given 150 mg. of heparin, and additional doses of 50 mg. were supplied every hour. Medical treatment was continued as necessary. TaCLV-Bypass was instituted within 20 min. and applied for the next 5 1/2 hr. The left ventricular cannula was inserted via the right subclavian artery. Within 3 min., the right atrial pressure had decreased to 5-8 mm. Hg. and the arterial pressure increased to 90-100/80-90 mm. Hg.

Before bypass the skin was cyanotic and had a mottled appearance. Within 10 min. after start of the bypass, the skin turned pink. The circulation in the right arm and leg did not appear different from that in the rest of the body. The hematocrit was 42% before and at the end of the bypass period. After 5 hr. of bypass the pH was 7.20 and the pCO_2 was 40 mm. Hg, the electrolytes were within normal range except for a high K of 5.2 mEq. /L., the platelet count was 165,000/mm.^{2}, the clotting time was over 50 min., and the PTT and fibrinogen were normal. No urine was produced.

After 5 1/2 hr. of bypass, massive uncontrollable bleeding occurred from the gastrointestinal tract, treatment was discontinued, and the patient died. At autopsy no abnormalities were observed in the heart, and there was no damage that could be related to the bypass. Throughout the upper part of the gastrointestinal tract multiple ulcers were found from which bleeding had apparently occurred. No poison has as yet been identified.

DISCUSSION

During advanced stages of cardiogenic shock, the cardiac output is decreased and tissue perfusion is inadequate. The left side of the heart is dilated with elevation of end diastolic left ventricular and left atrial pressures, the pulmonary veins are congested, and the arterial blood pressure is low[9]. If medical treatment fails, the mortality is 100%[10]. In these cases application of mechanical assist devices is justified. Decompression of the left ventricle and infusion of oxygenated blood into the arterial vascular bed is likely to improve the condition. During counterpulsation it is hoped that such is effected by the heart itself; if left ventricular function improves, cardiac output increases, and left ventricular end diastolic pressure decreases[11]. Techniques are available for non-invasive[12,13] and minimally invasive counterpulsation[11,14]. Clinical experience[11,15,16] seems to indicate that shock is reversed and that the heart can recover if counterpulsation is applied early. Long-term survival may then range from 0-55%. Counterpulsation is not effective during cardiac standstill or ventricular fibrillation[16]. In contrast, the circulation can still be maintained under these circumstances with bypass procedures. A bypass, however, requires dissection of blood vessels and, up until now, systemic heparinization is necessary. Complications such as embolism (air, clots, other particles), infection, blood damage, blood loss, and damage to blood vessels can occur.

Clinical experience with successful closed-chest partial cardiopulmonary bypass as a treatment for cardiogenic shock dates back as far as 1957[17]. More recently[18] a 50% recovery rate was reported. The procedure was time-limited because of the blood damage caused by extracorporeal oxygenation. Since membrane oxygenators became feasible[19] the bypass is being applied again as a circulatory assist[20]. Although a substantial amount of blood is diverted from the heart and infused into the arterial vascular bed there is experimental evidence that there is no effective decompression of the left ventricle[21]. The failing left ventricle is not able to pump out the blood flowing to the left atrium from the bronchial arteries and that which escapes the venous cannulas.

There is only limited clinical experience with closed-chest left heart bypass using a transvenous cannulation technique[22]. Although the shock could be reversed, no patients survived. Since the cannula removes blood from the left atrium, maximum decompression of the left ventricle cannot be obtained if the mitral valve is competent. With TaCLV-Bypass, the left ventricle is maximally decompressed and the blood removed from the left heart is returned to the arterial vascular bed. Artificial oxygenation is not necessary if pulmonary function is adequate.

In our first clinical experience with 2 patients the bypass could be instituted within 20-30 min. The outflow cannula did not cause damage to the heart or adjacent structures. The circulation did improve as evidenced from the skin color and temperature, as did the arterial and right atrial pressures, and, in the first patient, the pH, the urine production, and the return of consciousness. The anuria and acidosis in the second patient might be due to poison.

Usually the bypass was incomplete, the left ventricle ejected blood, and since the arterial pressure had increased, it is likely that myocardial work did increase rather than decrease. For this reason, equipment was designed to counterpulsate blood return (Figures 1-3); if applied during incomplete bypass it is expected to minimize myocardial work. In the first patient, the bypass was occasionally complete and a straight arterial pressure tracing was obtained (Figure 5) while the circulation was maintained with the roller pump. During such circumstances it might be advantageous to produce a pulsatile blood return. Initially there was cyanosis in both patients

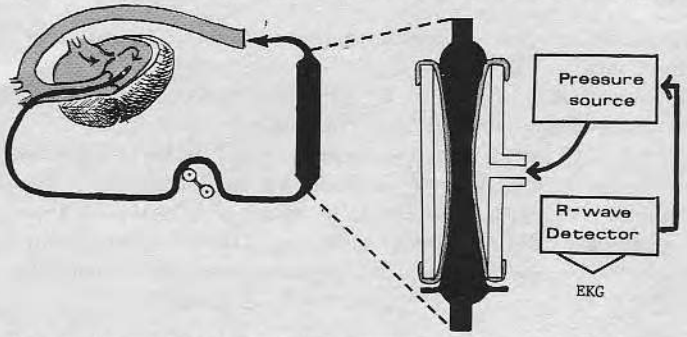

Figure 1. Schematic drawing of TaCLV-Bypass. Blood is removed from left ventricle with transarterial cannula and returned to aorta. (Figure 1a). Enlargement of arterial reservoir. A rigid cylinder, covered on the inside with a natural latex sleeve is fitted around reservoir for counterpulsation.

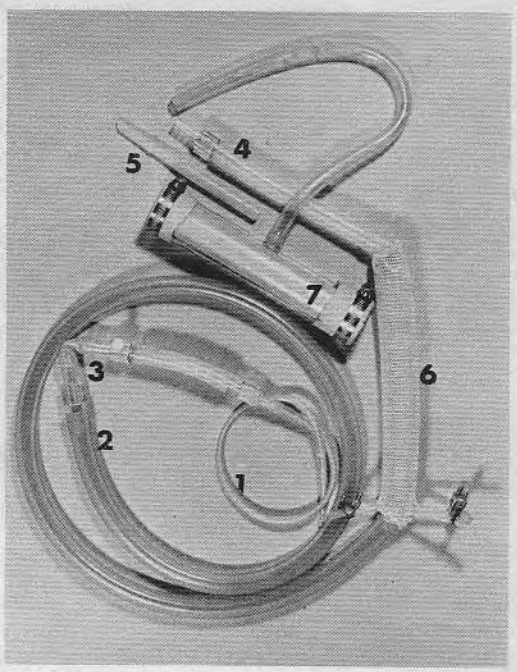

Figure 2. The blood circuit for TaCLV-Bypass. 1. Cannula to be inserted into left ventricle. 2. Inflow part of blood circuit. 3. Short piece of thin-walled silastic tubing, indicates position of outflow cannula and amount of suction produced by roller pump. 4. Outflow part of blood circuit. 5. Blood return cannula. 6. Arterial reservoir. Note the 3 side-lines. 7. Counterpulsation equipment.

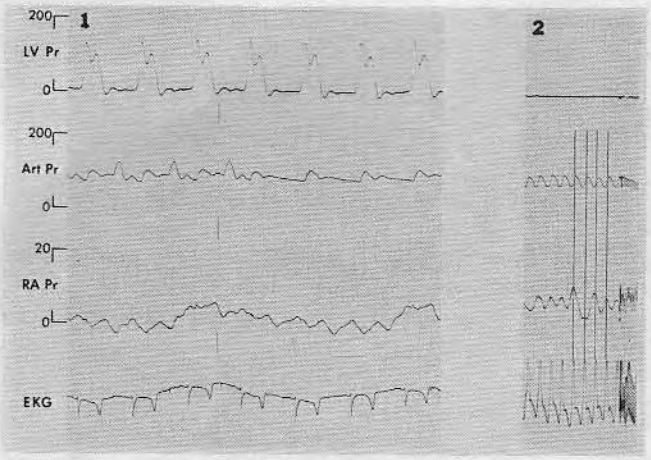

Figure 3. Tracings obtained from TaCLV-Bypass in a sheep. During the first half of period 1, blood return was counterpulsated. During period 2, the bypass is complete, the pressure in the left ventricle is atmospheric. Note that artificially produced pulsations in aorta are still synchronous with EKG. LV Pr. - pressure, left ventricle; Art. Pr. - pressure, thoracic aorta; RA. Pr. - pressure, right atrium. Pressures in mm. Hg.

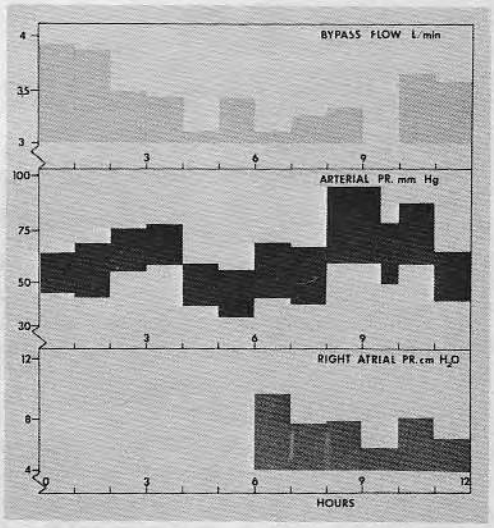

Figure 4. Bypass flow, arterial pressure and right atrial pressure during TaCLV-Bypass in patient 1.

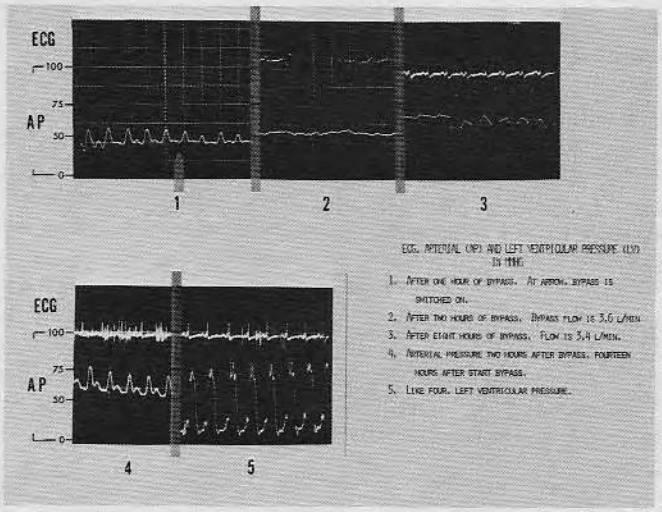

Figure 5. Tracings obtained during TaCLV-Bypass in patient 1. During period 2, left ventricle is bypassed completely. Art. Pr. - pressure in thoracic aorta. The left ventricular pressure, displayed at the lower right corner of the picture was measured through the outflow cannula while the bypass was switched off. Pressures in mm. Hg.

and in the first patient signs of pulmonary edema. The arterial oxygen saturation improved almost immediately during the bypass in the second patient. In the first patient this took 6 hr. The improvement of blood oxygen content could be the result of effective decompression of the left side of the heart. Physical signs of pulmonary edema disappeared during bypass in the first patient. If oxygenation does not improve within a short time, a membrane oxygenator might be included in the blood circuit. The temperature in neither of the patients decreased so that a heat exchanger does not seem to be necessary. In the first patient an extra perfusion line had to be inserted into the right femoral artery, distal from the cannulation site. Therefore, it seems wise that side lines connected to the arterial reservoir are provided. The bypass flow did not change abruptly, and the roller pump had to be slightly adjusted about every 30 min. if undue suction or low flow became apparent from the thin-walled piece of silastic tubing (indicator tube, 3 in Figure 2). One person could easily operate the bypass.

In both patients death was ultimately caused by massive bleeding from the gastrointestinal tract. Such bleeding is a known complication of massive myocardial infarction, especially during the advanced stages of shock. In the second patient, the bleeding was related to multiple ulcers - no clotting abnormalities other than those caused by heparinization could be detected. The heparin made the bleeding worse and these experiences initiated attempts to modify the blood circuit so that systemic heparinization is not necessary.

In the first patient it is likely that the sudden impairment of cardiac function was caused by a clot which occluded the right coronary artery. At autopsy, the clot could easily be removed. This finding suggests that diagnostic procedures, such as coronary angiography, be performed during the bypass if the heart does not recover within a reasonable time. Probably such studies could lead to surgical correction, eg., removal or bypass of the clot in this case.

The management of cardiogenic shock will change in the near future; if medical treatment fails, a non-invasive mechanical assist device, such as external counterpulsation, is applied. If the condition does not improve a bypass procedure is instituted. If during partial closed-chest cardiopulmonary bypass left ventricular end diastolic pressure is too high, the ventricle is decompressed with a transarterial cannula. If, during trans-arterial closed-chest left ventricular bypass, arterial oxygen content is too low, an oxygenator is used. If a bypass is incomplete blood return is counterpulsated, and if it is complete, pulsations are produced. Diagnostic procedures and surgical correction are carried out as necessary.

SUMMARY

Clinical experience with the application of Transarterial Closed-Chest Left Ventricular (TaCLV) Bypass in 2 patients has been described. During the bypass blood is removed from the left ventricle with a flexible, wide bore, thin-walled cannula which is inserted via the right axillary or subclavian artery. The blood is pumped back to the arterial vascular bed via a femoral artery. The method has been studied during experiments on 18 dogs and 42 sheep.

The blood circuit consists of a silastic tube, interrupted by a silastic reservoir. The tube is mounted in a roller pump. The reservoir serves to catch air bubbles and to depulsate the pump. Silastic side-lines are attached to the reservoir for additional perfusion of the right arm and the leg if necessary. With some additional equipment blood return can be pulsated and the pulses can be phased in between heart systoles (counterpulsation).

TaCLV-Bypass was applied in 2 patients with intractable shock. It took 20-30 min. to institute the bypass. A complete bypass was occasionally obtained, usually left ventricular pressure pulses were observed on the pressure tracing. The circulatory condition improved and cyanosis disappeared. One person could easily operate the bypass. The first patient was pumped for 11 hr. until bypass was discontinued because blood loss was suspected. Eight hours later the patient died from massive gastrointestinal bleeding. The same complications occurred after 5 1/2 hr. of bypass in the second patient. At autopsy, massive myocardial infarction was found in the first patient, while in the second, the heart appeared normal but multiple ulcers were found in the gastrointestinal tract and a poison was suspected of having caused the circulatory collapse. The prolonged shock-state and, in the second patient, the poison might have caused the profuse bleeding. Damage that could be related to the cannulas was not detected in the heart or adjacent structures.

Clinical results with other mechanical assist devices are described. It is suggested that diagnostic procedures such as coronary angiography be performed during the bypass if the heart does not recover. This could possibly lead to surgical correction. The management of patients with intractable shock is discussed.

REFERENCES

1. Zwart, H. H. J., Kralios, A., Collan, R., and Kolff, W. J. Transarterial closed-chest left ventricular (TaCLV) bypass. Trans. Amer. Soc. Artif. Int. Organs, 15:386, 1969.
2. Grode, G. A., Anderson, S. J., Grotta, H. M., and Falb, R. D. Nonthrombogenic materials via a simple coating process. Trans. Amer. Soc. Artif. Int. Organs, 15:1, 1969 and Andrade, J. D., Personnel communication.
3. Lyman, D. J. and Andrade, J. D. Platelet interaction with protein coated surfaces, an approach to thromboresistent surfaces. Thrombosis et Diathesis haemorrh., Suppl., in press.
4. Zwart, H. H. J. Complete left heart bypass without throcotomy. Thesis, 1966, S. O. L. Offsetdruk, Amsterdam, The Netherlands.
5. Geddes, L. A., Schuhman, R. E., Hoff, M. E., Moore, A. G., and Peters, J. L. Total maintenance of circulation in the closed-chest animal. Center Bull., 6:33, 1967.
6. Zwart, H. H. J., Kralios, A., Collan, R., and Kolff, W. J. TaCLV-bypass and coronary flow. Proc. 8th, ICMBE, Abstract, 26-7, 1969.
7. Zwart, H. H. J. and Kolff, W. J. Transarterial closed-chest left ventricular (TaCLV) bypass. Fed. Proc., Abstract, 780, 2914, 1969.
8. Zwart, H. H. J., Kralios, A., and Kolff, W. J. Transarterial closed-chest left ventricular bypass. Circulation Suppl. III, Abstract, 222, 1969.
9. Shillingford, J. P. and Thomas, M. Acute myocardial infarction and shock. Mod. Concepts Cardiovasc. Dis. 36:13, 1967.
10. Agress, C. M. Therapy of cardiogenic shock. Progr. Cardiovasc. Dis. 6:236, 1963.
11. Butner, A. M., Krakauer, J. S., Rosenbaum, A., Tjønneland, S., Sherman, J. L., Dresdale, D. T., and Kantrowitz, A. Clinical trial of phase-shift balloon pumping in cardiogenic shock: Results in 29 patients. Surg. Forum, 20:199, 1969.
12. Soroff, H., Birtwell, W., Levine, H., Bellas, A., and Deterling, R. Effects of counterpulsation upon the myocardial oxygen consumption and heart work. Surg. Forum, 13:174, 1962.
13. Cohen, L. S., Mitchell, J. H., Mullins, C. B., and Porterfield, D. Sequenced external counterpulsation in cardiogenic shock. J. Ass. Adv. Med. Instrum., in press.
14. Moulopoulos, S., Topaz, S., and Kolff, W. J. Extracorporeal assistance to the circulation. Trans. Amer. Soc. Artif. Int. Organs, 8:85, 1962.
15. Rosensweig, J, Chatterjee, S., and Merino, F. Treatment of acute myocardial infarction by counterpulsation. J. Thorac. Cardiovasc. Surg., 59:243, 1970.
16. Sugg, W. L., Rea, M. J., Webb, W. R., and Ecker, R. R. Cardiac assistance (Counterpulsation) in ten patients. Ann. Thorac. Surg., 9:1, 1970.
17. Stuckey, J. H., Newman, M. M., Dennis, C., Berg, E. H., Goodman, S. E., Fries, C. C., Karlson, K. E., Blumenfeld, M., Weitzner, S. W., Binder, L. S., and Winston, A. The use of the heart-lung machine in selected cases of acute myocardial infarction. Surg. Forum, 8:392, 1957.
18. Kennedy, J. H. and Norman, M. A. The use of a pump oxygenator in clinical cardiac failure. Mechanical assistance of the circulation. Stuttgart: Georg Thieme Verlag. 135, 1967.
19. Landé, A. J., Fillmore, S. J., Subramanian, V., Tiedemann, R. H., Carlson, R. G., Bloch, J. A., and Lillehei, C. W. 24 hours venous-arterial perfusion of awake dogs with a simple membrane oxygenator. Trans. Amer. Soc. Artif. Int. Organs, 15:181, 1969.
20. Landé, A. J. Personnel communication.
21. Torresani, J., Jausseran, J. M., Duport, G., Watel, J., Fornaris, E., Henry, E., and Jouve, A. Assistance cardiaque par dérivation veino-artérielle pulsée. Arch. Mal. Coeur, 62:1144, 1969.
22. Dennis, C., Grosz, C., Wesolowski, S. A., and Chin, C. J. External circulatory support in acute heart failure. J. Cardiovasc. Surg., 5:626, 1964.

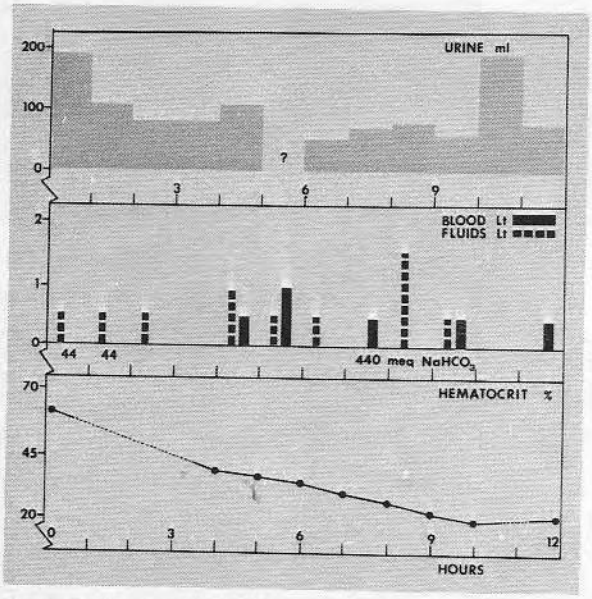

Figure 6. Urine production, fluids supplied, and hematocrit during TaCLV-Bypass in patient 1.

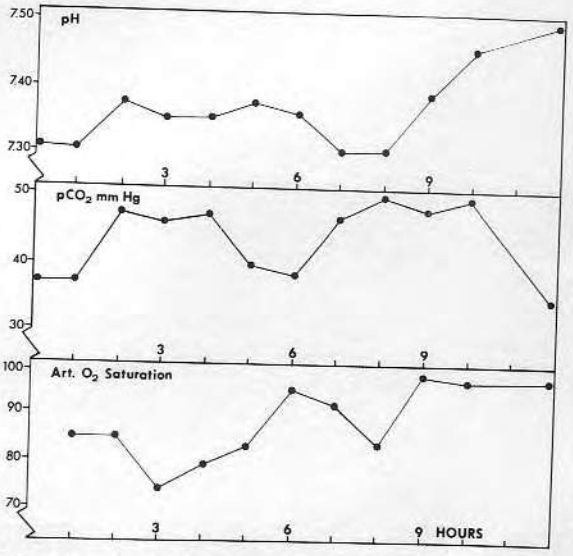

Figure 7. pH, pCO_2, and arterial oxygen saturation (Percent of normal) during TaCLV-Bypass in patient 1.

9 MOULOPOULOS, S.; TOPAZ, S., and KOLFF, W. J.: Diastolic balloon pumping with CO_2 in the aorta. Amer. Heart J. *63:* 669 (1962).
10 ROSENSWEIG, J.; CHATTERJEE, S., and MERINO, F.: Treatment of acute myocardial infarction by counterpulsation. J. thorac. cardiovasc. Surg. *59:* 243 (1970).
11 ROSS, J.: Left ventricular contraction and the therapy of cardiogenic shock. Circulation *35:* 611 (1967).
12 SCHAEFFER, J.; SCHWARZKOPF, H. J.; NIEDERMAYER, W.; HELD, L.; ULMER, F. und BIRKNER, K.: Änderungen der Herzdynamik durch arterielle Gegenpulsation. Pflügers Arch. ges. Physiol. *286:* 275 (1965).
13 SCHILLINGFORD, J. P. and THOMAS, M.: Acute myocardial infarction, hypotension and shock. Mod. Conc. cardiovasc. Dis. *36:* 13 (1967).
14 SUGG, W. L.; REA, M. J.; WEBB, W. R., and ECKER, R. R.: Cardiac assistance (counterpulsation) in ten patients. Ann. thorac. Surg. *9:* 1 (1970).
15 TORRESANI, J.; JAUSSERAN, J. M.; DUPORT, G.; WATEL, J.; FORNARIS, E.; HENRY, E. et JOUVE, A.: Assistance cardiaque par dérivation veino-artérielle pulsée. Arch. Mal. Cœur *62:* 1144 (1969).
16 ZWART, H. H. J.: Complete left heart bypass without thoractomy, an experimental study in dogs. Thesis (S.O.L., Amsterdam 1966).
17 ZWART, H. H. J.: Closed-chest left heart bypass as a treatment for myocardial infarction with shock following embolization of the left coronary artery in dogs. Arch. chir. neerl. *21:* 207 (1969).
18 ZWART, H. H. J. and KOLFF, W. J.: Transarterial closed-chest left ventricular (TaCLV) bypass. Abstract, Proc. Soc. exp. Biol. Med., p. 780 (1969).
19 ZWART, H. H. J.; KRALIOS, A.; COLLAN, R., and KOLFF, W. J.: Transarterial closed-chest left ventricular bypass and coronary flow. Abstract, Proc. 8th ICMBE (1969).
20 ZWART, H. H. J.; KRALIOS, A.; COLLAN, R., and KOLFF, W. J.: Transarterial closed-chest left ventricular (TaCLV) bypass. Trans. amer. Soc. artif. internal Organs *15:* 386 (1969).
21 ZWART, H. H. J.; KRALIOS, A., and KOLFF, W. J.: Transarterial closed-chest left ventricular bypass. Abstract, Circulation October (1969).
22 ZWART, H. H. J.; KRALIOS, A.; KWAN-GETT, C. S.; BACKMAN, D. K.; FOOTE, J. L.; ANDRADE, J. D.; CALTON, F. M.; SCHOONMAKER, F., and KOLFF, W. J.: First clinical application of transarterial closed-chest left ventricular (TaCLV) bypass. Trans. amer. Soc. artif. internal Organs *16:* 386 (1970).

Authors' address: Drs. H. H. J. ZWART, A. C. KRALIOS, C. S. KWAN-GETT, D. K. BACKMAN, J. L. FOOTE, J. D. ANDRADE and W. J. KOLFF, Division of Artificial Organs, Building 512, University of Utah, *Salt Lake City, UT 84112* (USA)

Mechanical Devices for Cardiopulmonary Assistance
Adv. Cardiol., vol. 6, pp. 157–172 (Karger, Basel 1971)

Transarterial Closed-Chest Left Ventricular Bypass for Desperate Heart Failure[1]

H. H. J. ZWART, A. C. KRALIOS, C. S. KWAN-GETT, D. K. BACKMAN, J. L. FOOTE, J. D. ANDRADE and W. J. KOLFF

Division of Artificial Organs, University of Utah, Salt Lake City, Utah

Myocardial infarction with shock, commonly called coronary shock, carries a mortality approaching 80% [2]. In such situation, the application of mechanical assist devices might be life-saving.

During advanced stages of coronary shock, the left ventricular output is decreased and tissue perfusion is inadequate. The left side of the heart is dilated, the intraluminal pressures are high and the lungs are congested. Pulmonary edema with desaturation is frequently encountered [13]. Overdistension renders the heart susceptible to arrythmias [3] and reduces left ventricular efficiency [11].

Treatment with mechanical assist devices must be directed towards restoration of blood flow to the tissues and decompression of the left side of the heart and the lungs. In 1966, a technique was developed by which this could be effected without thoracotomy [16]. A wide-bore, thin-walled, flexible cannula is inserted into the left ventricle via the right carotid (animals) or right axillary artery (humans) past the aortic valve. Blood is removed from the left ventricle and returned to the vascular bed via another peripheral artery (fig. 1). In previous animal experiments, it was demonstrated that this procedure of transarterial closed-chest left ventricular (TaCLV) bypass is feasible and relatively safe. A review of pertinent data from these experiments is presented in table I [16–22]. Recently, apparatus was developed for counter-pulsated blood return. A detailed description of the equipment for TaCLV bypass and the results of animal testing are presented.

1 Supported in part by the Max C. Fleischmann Foundation.

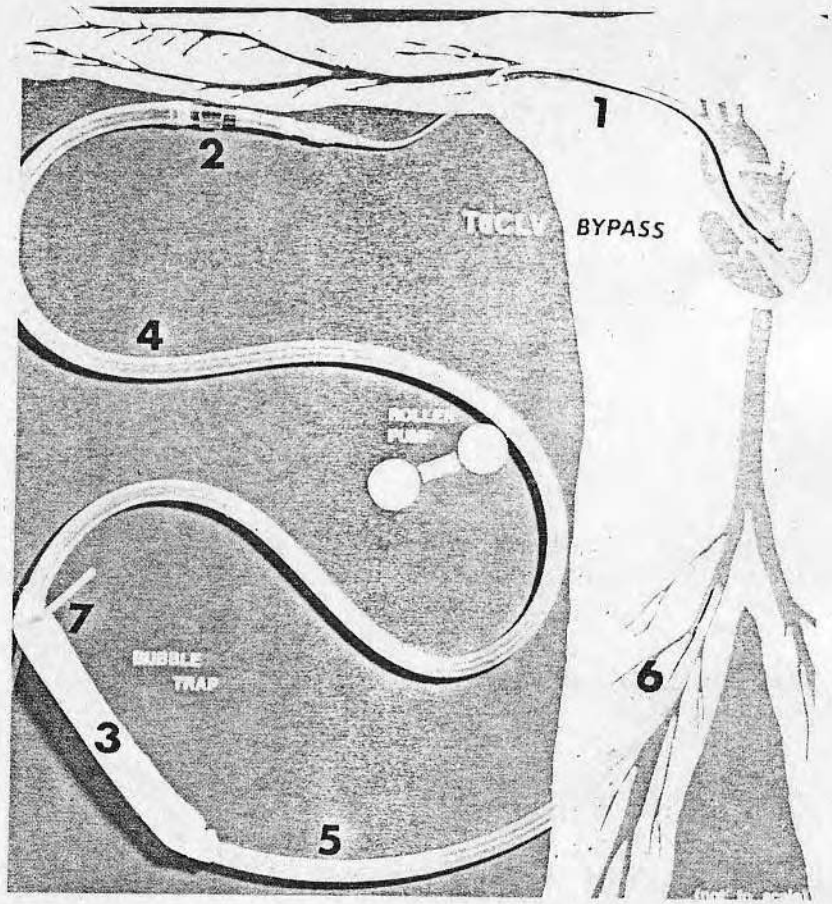

Fig. 1. Transarterial closed-chest left ventricular (TaCLV) bypass. A wide-bore, flexible, thin-walled cannula (1) is inserted into the left ventricle via a peripheral artery. A roller pump removes blood from the ventricle through the cannula and returns it to the arterial vascular bed. Thin-walled tubing (2) prevents undue suction by the pump to the left ventricle. Arterial reservoir (3), silastic tubing (4, 5), blood return cannula (6), 3 side lines from arterial reservoir (7). (Compare fig. 4).

Equipment of TaCLV Bypass

The circuit includes a blood outflow and a blood return cannula, blood tubes, a roller pump, and an apparatus for pulsatile or counter-pulsatile blood return.

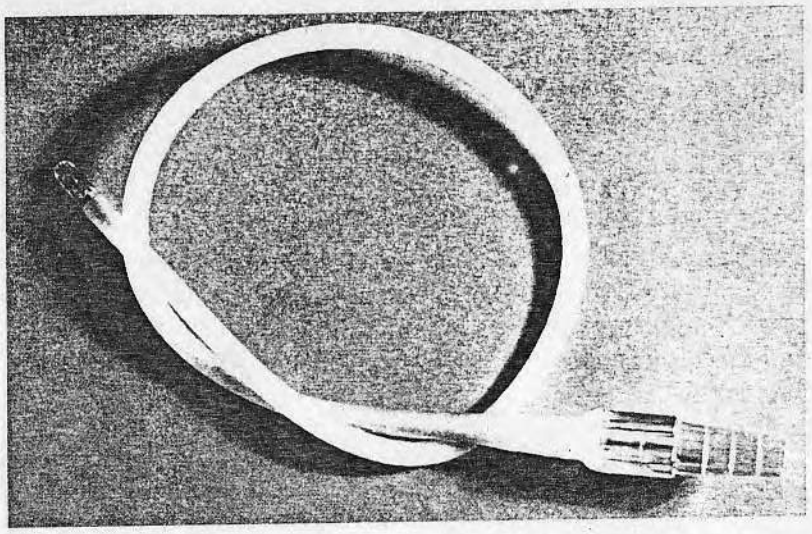

Fig. 2. Cannula for removal of blood from left ventricle. OD 6.0 mm, wall-thickness 0.3 mm, length 45 cm. Flexible, softens after insertion. Maximum capacity 6.2 l/min (blood, Hmt. 24, temp. 20 °C) at pressure difference of 150 mm Hg. Cannula is fabricated from polyurethane, reinforced with glass fiber.

The blood outflow cannula (fig. 1, No. 1 and 2) is 45 cm long, OD 6.0 mm, wall-thickness 0.3 mm. It is fabricated from polyurethane (Estane 5701-F1, Goodrich) reinforced with single-end glass-fiber (Owens-Corning). The maximum flow (blood, Hct. 24, temp. 20 °C) is 6.2 l/min at a pressure difference of 150 mm Hg. The base of the cannula carries a ¼–⅜ in connector. The cannula is flexible yet stiff enough for insertion without a stylet. Once in the body, the polyurethane softens so that the cannula adapts to the geometry of the heart and the blood vessels.

The cannula is connected with a 3-centimeter long ⅜ in ID ½ in OD silastic tube (fig. 1, No. 2). This piece of tubing in turn is connected with the blood circuit with a ⅜–½ in connector. The blood circuit consists of 6 ft of ½ in ID ¾ in OD silastic tubing which is interrupted by a reservoir (fig. 1, No. 3) leaving 5 (fig. 1, No. 4) respectively 1 ft (fig. 1, No. 5) of tubing at each end of the reservoir. The blood return cannula (Bardic 18–22 French) (fig. 1, No. 6) is connected to the blood circuit with a ½–⅜ in connector.

The silastic tubing for the blood circuit is mounted in a roller pump (Travenol 5 M 6002) at a point halfway between inflow part and arterial reservoir. The pump is set to be occlusive except for a backflow of 20 ml/min

against a pressure of 100 mm Hg. This pump setting seems to minimize blood damage [6]. The pump sucks at the base of the blood outflow cannula and it returns the blood through the blood-return cannula.

The reservoir is layered from uncured silastic sheet 0.060 in thick (Dow Corning) on a highly polished stainless steel mold. It has an OD of 1–¼ in and tapers off at both ends to a ½ in ID. Part of the reservoir is reinforced to prevent undue dilation. The reservoir is cured and glued over the silastic tubing of the blood circuit. The reservoir serves to catch air bubbles and to depulsate the roller pump so that a non-pulsatile blood return is produced. The latter is important during incomplete bypass because the left ventricle would be damaged if the pump produced a pulse wave during systole [12]. Three silastic side lines (fig. 1, No. 7) are connected to the inflow part of the reservoir. They serve to vent air and to perfuse the peripheral part of the cannulated arteries if necessary. The assembled blood circuit has a priming volume of 400 ml.

With the equipment described so far, transarterial bypass can be carried out effectively. Recently, apparatus was fabricated which, if added to the basic circuit, makes it possible to produce a pulsatile blood return or to counterpulsate the blood return. The first might be of importance during complete bypass. The latter is expected to be of value during incomplete bypass: it reduces the systolic and increases the diastolic pressure, thus decreasing the workload of the heart and increasing the coronary flow (concept of counterpulsation) [9].

The apparatus to produce pulsatile blood return (fig. 3) consists of an inflatable cuff to be mounted over the arterial reservoir, a pressure source, a buffer tank with a 3-way Solenoid valve and a pressure regulator, electronic apparatus to detect the R-wave of the ECG. The cuff is fabricated from a plexiglass cylinder 1–½ in ID 1–¾ in OD, covered on the inside with a natural latex sleeve. Air can be forced inbetween plexiglass and rubber sleeve through a side hole. It will cause the sleeve to collapse and this in turn will squeeze the blood out of the reservoir towards the blood return cannula so that a pulse and flow wave are produced in the aorta. Note that the blood is separated from the pressurized air by 2 independent layers of silastic. This minimizes the risk of air embolism. If the cuff is depressurized, the reservoir will be filled rapidly with blood from the roller pump and retrograde through the blood return cannula from the arterial vascular bed. Depending on the bypass flow, more or less blood will escape from the arterial system.

The pressure necessary to squeeze the reservoir effectively during a bypass with a flow of 1–4 l/min against a pressure sf 80–140 mm Hg using a

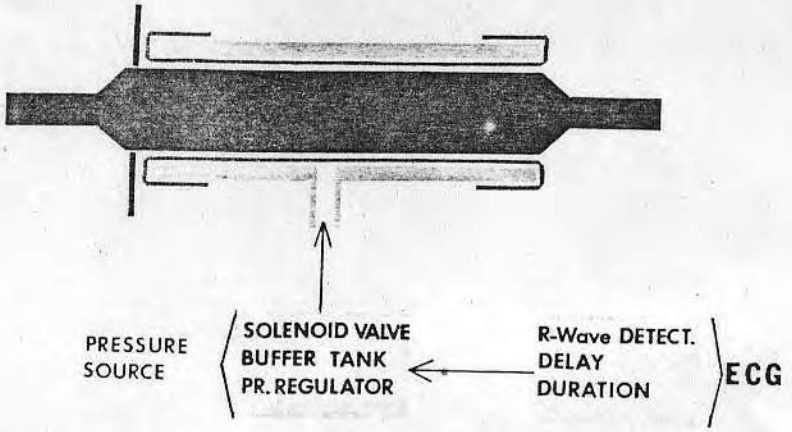

Fig. 3. Cuff to be mounted over arterial reservoir for pulsatile and counterpulsatile blood return. (Compare fig. 1 and 4.)

Bardic blood return cannula 20–24 Fr. is 20–30 PSI. No suction is needed for decompression of the cuff if the 3-way solenoid valve has an opening of at least ⅜ in. The ID of the tube connecting solenoid valve and cuff must be at least ⅜ in and no longer than 5 ft. The electronic instrument activates the solenoid valve at a chosen rate or it can be set to produce a pulse which is synchronized with the ECG. In the latter case, the pulse can be delayed with respect to the QRS complex and the duration can be varied.

Presently some 25 mg of albumin is added to the priming fluid of the blood circuit because there is evidence [8] that this will decrease platelet adhesion to the surface and probably also blood damage. In addition, attempts are being made to treat the blood circuit so that generalized heparinization is not necessary [5].

Operating Instructions for TaCLV Bypass

The equipment for transarterial bypass is mounted on a cart together with surgical instruments, drapes, fluids, and drugs, so that the bypass can be instituted without delay (fig. 4). The left ventricular cannulas are sterilized in ethylene oxide. The blood circuit and blood return cannula can be autoclaved. The blood circuit (without cannulas) is primed with saline 0.9%

Table 1. Compiled data on transarterial closed-chest left ventricular (TaCLV) bypass with literature references (18 dogs, 44 sheep and 2 humans)

1. The carotid and axillary arteries of sheep and the right axillary or subclavian artery of humans accept the left ventricular cannula [20, 22].
2. Insertion of the cannula into the left ventricle does not offer difficulties and can be carried out without the use of electronic or X-ray equipment [16, 20, 22].
3. The left ventricle can be bypassed completely in closed-chest animals or humans [4, 20, 22].
4. The aortic valve is competent during and after the bypass [18].
5. Coronary flow is not impeded during the bypass, during ventricular fibrillation increases [19].
6. The bypass is well tolerated, 6 sheep survived uneventful 4 h and 2 sheep survived 24 h of bypass; the plasma hemoglobin remained below 23 mg% [21].
7. Deep shock, produced in closed-chest dogs by embolizing the left coronary artery with microspheres, could be treated. In 4 out of 5 cases, the heart had recovered after 2 h of assist [17].
8. In 2 patients with cardiogenic shock who were beyond medical treatment, the shock could be reversed and the circulation could be restored. It required 20 and 30 min respectively to institute the bypass [22].
9. Usually the left ventricular cannula does not cause damage to the heart. Occasionally, small superficial hemorrhages are found on the endocardium [16].

(400 ml) and closed at both ends with tube clamps. Some 25 mg of albumin is injected into the circuit through the air vent of the reservoir, taking good care that no air is left in the circuit.

After dissection of the right carotid (animals) or right axillary or subclavian artery (humans) and a femoral artery, the left ventricular and blood return cannulas are inserted. The 3-centimeter long, thin-walled silastic tube (fig. 1, No. 2) is connected to the left ventricular cannula and closed off with a screw-clamp. After heparinization, the cannula is inserted into the artery and primed with blood by unscrewing the clamp.

The cannula is advanced until a distinct resistance is sensed: the aortic valve. The experience with cannulation in living humans is as yet limited (2 cases [22]). Resistances are anticipated at the junction of the subclavian artery with the carotid artery or with the aorta. They will be sensed, however, at an earlier stage of cannulation when only half of the cannula is being inserted. Arteriosclerotic plaques might also cause difficulties during advancement of the cannula. The aortic pressure pulse is barely noticeable at the silastic tubing as long as the cannula tip is in the aorta. As the cannula tip touches the aortic valve, it is withdrawn and advanced over about half

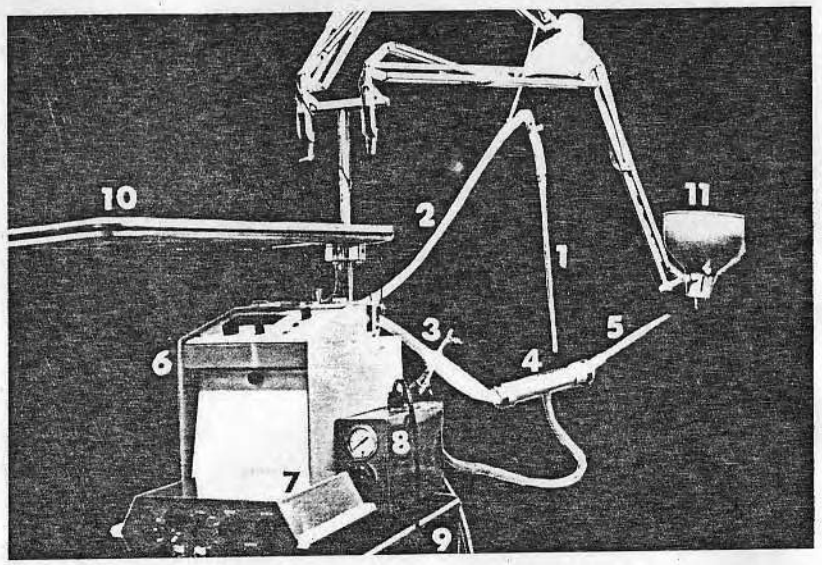

Fig. 4. Equipment for TaCLV-Bypass mounted on a cart. (1) LV outflow cannula, (2) blood circuit, (3) arterial reservoir, (4) cuff for pulsatile return, (5) blood return cannula, (6) roller pump, (7) R-wave detector, (8) solenoid valve and pressure regulator, (9) cart, (10) operating table, (11) surgical lamp.

an inch in quick motion, preferably synchronous with the heart beat. As the cannula tip enters the left ventricle, no resistance is sensed any more and the silastic tube shows distinctly the much larger pulse pressure of the left ventricle. The cannula is withdrawn carefully until the vigorous pulsations start to disappear and next advanced over 1 cm. The tip is now in the outflow tract of the left ventricle, which minimizes the risk of damage to the endocardium.

Preferably simultaneously, the blood return cannula is inserted into a femoral artery. The cannulas are connected with the blood circuit and the latter is mounted in the roller pump. If application of pulsatile blood return is anticipated, the cuff should be mounted over the blood return line. After removal of the tube-clamps, transarterial bypass can be started. The piece of thin-walled silastic tubing now serves to indicate the amount of suction at the cannula base. If 1 cm of the tubing is left free from the two connectors at both ends, it will collapse if the pressure is below minus 150 mm Hg. At a flow rate of 1–5 l/min the pressure in the left ventricle can be regulated

to be not less than atmospheric by preventing collapse of this tubing. In practice, it is not necessary to adjust the pump rate more often than once every 30 min. Once the bypass is functioning, equipment for pulsatile blood return can be made operational if desired. The cuff is mounted over the reservoir, connected with the solenoid valve and it, in turn, via the buffer tank and pressure regulator, to a pressure source. If the bypass is complete (feel the pulse) the electronic pulse generator can be set to activate the solenoid valve at any chosen rate. The pulse pressure is adjusted with the pressure regulator. In case the bypass is incomplete, it is necessary to insert a catheter into the arterial system, preferably near the heart, and to display the arterial pressure. The electronic pulse generator is connected with the ECG and set to synchronize the solenoid valve activation with the QRS complex. Duration and delay settings are adjusted until the pressure pulse produced by the bypass occurs during diastole.

Animal Experiments

After 48 h of fasting, six Columbia sheep of both sexes, weighing 45–60 kg were anesthetized with sodium methohexitol (Corvel, Indianapolis) 200–300 mg and Scopolamine 1–2 mg intravenously. Following endotracheal intubation, respiration was controlled with an Engstrom respirator (150, MIVAB), using room air 70% and oxygen 30%, frequency 16/min, volume 800 ml/stroke. Anesthesia was continued with sodium methohexitol. Experiments were divided in 3 groups:

Group I (sheep 1 and 2). During complete cardiopulmonary bypass, instituted for replacement of the heart with an artificial heart, the cuff was mounted around the reservoir in the blood return line and tested. The blood was returned via a carotid artery because femoral arteries of sheep do not accept cannulas over French size 18.

Group II (sheep 3 and 4). TaCLV bypass was applied for 2 h. During this period, ventricular fibrillation was produced and allowed to persist for 1 h. The blood circuit and the cannulas were treated for antithrombogenic properties [5]. The animals were allowed to survive.

Group III (sheep 5 and 6). TaCLV bypass was applied to test pulsatile and counterpulsated blood return. The circuit was treated, sheep 5 was not given heparin, sheep 6 received small dosage of heparin. In sheep 6 the chest was opened (midsternal split) and cardiogenic shock was produced by ligating coronary arteries. The shock was treated with transarterial bypass

or with arterio-arterial counterpulsation (same circuit, pump stop, blood circuit clamped between pump and arterial reservoir). The blood was returned via a carotid artery.

The arterial and right atrial pressure (AP and RAP) were measured in all sheep with catheters inserted via a femoral artery and vein. In group III, sheep 6, the left ventricular pressure (LVP) and the flow in the descending aorta, the left coronary artery and the blood return cannula were measured in addition. Pressures and flows were measured with Sanborn (Sanborn Company, Waltham, Mass.) and Biotronex (Biotronex Lab., Silver Spring, Md) transducers and recorded, together with the ECG, on an 8-channel Sanborn recorder.

The hematocrit, arterial oxygen saturation (American Optical Oxymeter), pH (Radiometer, Copenhagen) and clotting time were measured at regular intervals. The bypass flow was estimated from the rpm of the roller pump. The temperature was measured in the esophagus. At termination of the experiments, sheep of group I and II were sacrificed.

Results

Group I. For replacement of the heart with an artificial heart, it is necessary to maintain the circulation with cardiopulmonary bypass for about one hour. During this period, the non-pulsatile blood return of the heart-lung machine could be transformed to a pulsatile flow with a pulse pressure of 25–40 mm Hg in the thoracic aorta. A pressure of 20–30 PSI had to be applied to the cuff around the arterial reservoir (fig. 3) for 50–100 msec. The bypass period was too short for meaningful comparison between the condition of the sheep during pulsatile or continuous blood return.

Group II. Transarterial left ventricular bypass could easily be instituted without thoracotomy. No abnormalities were observed on the ECG during insertion of the left ventricular cannula. Data on hemodynamics and blood studies are presented in table II. Before ventricular fibrillation was produced, the bypass was incomplete, the flow ranged between 3.4 and 4.6 l/min (mean 3.7), and RAP, AP and ECG did not change. During ventricular fibrillation the bypass flow ranged between 1.8 and 2.6 l/min (mean 2.3), RAP increased to 5–18 mm Hg (mean 11) and AP fell to 55–80 mm Hg (mean 72). No extra fluids or vasopressors were supplied to the sheep. After 1 h of ventricular fibrillation, the hearts could be defibrillated externally at the first attempt. The ECG showed normal sinus rhythm.

Table II. Hemodynamics and blood studies during different stages of transarterial bypass in sheep 3 and 4

Sheep number	Stage	Mean RAP mm Hg	AP mm Hg	Bypass flow l/min	Hematocrit %	pH	Art. O_2 saturation % of 100	Clotting time min
3	30 min before ventricular fibrillation	2	110/90	3.4	32	7.62	92	12
	during ventricular fibrillation	11	78	2.8	30	7.58	94	3
	30 min after defibrillation	3	125/95	3.2	31	7.59	90	3
4	30 min before ventricular fibrillation	4	100/90	3.6	28	7.68	95	3
	during ventricular fibrillation	17	75	2.7	26	7.63	93	4
	30 min after defibrillation	2	110/75	3.4	25	7.65	96	3

The hematocrit decreased somewhat in both sheep during the bypass, the plasma remained clear. The pH was high and the oxygen saturation normal. The clotting time was slightly prolonged (12 min) at start of the bypass in sheep 3, it was normal (less than 4 min) in all other samples of both sheep. The esophageal temperature remained stable (39° ± 0.7 °C). The pulmonary inflation pressure was normal (18–28 cm H_2O) throughout the experiments in both sheep. The eyelid reflexes were present before, during and after the experiments.

Both sheep woke up and stood on their legs within 1 h after anesthesia had been discontinued. They recovered uneventful from the experiments and are still doing well. One of the sheep delivered 2 healthy lambs 60 days after it was operated on (fig. 5). Small clots were found around the connectors and fibrin deposits in the arterial reservoir.

Group III. As sheep 3 and 4, the sheep of this group tolerated the bypass well. The clotting time was normal in all blood samples of sheep 5. In sheep

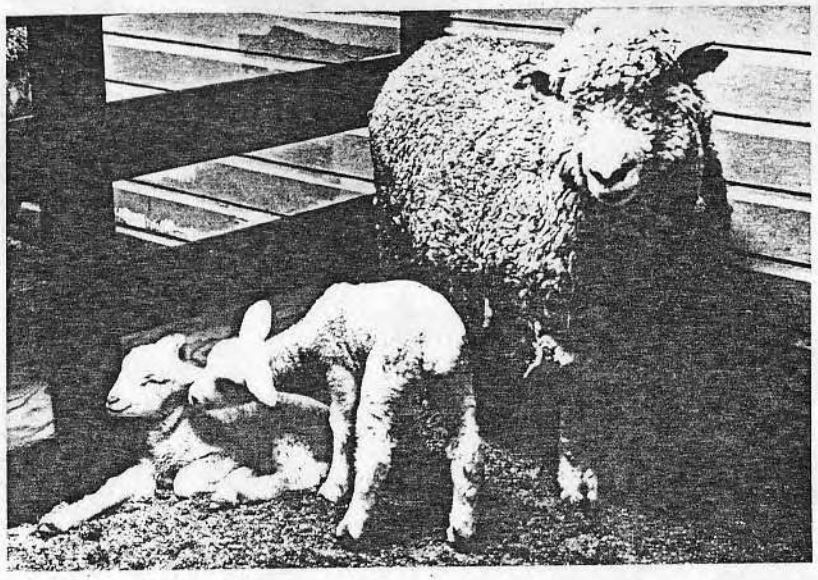

Fig. 5. Sheep 4 (group II) was in ventricular fibrillation for 60 min. The circulation was maintained with TaCLV-bypass. She delivered 2 healthy lambs 60 days later.

6, small amounts of heparin were supplied intravenously to keep the clotting time at 10 min in an attempt to prevent the build-up of clots around the connectors.

The equipment for pulsatile and counterpulsatile blood return functioned properly. During complete bypass a pulse pressure of 20–50 mm Hg could be produced in the thoracic aorta at a rate of 60–180 min. During incomplete bypass, the blood return could be counterpulsated even during arrythmias (fig. 6) up to a heart rate of 130 beats/min. At high heart rates or during serious arrythmia, the bypass became complete, making counterpulsated blood return unnecessary (fig. 6). In agreement with previous experiments [20] the LV pressure in sheep 6 could be kept around atmospheric during complete bypass (fig. 6).

Cardiogenic shock was produced by ligating coronary arteries in sheep 6. In the initial stage of shock, the condition could be improved equally well with bypass or arterio-arterial counterpulsation. During the advanced stages of shock, however, counterpulsation alone did not change the condition whereas the circulation could be restored with bypass (fig. 7).

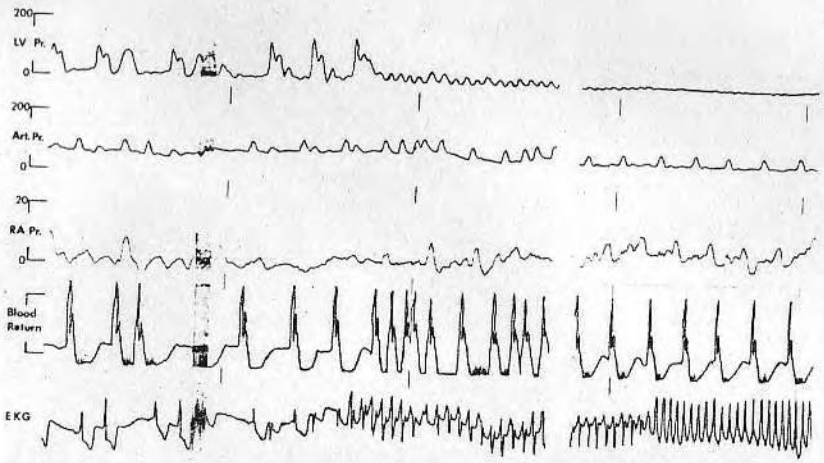

Fig. 6. Tracings obtained during advanced stage of coronary shock in sheep 6 (group III). Pressures in mm Hg. Paper speed is 25 mm/sec. Flow in blood return cannula was measured with non-calibrated electromagnetic flow probe. In the left panel blood return was counterphased to left ventricular ejection. In the right panel the bypass its complete, LV pressure is around atmospheric and blood return is pulsated with a free running pulse without synchronization with the ECG.

At autopsy, no abnormalities were found in the hearts that could be related to the left ventricular outflow cannula. Small clots were present around the connectors and fibrin deposits in the arterial reservoir notwithstanding the partial heparinization in sheep 6. No damage or wear was detected in the arterial reservoir.

Discussion

The application of a mechanical cardiocirculatory assist is an emergency procedure, even more so because the decision to use the device is often made only at an advanced stage of shock. It is therefore important that institution of the assist be a simple procedure, that complicated equipment be avoided and that the apparatus be reliable. Transarterial left ventricular bypass in its simplest form meets these requirements.

The procedure involves dissection of 2 arteries, the chest remains closed, general anesthesia is not necessary, and no electronic or X-ray equipment needs to be available. The bypass could be instituted within 30 min in our first 2 patients [22]. The pump and the blood circuit are simple and reliable.

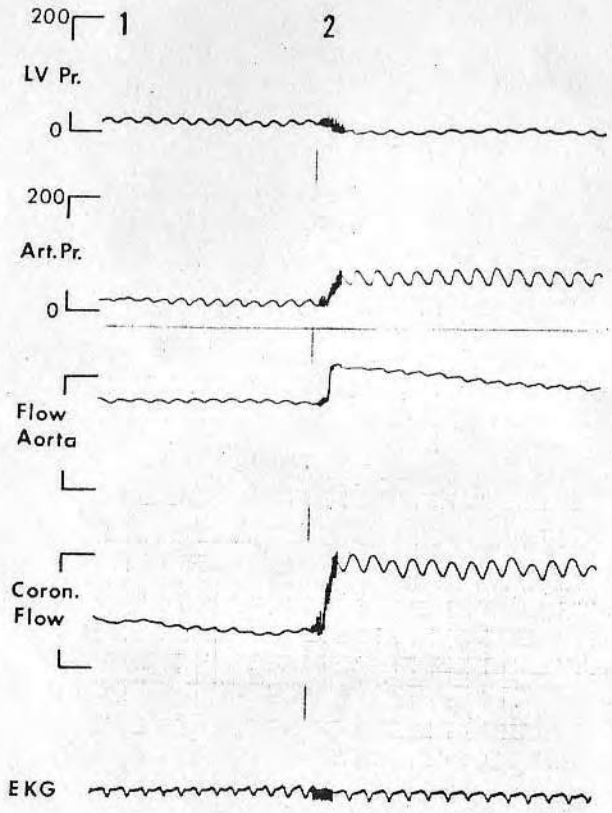

Fig. 7. Tracings obtained during advanced stage of coronary shock in sheep 6 (group III). Pressures in mm Hg. Paper speed is 5 mm/sec. Flow in descending aorta and left main coronary artery were measured with non-calibrated electromagnetic flow probes. During period 1 the shock was treated with arterio-arterial counterpulsation alone. At 2 the bypass was switched on.

The method has the additional advantage that, if fitted in an ambulance it could be applied everywhere.

The equipment for pulsatile or counterpulsated blood return functioned properly: pulse waves with more than satisfactory pulse pressures (20–50 mm Hg) could be produced in the thoracic aorta. The system is quick enough to follow a heart rate of 130 beats/min. However, the necessary apparatus, including that for monitoring of blood pressure and ECG,

complicates the method. It remains to be established that the produced pulsations are of much additional benefit. It is unlikely that for immediate application of the bypass, pulsatile blood return is essential. Therefore it is advised to use this equipment only after the condition has stabilized and if apparatus and personel are readily available.

The treatment of the circuit in order to prevent generalized heparinization is imperfect although sheep 3 and 4 did not receive heparin and survived bypass of 2 h without ill effects. It should be realized that if clots are found in the circuit, it is most likely that many emboli have been produced during the pybass [7]. Since prolonged heparinization causes considerable capillary bleeding from even small wounds and because heparin might damage platelets [1], investigations are continued to obtain properly treated blood circuits [5, 8].

It is of importance that the circulation can be maintained during ventricular fibrillation. Even lambs survived the experiment while in the uterus. With counterpulsation alone (external, balloon, or arterio-arterial counterpulsation) animals [9] and humans [10, 14] cannot be kept alive during ventricular fibrillation. If the circulation is maintained with closed-chest cardiopulmonary bypass (veno-arterial bypass with oxygenation) the left ventricle is not maximally decompressed [15]. During arrhythmias or serious pump failure, the hemodynamic situation is comparable with ventricular fibrillation: minimal cardiac output, high end-diastolic LVP and low AP. Such a condition was produced in sheep 6 by ligating coronary arteries. It could be treated with left ventricular bypass, the left ventricule was decompressed to atmospheric pressure and AP increased.

Summary

A method for treatment of desperate left ventricular failure has been developed. Blood is removed from the left ventricle with a flexible, wide-bore, thin-walled cannula, which is inserted via a peripheral artery, past the aortic valve. The blood is returned to the vascular bed via another peripheral artery. With this transarterial closed-chest left ventricular (TaCLV) bypass, the left ventricle can be decompressed to atmospheric pressure, the circulation can be maintained even during ventricular fibrillation and cardiogenic shock can be treated.

The equipment for transarterial bypass is described in detail and instructions for use are given. The external blood circuit consists of a silastic tube, mounted in a roller pump. Between the pump and the blood return cannula, the circuit includes a reservoir which serves as a bubble trab and a depulsating device. Additional apparatus is available for the

production of pulsatile or counterpulsated blood return. For institution of the bypass, it is not necessary to have electronic or X-ray equipment available. All necessary apparatus is mounted on a cart and is portable. Attempts have been made to treat the blood circuit so that generalized heparinization is not necessary.

Experiments were performed on 6 sheep to test the equipment for pulsatile and counterpulsated blood return and antithrombogenic properties. Pulse waves with a pulse-pressure of 20–50 mm Hg and a frequency of up to 180 min could be produced in the thoracic arota. Counterpulsatile blood return was effective up to a heart rate of 130 beats/min. At heart rates over 120, the bypass became complete making counterpulsation unnecessary. On examination of the blood circuit following the experiments, small clots were found around the connectors and fibrin deposits in the arterial reservoir. Two sheep survived 2 h of bypass during which ventricular fibrillation was produced and allowed to persist for 1 h. One of these sheep delivered 2 healthy lambs 60 days later. In another sheep, profound cardiogenic shock was produced by ligating coronary arteries. The shock could be treated with transarterial bypass, whereas arterio-arterial counterpulsation was ineffective.

This equipment is suggested for transarterial bypass in its simplest form during the initial, acute stage of treatment. After the condition has stabilized, the use of pulsatile or counterpulsated blood return can be considered. It remains to be established whether either mode of blood return is of much additional benefit.

References

1 AEPLI, R.: Action traumatique exercée sur le sang par les matières servant à la fabrication des appareils «cœur-poumons». Helv. physiol. pharmacol. Acta *18:* 119 (1960).
2 AGRESS, C. M.: Therapy of cardiogenic shock. Progr. cardiovasc. Dis. *6:* 236 (1963).
3 CHARDACK, W. M.; GAGE, A. A.; MCRONALD, R. E., and SOUTHER, S.: Fibrillation in empty and loaded ventricles. Arch. Surg., Chicago *93:* 795 (1966).
4 GEDDES, L. A.; SCHUMAN, R. E.; HOFF, H. E.; MOORE, A. G., and PETERS, J. L.: Total maintenance of circulation in the closed-chest animal. Center Bull. *6:* 33 (1967).
5 GRODE, G. A.; ANDERSON, S. J.; GROTTA, H. M., and FALB, R. D.: Nonthrombogenic materials via a simple coating process. Trans. amer. Soc. artif. internal Organs *15:* 1 (1969).
6 KOLOBOW, T.; ZAPOL, W., and PIERCE, J.: High survival and minimal blood damage in lambs exposed to long-term (1 week) veno-venous pumping with a polyurethane chamber roller pump with and without a membrane blood oxygenator. Trans. amer. Soc. art. internal Organs *15:* 172 (1969).
7 KUSSEROW, B.; LARROW, R., and NICHOLS, J.: Observations concerning prosthesis-induced thromboembolic phenomena made with an *in vivo* embolism test system. Trans. amer. Soc. artif. internal Organs *16:* 58 (1970).
8 LYMAN, D. J. and ANDRADE, J. D.: Platelet interaction with protein coated surfaces, an approach to thromboresistant surfaces. Thromb. Diath. haemorrh. (suppl., in press).